NAZARBAYEV UNIVERSITY

CHME 400 Capstone Project

Design of Plant for Industrial Production of Butadiene from Butane

Nazarbayev University

School of Engineering and Digital Sciences

Chemical and Materials Engineering Department

Under the guidance of Professor Shah,

Professor Golman, Professor Mentbayeva

Group "C(H)MEshariki"

Azel Tuyakova 202060551

Adil Zulkarnayev 202182028

Kamilya Kossayeva 202148144

Darkhan Nurgumarov 201932212

Aigerim Sarsengaliyeva 202043796

Zhandarbek Sapargaliyev 202051563

Section	Topic	Azel	Zhandarbek	Adil	Aigerim	Darkhan	Kamilya
Chapter 1. Process Introduction							
1.1	Butadiene Overview				1st		
1.2	Purity and Production rate			1st			2nd
1.3	Mechanism section				1st		
1.4	Chemical Reaction Analysis	1st					
1.5	Introduction to the major unit operations in the process		1st				
Chapter 2. Process Summary							
2.1	Catalytic dehydrogenation overview					1st	
2.2	Selected Chemical reaction		1st				
2.3	Process Summary	1st					2nd
2.4	Overall material balance		1st				
Chapter 3. Major unit design							
3.1	E-101 Design	1st					
3.2	R-101 Design		1st				
3.3	C-102 Design				1st		

3.4	E-103 Design			1st			
3.5	T-101 Design						1st
Chapter 4. Minor unit design							
4.1.1	E-100	1st					
4.1.2	E-102						1st
4.1.2	E-104		1st				
4.2	C-101, C-102				1st		
4.3	Storage Tanks	1st		2nd			
4.4	T-102		1st				
4.5	T-103					1st	
4.6	RC–101			1st			
4.7	F-101					1st	
Chapter 5. Plant Location and Layout							
5.1	Location of the Plant	1st			2nd		
5.2	Plant Layout			2nd	1st		
Chapter 6. Environment and Waste Streams							
6.1	Overview of Waste Streams						1st

6.2	Law Regulations			2nd			1st
6.3	Safety Measures for Incinerating Hydrogen Stream			1st			
6.4	Energy Recovery from Waste Stream Combustion			2nd			1st
6.5	Water Stream Outlet			1st			
6.6	Catalyst Usage and Disposal						1st
6.7	Fire safety						1st
Chapter 7. Total Investment and Profitability							
7	Total Investment and Profitability	2nd	1st				
Chapter 8. Conclusions and future work							
8	Conclusions and future work			1st			

Table of contents:

Chapter 1. Process Introduction

1.1. Butadiene Overview

1,3-Butadiene (BD), a non-corrosive, flammable and colorless gas with the chemical formula C_4H_6, is a highly important industrial chemical which is known for its versatility and widespread use. Being a primary product of the petrochemical industry, its building components are essential for the production of a wide range of consumer and industrial goods, such as vehicles, construction materials, appliance components, electronics, clothing, packaging, and household items [1].

Table 1.1.1 Physical and chemical properties of Butadiene [2]

Properties		Chemical structure
IUPAC Name	Buta-1,3-diene	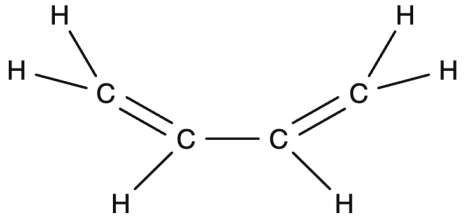
Molecular Formula	C_4H_6, CH2=(CH)2=CH2	
Appearance	Colorless gas	
Molecular Weight	54.09 g/mol	
Melting Point	-108.966 °C	
Boiling point	-4.5 °C	
Density	0.6149 g/cu	

Butadiene has two isomers: 1,3-butadiene and 1,2-butadiene. 1,3-butadiene is mainly produced as a byproduct of steam cracking for ethylene manufacture in regions like the U.S., Europe, and Japan, although some areas still use ethanol for butadiene fabrication. Older methods like n-butane dehydrogenation have largely been phased out with decreased relevance. The second isomer, 1,2-butadiene, is a minor byproduct of 1,3-butadiene production and has no significant commercial use [3].

1.2. Purity and production rate

1.3-Butadiene is sold at different purity grades for different uses. A technical-commercial grade of 1,3-Butadiene is 98 mol% purity [4]. Analytical, polymer, rubber and liquid grades in a range of 99.0-99.5% purity [4]. Nowadays, according to the Russian Federation Standard (GOST), depending on the purpose, butadiene is produced in grades A (First and Superior Quality) and B [5]. Grade A is used for the production of synthetic rubbers by stereospecific polymerization, production of synthetic rubbers and latexes by emulsion polymerization, and production of chloroprene, while grade B is used for the production of synthetic rubbers and

latexes by emulsion polymerization, and production of chloroprene. Grade B requires 98.0% purity [5]. Grade A requires 99.0% purity for the First Quality and 99.3% purity for the Superior Quality [5]. Russian companies such as “ТИТАН” (“Titan”), “Татнефть” (Tatneft) and “Синтез-Каучук” (“Syntez-Kauchuk”) produce butadiene in these 3 grades [6-8]. Russian company “БК Групп” (“BC Group”) produces it at purity more or equal to 99.3% [9]. Korean “LG Chem” requires butadiene with a minimum purity of at least 99% for its products [10]. Based on this data and available information of butadiene market and production processes, the optimal purity grade is to be 99.5%. Highly pure butadiene ensures most favorable performance and quality of end products. Achieving these levels of purity requires advanced purification processes, including distillation and extraction.

Kazakhstan government is applying Russian GOST for production of chemical materials, which is why production quality specifications are taken from them:

Table 1.2.1 Quality specifications of butadiene (Russian GOST) [9]

Property	**Grade A (Superior quality)**
Appearance	Colorless or yellowish liquid
Mass fraction of 1,3-butadiene, %, not less than	99.3
Mass fraction of light volatile hydrocarbons, %, not more than	0.10
Mass fraction of cyclopentadiene, %, not more than	0.001
Mass fraction of nitrogen compounds (as nitrogen), %, not more than Including mass fraction of ammonia (as nitrogen), %, not more than	0.003 0.001
Mass fraction of carbonyl compounds (as acetone), %, not more than	0.005
Mass fraction of monosubstituted acetylene hydrocarbons, %, not more than	0.005
Mass fraction of allenic hydrocarbons, %, not more than	0.006
Mass fraction of heavy residue, %, not more than	0.10
Mass fraction of copper	Not regulated
Mass fraction of peroxide compounds, %, not more than	0.0003

Undissolved moisture content	Absence

Production rate for this process was decided as 90,000 tons per year by calculations using interpolation of data from the US (see Appendix A.2). This number is well aligned with the plans of “ТОО Бутадиен” (“LLP Butadiene”) company which plans to produce around 120 thousand tons per year including the Russian market [11].

1.3. Mechanism Section

Butadiene is commercially produced through 3 main processes [1]:

1. Steam cracking of paraffinic hydrocarbons: in this method, butadiene is obtained as a co-product during ethylene production.
2. Catalytic dehydrogenation of n-butane and n-butene: known as the Houdry process, this approach dehydrogenates n-butane and n-butene to produce butadiene.
3. Oxidative dehydrogenation of n-butene: this process involves the oxidative dehydrogenation of n-butene to yield butadiene.

Table 1.3.1 shows a comparison of three butadiene production processes: steam cracking, oxidative dehydrogenation and catalytic dehydrogenation.

Table 1.3.1. Comparison of butadiene production processes

Comparison Parameters	**Steam Cracking**	**Oxidative Dehydrogenation**	**Catalytic Dehydrogenation**
Primary feedstock	Paraffinic hydrocarbons	n-butane	n-butane, n-butene
Main products	Ethylene, butadiene	Butadiene	Butadiene
Catalysts	None	Metal oxides (e.g. Mo-V-MgO, Fe_2O_3/Al_2O_3, Fe_2O_3/SiO_2,) [13, 16]	Platinum/Alumina, Chromium/Alumina based catalysts [14, 15]
Energy consumption	**High**, since energy intensive process (exothermic reaction) [17]	**Low**, since exothermic reaction [13]	**Medium**, since endothermic reaction [15]

Temperature	790–830°C [1]	500-620°C [15]	575-625°C [18]
Environmental impact	**High,** - Different emissions from combustion of carbon (CO_2, CO, CH_4, N_2O, NO_2, SO_2, etc.) [17] - High energy consumption [17]	**Low**, - ODH operates at lower temperatures [13, 19] - Relatively high selectivity - Relatively lower energy consumption	**Medium**, - Coke depositions due to quick deactivation of catalysts [13] - Operates at comparatively lower temperatures - Relatively high selectivity
Butadiene yield	About **1–15 wt.% C4** (mainly butadiene and butenes) [12]	About **23-83%** [20]	About **34-82%** [21]
Production cost	**High**, - Complicated equipment setup [18] - Need of by-product management [18] - High energy requirements [17] - Low selectivity - Large scale of production	**Low**, - Comparatively lower cost of raw materials [19] - Lower energy requirements [13] - No need for external hydrogen: directly oxidizes hydrocarbons	**Medium**, - Lower cost of raw materials [22] - High cost of catalysts [23] - Relatively medium energy requirements [15]

Steam cracking consumes a lot of energy and has a significant impact on the environment, allowing the production of ethylene and butadiene. Whereas, oxidative dehydrogenation results in low butadiene yield. Therefore, catalytic dehydrogenation was chosen as the process method.

1.4. Chemical Reaction Analysis

Figure 1.4.1. illustrates the key reactions implied in the manufacturing of butadiene by butane. The mechanism of reactions is dehydrogenation. The process of production of butadiene from n-butane is carried via 2 main reactions:

(1) Dehydrogenation of n-butane to 1-butene and 2-butene
(2) Further dehydrogenation of 1-butene to 1,3-butadiene

Studies and identification of the reaction intermediates suggest that n-butane first undergoes dehydrogenation primarily to 1-butene. 1-Butene then undergoes secondary dehydrogenation to produce 1,3-BD [24]. Additional reactions include polymerization of 1-butene to trans-2-butene and cis-2-butene [20], and formation of shorter hydrocarbon chains such as ethane and propane as a result of cracking [25].

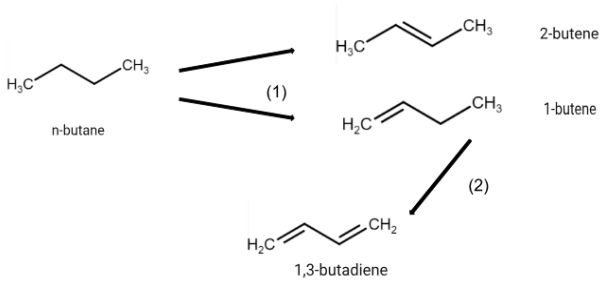

Figure 1.4.1. 1,3-butadiene formation reaction sequence

The butane dehydrogenation process is a catalytic reaction, which means the presence of a catalyst is required. The mechanism of the n-butane dehydrogenation into 1-butene and 1,3-butadiene, including the catalyst, is illustrated in Figure 1.4.2. The mechanism includes a combination of two catalysts (one catalyst supported by another catalyst) this is done for economic reasons. The butane molecule adsorbs on the active site of the catalyst by weakly binding [26]. This leads to an intermediate stage, where the hydrogen atom is abstracted and the butyl part is connected to the active site [26]. When abstraction of a second hydrogen atom occurs 1-butene is produced, because it is favored kinetically [26]. 1-Butene undergoes further dehydrogenation to 1,3-butadiene and eventually desorbs from the catalyst surface with another hydrogen molecule [26].

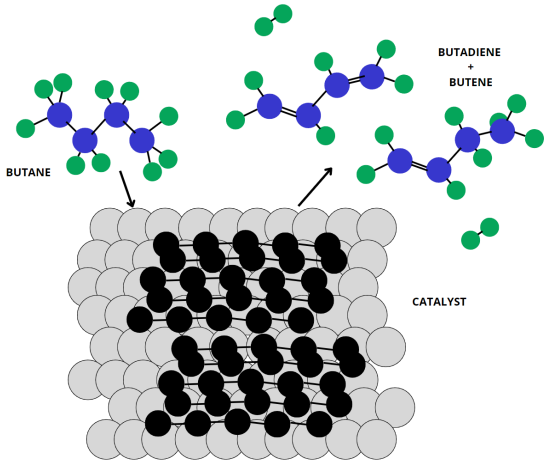

Figure 1.4.2. Mechanism of butane dehydrogenation

1.5. Introduction to the major unit operations in the process

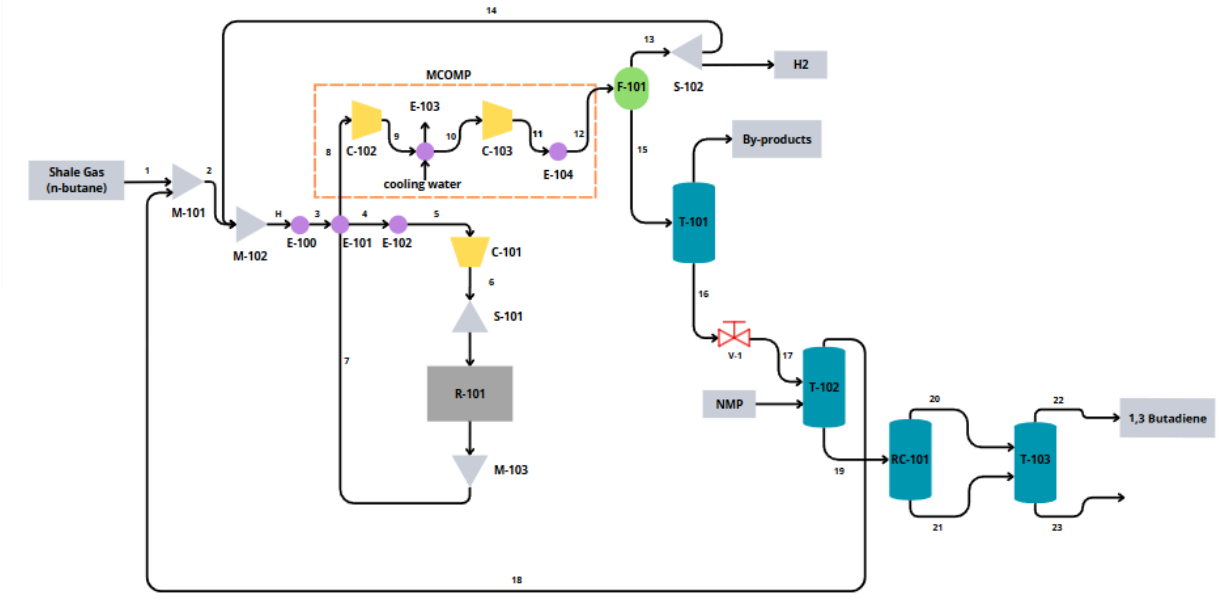

Figure 1.5.1. Process Flow Diagram

The process will include a series of key unit operations, such as mixing, heating, reaction, compression, separation, and distillation. Each step is designed to optimize the yield of 1,3-butadiene while efficiently managing by-products and recycling streams. The operation scheme is built and described based on the benchmark process provided by Brencio [25].

Feed

First of all, the feed is supplied along with recycled n-butane, in order to raise the total concentration of n-butane in the feedstock and guarantee a consistent supply to the reaction section. Recycled hydrogen is then added to this combination, serving as a diluent. The production of ethylene, ethane, methane, and propylene is regulated by the hydrogen by lowering the partial pressure of n-butane in the reactor. Maintaining the reactions' selectivity towards the intended product, 1,3-butadiene, depends on this step.

Preheating

Using the reactor's hot effluent gases, the preheating stage raises the mixed stream's temperature to optimal (≈ 623°C) for the dehydrogenation reaction. By recovering heat from the reactor effluent and minimizing the requirement for external heating sources, the heat exchange process saves energy.

Reaction zone

The preheated feed enters a series of four parallel fixed-bed reactors operating at high temperature (623°C) and pressure of 6 bars. This zone is where n-butane dehydrogenates to produce 1,3-butadiene and several byproducts such as propylene and ethylene. The catalyst has a lot of surface area thanks to the packed-bed arrangement, which encourages effective reaction kinetics. Coke is another product of the reaction that accumulates on the catalyst surface and must be periodically removed.

Effluent cooling and compressor (MCOMP)

The reactor's 1,3-butadiene-rich effluent gas is compressed in a multistage compressor with interstage cooling after being chilled initially. The temperature drops as a result of compression, which also raises pressure. The next flash separation, in which hydrogen is extracted from the hydrocarbon mixture, will be satisfied by maintaining the current conditions. In order to distribute the energy load evenly across the units rather than just on one compressor, the multistage compressor system is employed. Such a method is more effective since it lessens wear and risks related to high temperatures because the temperature of gas increases with pressure.

Hydrogen separation

Because of the variations in their boiling temperatures, the hydrogen and the heavier hydrocarbons are separated in the flash drum. In order to maintain the necessary H_2/n-butane ratio, the hydrogen-rich vapor stream is divided into two parts. The first half is recycled back to the reactor inlet. The remaining hydrogen will be burned to produce energy used in the plant.

Depropanization

The depropanizer column separates the lighter hydrocarbons (C3 and lighter) from the C4+ components. The lighter components are collected at the top and are usually considered undesirable by-products. They are sent to a furnace for disposal, where they generate a hot exhaust gas stream used to preheat air for the catalyst regeneration process. The C4+ mixture (rich in n-butane and 1,3-butadiene) collected at the bottom is then sent for further processing.

Extractive Distillation

The C4+ mixture is fed into the first extractive distillation column, where 1,3-butadiene will selectively be separated from other C4 components, such as unreacted n-butane. The overhead stream, containing mostly n-butane, is recycled back to the feed inlet. The bottom product, containing 1,3-butadiene and some heavier C4+ components, is sent to the rectifier for further purification.

Pressure reduction

The pressure of the C4+ mixture is reduced using a valve. This pressure reduction prepares the stream for the subsequent extractive distillation steps, where lower pressures facilitate the separation of 1,3-butadiene from other C4 components.

Final rectification

In the rectifier column, the remaining 1,3-butadiene is separated from the solvent added during extractive distillation, achieving the desired high purity. The purified butadiene is collected at the top of the column, while the bottom stream is recycled back to the extractive distillation column for reuse. The heavier C4+ and C5 components are removed from the bottom of the rectifier as waste or lower-value by-products.

Chapter 2. Process Summary

2.1. Catalytic dehydrogenation overview

As it was stated before, the main mechanism of our plant was selected to be a catalytic dehydrogenation process. According to the American Chemistry Council, the catalytic dehydrogenation of n-butane involves two main stages: first, converting n-butane to n-butenes, and then further transforming it into butadiene. Both stages are endothermic reactions [27].

A Houdry Catadiene process (Figure 2.1.1) is a primary process in the catalytic dehydrogenation of n-butane, where n-butane is dehydrogenated to n-butenes and then to butadiene over platinum/alumina or chromium/alumina catalysts occurs [27, 28]. The reactors typically operate at conditions as: absolute pressure of 0.14 bar - 0.24 bar and temperatures of 575°C-625°C [28]. For continuous operation, three or more reactors are used: one is on-line, another is being regenerated, and a third is purged in preparation for regeneration [27].

The temperature of the catalyst bed decreases during the endothermic reaction and a certain amount of coke is formed at the end. Using preheated air, the coke is burned during the regeneration process, providing nearly all the heat needed to reach the target reaction temperature. The output from the reactor is sent to a quench tower for cooling. The resulting stream is compressed before entering the absorber/stripper system, which produces C4 concentrate. The concentrate is then processed in a butadiene extraction system to make high-purity butadiene [27]. One of the advantages of catalytic dehydrogenation over oxidative dehydrogenation is that free hydrogen is formed in substantial amounts and can be sold for additional profit [14].

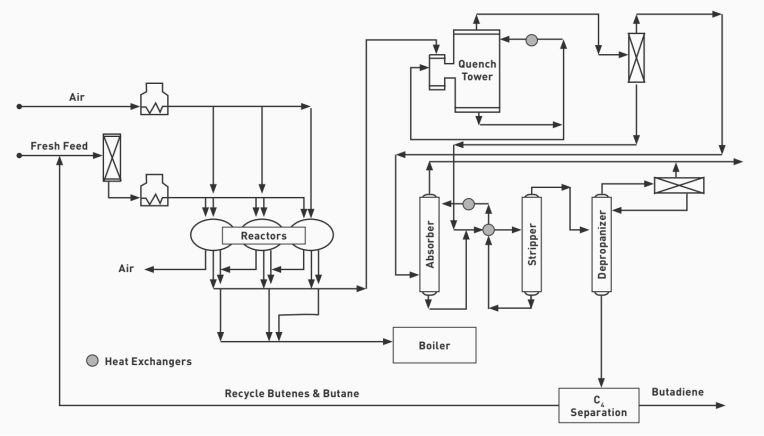

Figure 2.1.1. Catadiene Process [27].

2.2 Selected Chemical reaction

Catalytic dehydrogenation reaction in our process was selected based on the catalyst proposed by Tanimu [29]. Reaction mechanism with Ni−Fe−Co−Bi−O supported on γ-Al_2O_3 catalyst consists of 2–step dehydrogenation as the main reaction and cracking of butene intermediates as a side reaction (see Figure 2.2).

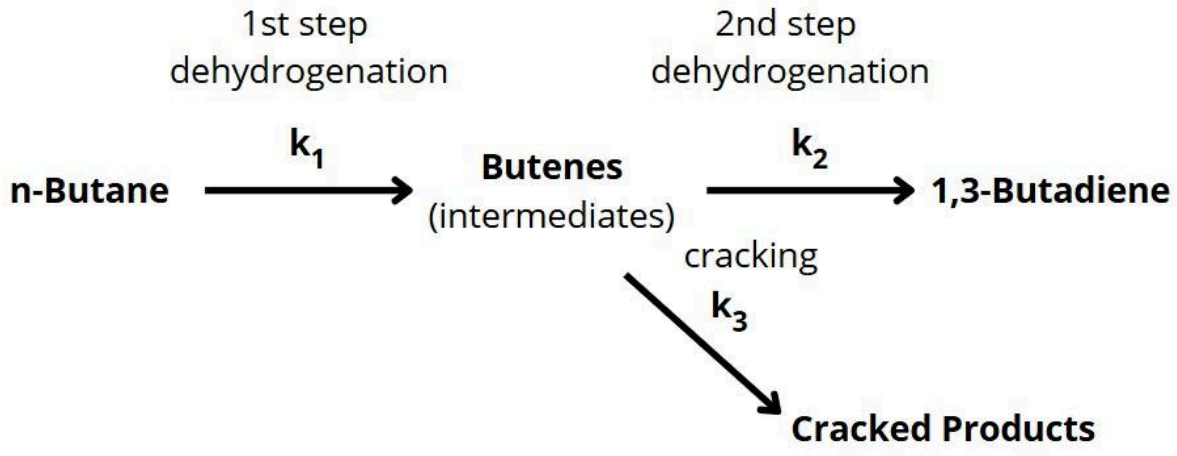

Figure 2.2.1 CDH of *n*-Butane to Butadiene and Cracked Products through Butene Intermediates

Table 2.2. Reactions

Reaction		Main product(s)	Type
R1	$C4H10 \rightarrow C4H8 + H2$	Butenes	Main
R2	$C4H8 \rightarrow C4H6 + H2$	1,3 - Butadiene	Main
R3	$C4H8 \rightarrow cracking\ products$	Ethylene and Propylene	Side

Rate expression for each reaction was based on the concentration of reactants in each reaction. R1 is shown to follow elementary rate law, while R2 and R3 demonstrate the dependence of reaction rate on the concentration of 1-Butene raised to the power of 0.5. Equations are presented as:

$$-r_{nB} = -\frac{dy_{nB}}{d\tau} = k_{12}C_{nB} * MW_{nB}$$

$$r_{Bu} = \frac{dy_{Bu}}{d\tau} = (k_{12}C_{nB} - k_{23}C_{Bu}^{0.5} - k_{24}C_{Bu}^{0.5}) * MW_{Bu}$$

$$r_{Bd} = \frac{dy_{nB}}{d\tau} = k_{23}C_{Bu}^{0.5} * MW_{Bd}$$

$$r_{Cr} = \frac{dy_{Cr}}{d\tau} = k_{24} C_{Bu}^{0.5} * MW_{Cr}$$

where,

r_{nB} - rate of disappearance of n-butane

r_{Bu} - rate of appearance and disappearance of the butene intermediate

r_{Bd} - rates of appearance of 1,3 - BD

r_{Cr} - rates of appearance of cracking products

k_j - rate constant for reaction j

y_i - mass fraction of species i

τ - contact time, ratio of weight of catalyst to butane mass flow rate

It can be seen that the catalyst decay was not considered, as well as concentration of oxygen, which makes the provided model suitable for our process.

Rate constants were calculated using Arrhenius equation:

$$k_j = k_j^o exp[\frac{-E_j}{RT}]$$

where,

k_j^o - pre-exponential factor, mol/$g_{cat.}$ min

R - universal gas constant, J/K · mol

T - temperature, K

E_j - activation energy, J/mol

Most importantly, the kinetic model of authors was built based on five key assumptions. It was assumed that mass transfer limitations were negligible, allowing for the focus on reaction kinetics rather than diffusion effects. Catalyst deactivation was not considered, implying that the catalyst remained fully active throughout the process. The model also assumed an excess of molecular oxygen, resulting in negligible butane conversion due to the abundant oxygen supply. The effectiveness factor was set to unity, indicating that the catalyst particles were fully effective in facilitating the reaction. Additionally, only catalytic reactions were considered, excluding any non-catalytic pathways.

Based on calculations of justification of kinetics it was concluded that reasonable extrapolations up to processes' industrial operating conditions can be made. To do so, the temperature of the inlet stream was changed to 625°C and another sensitivity analysis was performed which identified the dependance of conversion on mass of a catalyst. Aspen demonstrated a good conversion at atmospheric pressure but with high catalyst load (Figure 2.2.2). In further analysis the pressure will be increased to reduce the needed amount of catalyst and sustain a reasonable conversion.

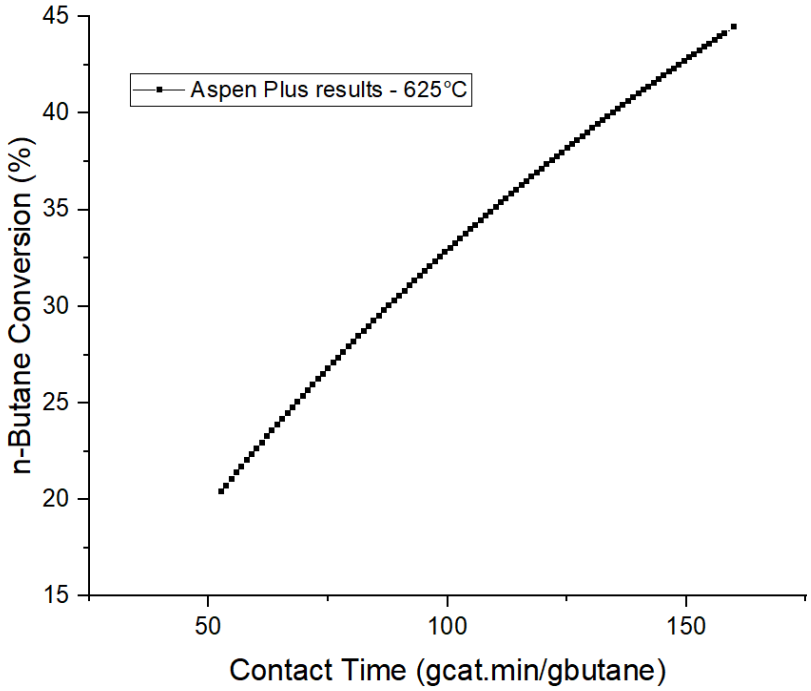

Figure 2.2.2. n-Butane conversion (%)

Thermodynamic Model

In order to simulate the whole process in Aspen Plus v14, Peng-Robinson model was chosen. The model accurately explains the behavior of the gas mixture in the reactor and compressor, which is justified by little deviation with experimental data taken from the literature.

2.3 Process summary

2.3.1 Preheating

The mixture is preheated using 2 heat exchangers and a furnace to reach the reactor operating temperature. The composition of the stream remains unchanged and only heated. The operating conditions of the units are presented in Table 2.3.1.

Table 2.3.1. Inlet and outlet parameters in preheating zone

Preheating	Pressure, bar				Temperature, °C			
	Inlet		Outlet		Inlet		Outlet	
E-100	1		1		-10.54		85.43	
E-101	Hot fluid	Cold fluid	Hot fluid	Cold fluid	Hot fluid	Cold fluid	Hot fluid	Cold fluid
	4.55	1	4.5	0.89	490.88	85.43	354.27	268.87
E-102	1		1		268.87		623	

2.3.2 Reaction Zone

Reactor zone contains a C-101 compressor unit, followed by 4 parallel fixed bed reactors. The main purpose of the compressor is to increase the inlet pressure of feed and compensate for the catalyst load, while maintaining the similar conversion. Compressor increases the pressure of gaseous feed from 1 bar to 6 bar, simultaneously increasing its temperature from 511°C to operating 623°C. Reactor converts butane and butene in the feed to the butadiene product. It works as an adiabatic unit making it lose heat as a result of endothermic reaction, and subsequently cooling to 491°C and dropping pressure to 4.55 bar. Inlet/outlet parameters and flow rates of reaction zone units can be seen in tables 2.3.2 and 2.3.3. The resultant product stream is sent to MCOMP unit for further processing.

Table 2.3.2. Reactor zone units inlet and outlet parameters

Reaction zone units	Pressure, bar		Temperature, °C	
	Inlet	Outlet	Inlet	Outlet
C-101	1	6	511.00	622.80
R-101	6	4.55	622.80	490.89

Table 2.3.3. C4 flow rates in reactor

R-101	Inlet	Outlet
n-Butane flow rate (kmol/h)	722.66	435.67
1-Butene flow rate (kmol/h)	1,146.84	1,186.74
Butadiene flow rate (kmol/h)	814.36	1,060.53

2.3.3 Multistage compressor system (MCOMP)

After the reaction zone, stream 7 is directed into a multistage compressor (MCOMP) and exits as stream 12. The system consists of two compressors (C-102, C-103) and two heat exchangers (E-103, E-104). The gas is compressed in a multistage compressor with interstage cooling. During compression, the temperature decreases from 320°C to 14 °C while the pressure increases from 4.5 to 7 bar. MCOMP allows this process to be carried out more gradually, ensuring effective control of pressure and temperature with fewer stages.

Table 2.3.4. Inlet and outlet parameters of Multistage Compressor (MCOMP)

MCOMP Equipment	Pressure, bar		Temperature, °C	
	Inlet	Outlet	Inlet	Outlet
C-102	4.55	9.53	318.15	360.08
E-103	9.53	9.53	360.08	166.04
C-103	9.53	20.2	166.04	206.22
E-104	20.2	20.2	206.22	14

2.3.4 Hydrogen Removal

Hydrogen is removed from the process stream using the F-101 flash drum unit. Operating conditions are 14°C and 20.2 bar. The top stream of F-101 contains almost all hydrogen from the feed and bottom stream consists of around 0.97 of all C4 hydrocarbons from the feed. Part of the top stream is sent to recycle back to the system, while the liquid bottom stream is sent to the depropanizer unit (see Table 2.3.5).

Table 2.3.5. Split fractions of F-101 units.

Component	Split fractions	
	Top stream	Bottom stream
n-Butane	0.024	0.976
1-Butene	0.030	0.970
Butadiene	0.038	0.962
Hydrogen	0.999	0.001

2.3.5 Depropanizer column

Hydrogen and light hydrocarbon gases (ethylene, propylene, propane) are separated and removed from heavier hydrocarbons present in the liquid stream exiting the F-101 flash drum. This step is needed to remove unnecessary gases as an overhead product and prepare the bottom stream for further separation. The column with 25 stages, condenser temperature of 2.8 °C, distillate rate of 15 kmol/h, reflux ratio of 16 ensure proper separation efficiently recovers propane in the top stream, which can be burnt later, while heavier hydrocarbons exit through the bottom. This separation step is critical to ensure product purity requirements are met and to optimize downstream processing units (see Table 2.3.6 for composition details).

Mole Flows (kmol/hour)	15	By-products	16	Recovery of feed in By-products	Recovery of feed in stream 16
Temperature, °C	14	92.3	103.831		
Pressure, bar	20.2	20.2	20.2		
Vapor fraction [-]	0	1	0		
n-Butane	425.10	1.48	423.62	3.49E-03	9.97E-01
1-Butene	1,151.5	3.56	1,147.93	3.09E-03	9.97E-01
1,3-Butadiene	1,019.8	4.90	1,014.88	4.80E-03	9.95E-01
Ethylene	0.31	0.31	0.00	1.00	2.70E-09
Propylene	0.95	0.86	0.08	9.11E-01	8.86E-02
Propane	1.93	1.87	0.06	9.70E-01	2.99E-02
H2	0.90	0.90	0.00	1.00	0.00
NMP	1.09	0.00	1.09	9.49E-10	1.00
H2O	272.26	1.10	271.16	4.06E-03	9.96E-01
Total	2,873.82	14.99	2,858.82	5.22E-03	9.95E-01

Table 2.3.6. Composition of streams and feed recoveries in product stream of T-101 unit.

2.3.6 Purification

Depropanized stream together with the NMP solvent stream is fed into the first extractive distillation column T-102, operating at a pressure of 5 bar and within a temperature range 31.27°C - 104.28°C. The top products are returned to the main feed, while the bottom stream 17 is directed to the rectifier (RC-101), where butadiene, butane and butene mixture (stream 18) is separated from the NMP solvent (stream 19) at 5 bar and in temperature interval 104.28°C - 136.35 °C. Next, to reach a final purity of 99.5 wt% butadiene, these streams enter the second extractive distillation column T-103. This column operates at the same pressure of 5 bar and a temperature range 36.40°C - 136.79°C, producing butadiene product stream at the top (99.5 wt% purity) and NMP stream at the bottom.

Table 2.3.7. Inlet and outlet parameters of Distillation columns and Rectification column

Equipment	Pressure, bar		Temperature, °C	
	Top	Bottom	Top	Bottom
T-102	5	5	31.27	104.28
RC-101	5	5	104.28	136.35
T-103	5	5	36.40	136.79

2.4 Overall material balance

The material balance is given in Table 2.4. Process flow diagram can be seen in figure 1.5.1.

Table 2.4.1. Material balance for the process

Mass Flows (kg/hour)	1	2	H	3	4	5	6	7	8
n-butane (C4H10)	17,455	41,781	42,002	42,002	42,002	42,002	42,002	25,321	25,321
Butene (C4H8)	0	63,634	64,345	64,345	64,345	64,345	64,345	66,583	66,583
Butadiene (C4H6)	0	43,257	44,051	44,051	44,051	44,051	44,051	57,367	57,367
Ethylene	0	0	2	2	2	2	2	16	16
Propylene	0	4	5	5	5	5	5	45	45
Propane (C3H8)	88	90	93	93	93	93	93	93	93
H2	0	0	604	604	604	604	604	1678	1678
NMP	0	108	108	108	108	108	108	108	108
H2O	0	4,907	4,908	4,908	4,908	4,908	4,908	4,908	4,908
Total	17,543	153,781	156,118	156,118	156,118	156,118	156,118	156,118	156,118

Table 2.4.2. Material balance for the process

Mass Flows (kg/hour)	9	10	11	12	13	14	H2	15	Byprod
n-butane (C4H10)	25,321	25,321	25,321	25,321	612	220	392	24,708	86
Butene	66,583	66,583	66,583	66,583	1,975	711	1,264	64,607	200

(C4H8)									
Butadiene (C4H6)	57,367	57,367	57,367	57,367	2,205	794	1,411	55,161	265
Ethylene	16	16	16	16	7	2	4	9	9
Propylene	45	45	45	45	5	2	3	40	36
Propane (C3H8)	93	93	93	93	8	3	5	85	82
H2	1,678	1,678	1,678	1,678	1,677	604	1,073	2	2
NMP	108	108	108	108	0	0	0	108	0
H2O	4,908	4,908	4,908	4,908	3	1	2	4,905	20
Total	156,118	156,118	156,118	156,118	6,492	2,337	4,155	149,626	700

Table 2.4.3. Material balance for the process

Mass Flows (kg/hour)	16	17	NMP	18	19	20	21	22	23
n-butane (C4H10)	24,622	24,622	0	24,326	296	296	0	0	296
Butene (C4H8)	64,408	64,408	0	63,634	774	774	0	0	774
Butadiene (C4H6)	54,896	54,896	0	43,257	11,639	9,471	2,168	11,356	283
Ethylene	0	0	0	0	0	0	0	0	0
Propylene	4	4	0	4	0	0	0	0	0
Propane (C3H8)	3	3	0	3	0	0	0	0	0
H2	0	0	0	0	0	0	0	0	0
NMP	108	108	1,131,859	108	1,131,859	0	1,131,859	0	1,131,859
H2O	4,885	4,885	282,965	4,907	282,943	168	282,775	55	282,775
Total	148,925	148,925	1,414,824	136,238	1,427,511	10,709	1,416,803	11,411	1,418,156

Chapter 3. Major Equipment Design

3.1 Heat Exchanger E-101 Design

3.1.1 Heat Exchanger E-101 description

Heat exchanger, E-101, is a system of 4 parallel heat exchangers operating at the same conditions. Each E-101 is a shell and tube heat exchanger with one shell pass and one tube pass. The reactor outlet at the temperature of 490.88°C is utilized to heat the reactor inlet at the temperature of 85.43°C. Both streams are a vapor mixture of hydrocarbons with the same components and mass flow rate but different mole fractions. The components of the streams are butane, butene, butadiene, propane, propylene, ethylene, hydrogen, water, and NMP. The reactor outlet as hot fluid is placed on the tube side due to its high pressure (4.55 bar) for safety reasons and better heat transfer efficiency. The reactor inlet as cold fluid at 1 bar is placed on the shell side of the heat exchanger.

3.1.2 Heat Exchanger E-101 Design Specifications

Table 3.1.1 summarizes the heat exchanger design specifications. Parameters for tube side design were taken in accordance with the Tubular Exchanger Manufacturers Association (TEMA) specifications. Other parameters were calculated according to the correlations given in the Chemical Engineering Design book by Towler and Sinnott [30]. The detailed calculations and applied equations are given in ESI, Appendix B.1. The fluid properties at mean temperatures of the streams were chosen for calculations and were evaluated using Aspen Plus mixture analysis (Appendix B.1. Table B.1.3 and B.1.4).

In the calculations, initially the overall heat transfer coefficient was assumed to be 60 $W/m^2°C$, which is recommended for organic vapors. The mass flow rate and heat duty were divided equally to 4 parallel heat exchangers in order to keep shell diameter acceptable by the TEMA standards (Appendix B.1. Table B.1.2).

The velocity on the tube side was kept in the range 10-15 m/s as it is suggested for vapors at this pressure (Appendix B.1. Table B.1.5). Parameters such as tube outside diameter, inside diameter, thickness were chosen according to the TEMA (Appendix B.1. Table B.1.6). Whereas, the length and number of tubes were suggested by Aspen Plus simulation (Appendix B.1. Table B.1.6). Number of tube passes equals 1, this was used in order to avoid temperature crossover, which was indicated in the Aspen simulation at 2 and more tube passes.

In the shell side design, the triangular pitch was chosen for a more compact design and based on the high Re numbers of the fluids. Moreover, the pressure drop on both sides using this configuration was acceptable, therefore it was not changed to the rectangular pitch. The shell

diameter (1.5m) was suggested by the Aspen simulation, which is accepted by the standards (< 2m).

Heat transfer coefficient from Aspen (158.4 W/m^2°C) and calculations (149.5 W/m^2°C) have little deviation and show good efficiency of the heat exchanger. It exceeds the initially assumed value. The stainless steel SS321 was selected as the construction material with thermal conductivity 21.4 W/m°C at 500°C.

The pressure drops on both sides were calculated and found by the Aspen Plus simulation. They have little difference and are acceptable by both the TEMA standards and allowable pressure drop by the Aspen Plus (Appendix B.1, Table B.1.9).

It should be noted that the little deviations between hand calculations and Aspen Plus values are associated with the fact that Aspen uses higher correction factor (0.98) resulting in lower minimum required area. This was corrected further by overdesigning the unit by 20%.

Table 3.1.1. Heat exchanger E-101 Design Specifications

Heat exchanger, E-101	Type: BEM, 1-1 shell and tube, horizontal			
Performance				
Fluid location	Tube Side		Shell Side	
Fluid type	Hot fluid		Cold fluid	
Fluid	Reactor outlet		Reactor inlet	
Mass flow rate, kg/s	43.364		43.364	
Stream	In Stream	Out Stream	In Stream	Out Stream
T, °C	490.88	354.27	85.43	268.87
P, bar	4.55	4.5	1	0.89
Pressure drop, bar	0.0487		0.1109	
Velocity, m/s	12.3		26.15	
Heat Exchanged, kW	17,677.6			
MTD (corrected), °C	241.37			

Heat transfer rate, $W/m^2°C$	Service	148.6
	Dirty	148.5
	Clean	158.4
Design Specifications		
Area total required, m^2	493	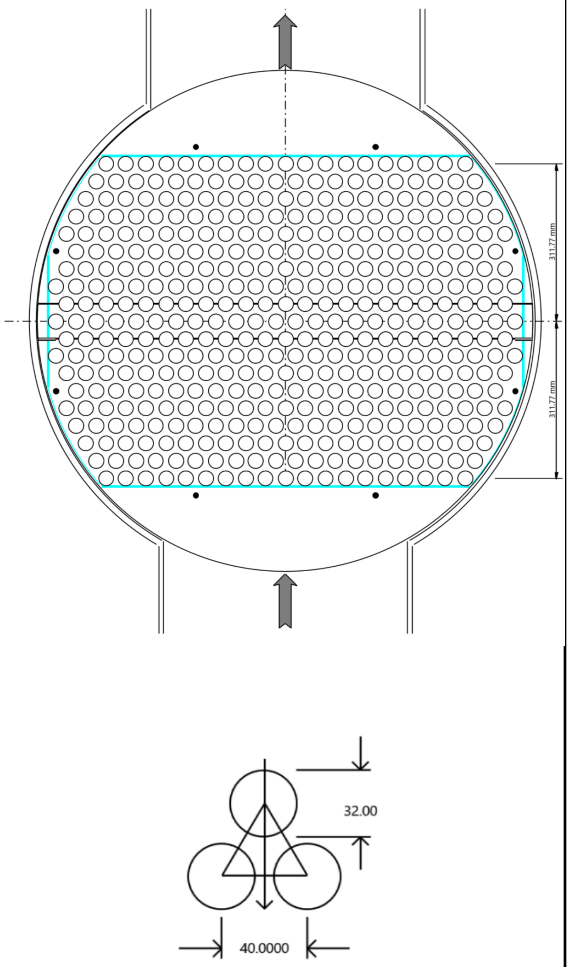
Area total overdesigned, m^2	591.6	
Area, m^2	123.2	
Area overdesigned, m^2	147.84	
N_{tubes}	418	
$N_{tube\ passes}$	1	
Tube OD, m	0.032	
Tube thickness, m	0.0017	
Tube length, m	3.15	
Pitch, m	0.04	
Pitch type	Triangular	
Construction material	Stainless steel 321	
Shell ID, m	1.5	
Shell OD, m	1.516	
Baffle type	Single segmental Horizontal cut (47.69%)	
Baffle spacing, m	0.825	

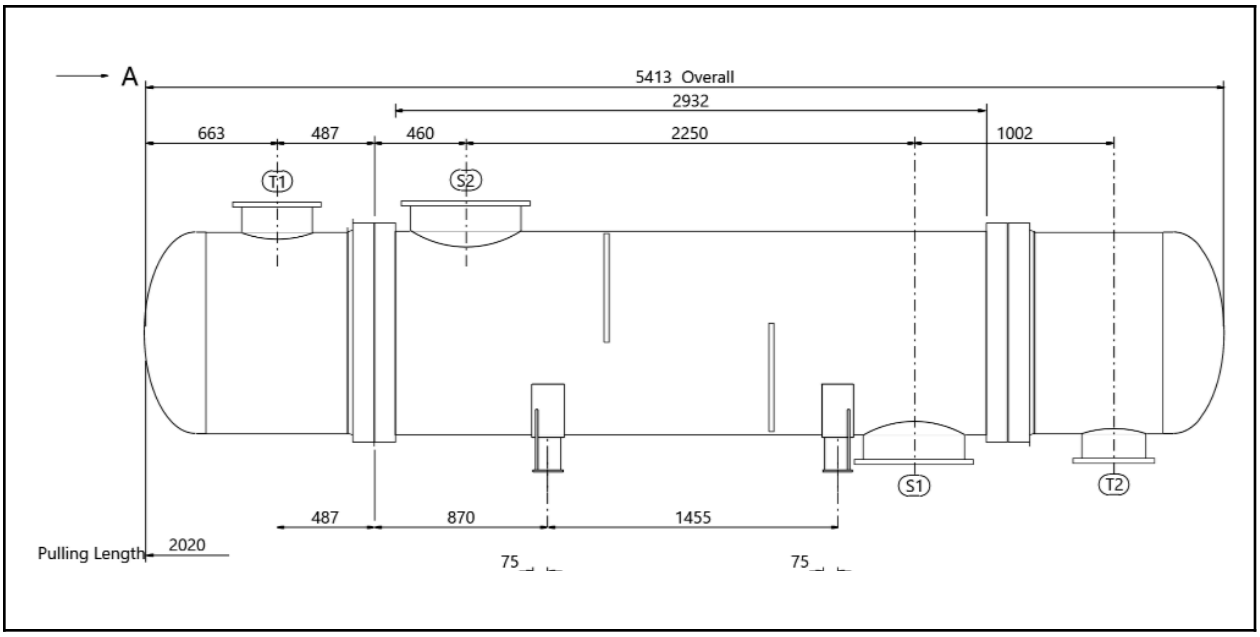

3.1.3 Material selection

Stainless steel 321 was chosen as the construction material due to high-temperature resistance and proneness to carbide precipitation (321 SS datasheet is given in ESI). The temperature that the material should withstand is 500°C. The thermal conductivity for operating temperature is given as 21.4 W/m°C. Additionally, the streams on the tube and shell sides contain water and hydrocarbons. SS 321 has good resistance to the corrosion associated with water and carbide precipitation.

3.1.4 Cost estimation

The cost for one heat exchanger was estimated based on Chapter 7 from the Chemical Engineering Design book by G. Towler [31]. The calculations include factors for SS 321, overdesigned required area. Since the production was placed in China the location factor (0.61) and distance to the plant (Taraz city) as additional 20% were considered (Appendix B.1, Table B.1.10). The cost for one heat exchanger was estimated as 204,195 USD and 248,419 USD by two calculation methods (Appendix B.1. Table B.1.11). Overall, four parallel heat exchangers will cost 816,780 USD.

3.2 Reactor R-101 Design

3.2.1 Initial Input

The reactor design was primarily based on the kinetics justified in the previous report, and the reactor type will remain an adiabatic fixed-bed reactor. Our utilized catalyst is a (Ni,Fe,Co)-Bi-O/gamma-Al2O3 alloy with the following composition: 10 wt% Nickel, 5 wt%

Iron, 5 wt% Cobalt, 30 wt% Bismuth, and 50 wt% gamma-Al2O3. The density of particles was estimated to be 5,389 kg/m3 using the density formula for metal alloys (See Appendix B.2), and particles were assumed to be perfect spheres with a 3 mm diameter. Literature reports that the bed voidage of 0.38 is obtainable with perfectly sphered particles, so the bed voidage of our designed reactor was taken to be 0.4. To reduce the load per reactor, it was decided to divide the feed into 4 parallel reactors, which also allows lower pressure drop and better operational control.

Reaction kinetics were based on a paper published by Tanimu [29]. The selected catalyst is reported to have the power-law based kinetics (see section 2.2). The following parameters were taken to be tested using Python and Aspen plus:

Table 3.2.1. Kinetic Parameters

Parameter	Units	Value
k_1^o	mol/$g_{cat.}$ min	0.857 ± 0.014
k_2^o		1.930 ± 0.089
k_3^o		0.198 ± 0.048
E_1	J/mol	34400 ± 2420
E_2		68800 ± 7570
E_3		88500 ± 9160

Validation graph is shown in Appendix B.2.

3.2.2 Reactor Sizing (Details in Appendix B.2)

According to Tanimu [29], the required mass of catalyst to mass of butane ratio should be 158.1 g_{cat}.min/g_{butane} to obtain the aimed 41.21% butane conversion. Taking into account the 43.36 kg/s mass feed, it was calculated that around 411 tons of catalyst would be required to achieve a favourable amount of production. Because this amount is too high, it was decided to find a way to maintain similar conversion at lower catalyst weight. The increase in operating pressure from 1 bar to 6 bars resulted in a modest decrease in conversion (39.72) followed by substantial reduction in the mass of the catalyst to 100 tons. The required volumes of catalyst and individual reactors were calculated as follows:

$$V_{catalyst} = m_{cat} / (\rho_{cat} * N) \quad (3.2.1)$$

$$V_{1.reactor} = V_{cat} / (1 - \varepsilon) + 20\% \quad (3.2.2)$$

where, V is volume in m^3, m is mass in kg, ρ is density in kg/m^3, and ε is dimensionless bed voidage. N is the number of reactors mentioned earlier. A 20% increase in reactor volume is taken as overdesign to account for kinetic uncertainty and ensure safety by avoiding the possible undersizing.

Equations (3.2.1) and (3.2.2) demonstrate that the required volume of catalyst per reactor is 4.64 m^3, and the volume of one reactor with overdesign is 9.28 m^3.

Once the volume is obtained, the next step is to calculate the length and diameter of the reactor. Calculations involved the sensitivity analysis in Aspen Plus to determine which length and diameter pairs bring about optimal pressure drop and feed velocity. It was found that a 1.5 m diameter and 5.22 m high reactor demonstrates a reasonable 1.45 bar pressure drop, along with 4 m/s of actual velocity in a reactor. Such configuration gives a residence time of 3 seconds, which ensures proper contact and conversion of butane.

3.2.3 Material Selection (Details in Appendix B.2)

Rough design conditions (6.2 bar, 650°C) force us to refuse simple materials such as carbon steel and select stronger alloys. Two reliable and widespread material types are Inconel and Stainless steel. The comparison was done between Inconel 625 (N06625) and Stainless steel 310S (S31008). Analysis revealed that N06625 is more suitable in our process than S31008 (see Appendix B.2, Material selection for detailed comparison). Wall thickness calculations were performed using the formula:

$$t = \frac{P*D}{2*(S*E*W+P*Y)} \quad (3.2.3)$$

where t is wall thickness (mm), P is design pressure (MPa), D is pipe outside diameter (mm), W is weld strength reduction factor, Y is coefficient of material used, and S is allowable stress (MPa). S, E, W, and Y variables were found from ASME Part D [32] specifications. Knowing that the needed inside diameter is 1.5 meters, it was possible to estimate that the needed minimum wall thickness is 5.23 mm. However, the closest ASME Standard is 9.53 mm for 1219 OD pipe. So, the value of this standard will be used for our reactor. This adjustment allows an increase in the corrosion allowance from 1.7 mm to 6 mm.

3.2.4 Pressure Drop (Details in Appendix B.2)

Primarily, pressure drop across the reactor was found using Aspen Plus and then was justified using hand calculations. The main equation for pressure drop is Ergun's equation, which is the empirical correlation for fixed bed reactors.

$$\frac{\Delta P_{drop}}{L} = \frac{180*\mu*(1-\varepsilon)^2*u}{d^2*\varepsilon^3} + \frac{1.75*\rho*(1-\varepsilon)*u^2}{d*\varepsilon^3} \quad (3.2.4)$$

where d is particle diameter (m), u is superficial velocity (m/s), L is reactor length (m), μ is fluid viscosity (Pa.s), and ΔP_{drop} is pressure drop (Pa). Calculations show 2.87 bar of pressure drop.

Besides pressure drop due to friction between particle and fluid, pressure increase due to gas expansion should be considered. It can be expressed as the ratio between outlet and inlet moles of gases:

$$\Delta P_{inc} = (n_{out}/n_{in} - 1) * P_{op} \quad (3.2.5)$$

where P_{op} is operating pressure, n_{out} and n_{in} are number of moles of gases at outlet and inlet, respectively, while ΔP_{inc} is pressure increase. Expansion seems to add 0.98 bar into the system, according to calculations. This results in 1.89 bar of total pressure drop, which closely aligns with the Aspen Results mentioned in the "Sizing" section, the difference being 18%.

3.2.5 Reactor Cost Estimation

Reactor cost estimation was based on Chapter 7 of the Chemical Engineering Design book by G. Towler [31]. As specific reactor cost estimations were not provided, it was decided to roughly calculate the cost using the constants for a vertical Pressure Vessel. The price of a pressure vessel is based on the mass of the shell, which in our case was calculated using the density of Inconel 625 (844 kg/m^3) and calculated shell volume with an inside diameter of 1.5 meters and wall thickness of 9.53 mm.

The cost curve correlations resulted in around 14.6 thousand USD for the reactor. Considering the Lang factor of 4 and the material coefficient for Inconel (1.7), this yielded 99.6 thousand USD. The alternative way of calculation, considering equation (7.12) of the chapter, resulted in a much lower 65.3 thousand USD.

To consider the location of our plant, the indigenous China values were used (0.61). An extra 20% was added as an effect of approximately 2000 miles between Taraz and China, resulting in an overall 0.732 location factor. Cost escalation was estimated in the CEPCI factor, which was 532.9 in the book as of January 2010 and rose to around 800 in June 2024. Accounting for those factors, our estimated cost of 1 reactor is between 71.8 and 109.5 thousand USD (± 30%).

Table 3.2.2. The cost estimates for individual reactor

Lang estimation	99,634	Location	72,932	Cost Escalation	109,487	USD
Formula (7.12)	65,348	Location	47,834	Cost Escalation	71,810	USD

3.2.6 Sensitivity tests.

Aspen was utilized to conduct sensitivity analysis to check the changes in conversion of n-butane in the reactor with 3 varying inputs: catalyst load, temperature and pressure.

Temperature tests were performed in the range of 600-650°C to account for 25°C change to operating temperature of the reactor. Figure 3.2.1 shows that the simulations show proper work of the reactor in sudden temperature rise or drop. It can be stated that the reactor will be able to withstand these changes, resulting in a conversion range of 0.38-0.43 . Similar test with pressure was done. The range was 5-7 bars. Figure 3.2.2 demonstrates the proper work of the reactor with conversion in range 0.34-0.45. Lastly, the catalyst load range of 85,000-110,000 kg was tested. Results reveal that conversion of n-Butane doesn't fall below 0.37, meaning a sufficient work of the reactor (see Figure 3.2.3).

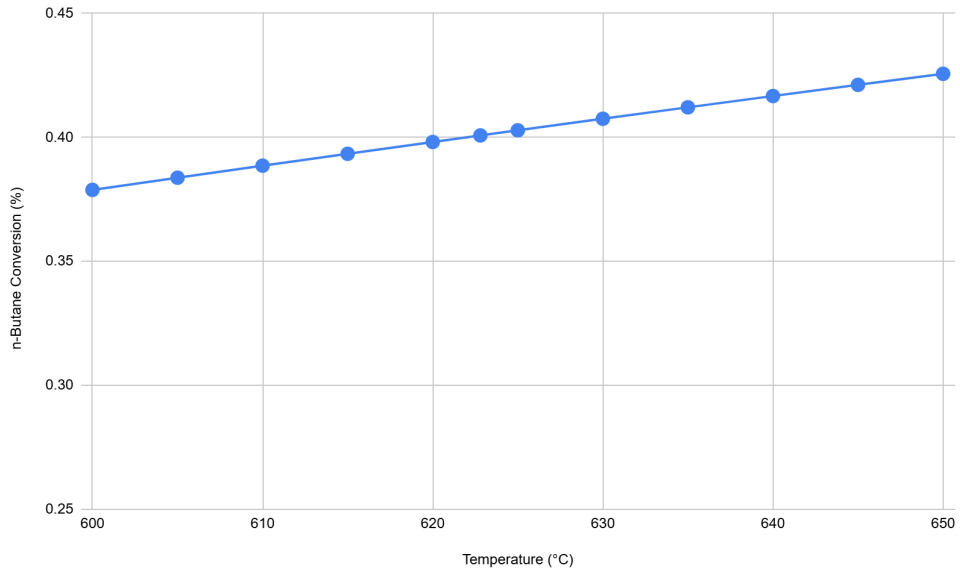

Figure 3.2.1. Temperature vs. n-Butane conversion graph

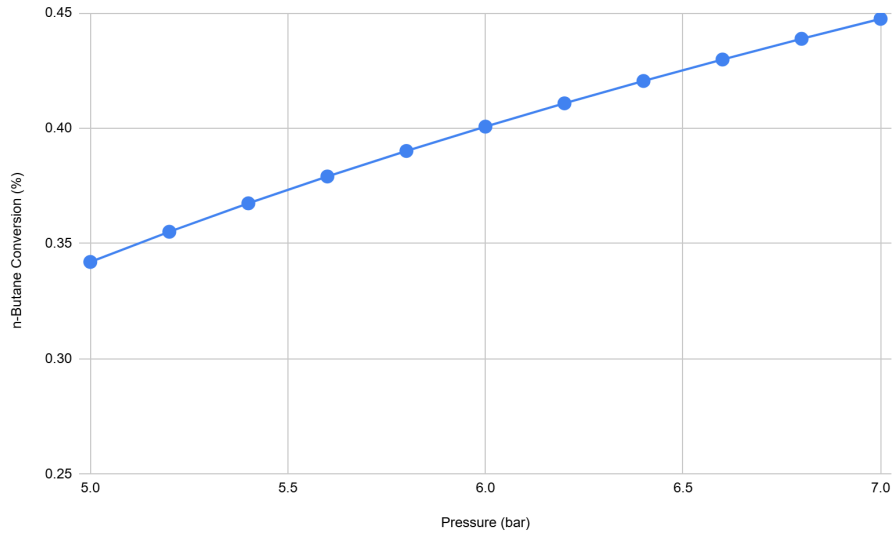

Figure 3.2.2. Pressure vs. n-Butane conversion graph

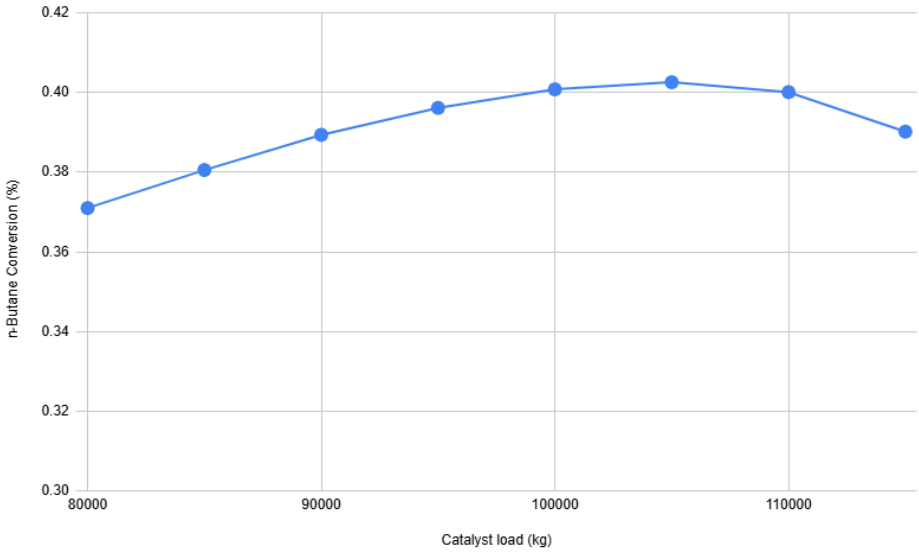

Figure 3.2.3. Catalyst load vs. n-Butane conversion graph

3.2.7 Reactor R-101 Design Specifications

Given all the above calculations, the specification sheet of the R-101 unit is given as follows:

Table 3.2.3. Reactor R-101 Design Specifications

Operating Conditions			
Temperature, °C		625	
Pressure, bar		6	
Catalyst		(Ni,Fe,Co)-Bi-O/γ-Al2O3	
Type and sizing			
Type of reactor	Fixed bed reactor, adiabatic	Outside diameter, m	1.52
Material	N06625	Wall thickness, mm	9.53
Number of reactors	4	Length, m	5.22

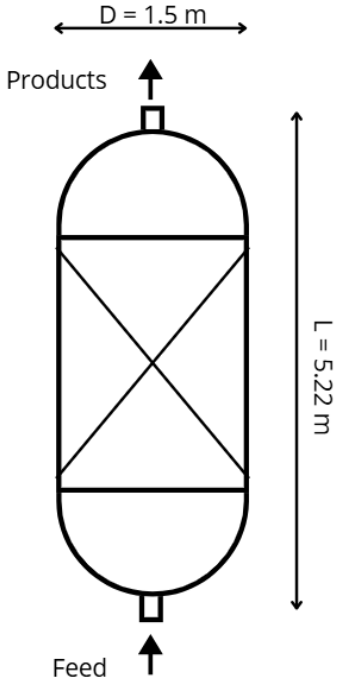

Diagram of R-101

3.3 Compressor C-102 design

3.3.1 Compressor type selection

The multistage compressor system (MCOMP) is designed to compress a gas stream (with a total mass flow rate of 156,109 kg/h), which contains n-butane, butene, butadiene, ethylene, propylene, propane, hydrogen, and water vapor. The initial pressure of the gas is 4.5 bar, and it must be increased to 20.2 bar across two compression stages, with intermediate cooling via heat exchangers to control temperature and improve efficiency (the reasoning behind selecting 20.2 bar as the final pressure is provided in the Appendix B.3, Operating discharge pressure of MCOMP). The choice of compressor must consider efficiency, reliability, and operational costs. Given the process conditions, high flow rate, moderate-to-high pressure ratio, and the presence of a hydrocarbon gas mixture - a centrifugal compressor was determined to be the most suitable option:

- High flow rate capability: (~136.6 tons/hour) of gas, which is very high for industrial production [33].
- Moderate-to-high pressure ratio: e.g. horizontally split compressors (up to 100 bar) and radially split compressors (up to 1034 bar) both exceed the 20 bar discharge pressure in the process [34].

- High power capability: compressors operate across a wide power range, from 75 kW to over 97 MW, making them ideal for high-flow, high-pressure industrial applications [34].

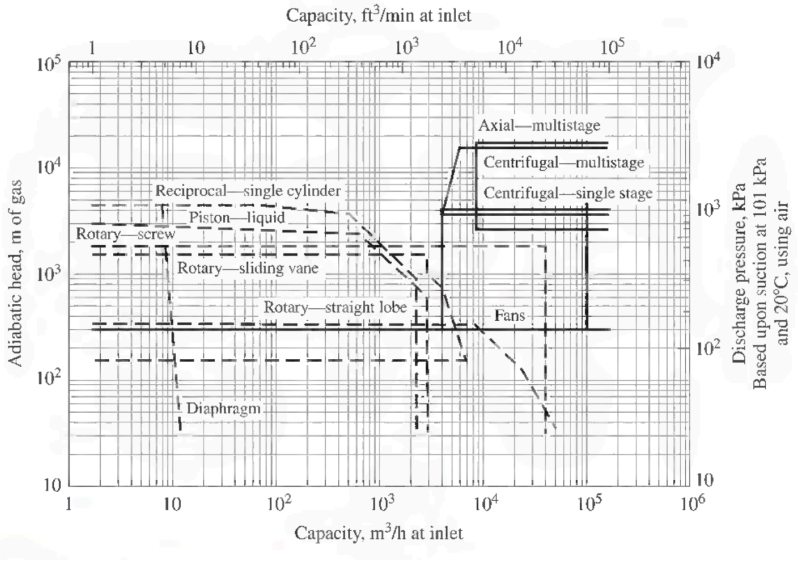

Figure 3.3.1. Compressor coverage chart based on the normal range of operation of commercially available types shown [35]

Additionally, according to Figure 3.3.1, in comparison with other types of compressors, the most appropriate compressor type for the process is a centrifugal compressor. The operational range of centrifugal compressors aligns well with our required head (10,000 m) and capacity (44,000 m³/h), ensuring efficient performance. As well, multistage centrifugal compressors are suitable for achieving the necessary pressure ratios while maintaining reliability and energy efficiency [35].

3.3.2 Design considerations for compressor C-102

The compressor design was developed using the approximate rating of centrifugal compressors outlined in *Ludwig's Applied Process Design for Chemical and Petrochemical Plants* by A. Kayode Coker [33] and *Process Centrifugal Compressors* by Klaus H. Lüdtke [36]. For this system, the first compressor is designed as a major unit, where pressure is increased from 4.5 bar to 20.2 bar. The type of horizontal split casing is chosen for the compressor (the reasoning is explained in Appendix B.3, Compressor characteristics and dimensions).

According to Table B.3.1 (Appendix B.3), the most suitable compressor frame for MCOMP system is 46M, as it closely matches the required specifications, providing the optimal balance of flow capacity, and pressure range. This compressor frame can effectively handle the required pressure increase from 4.5 bar to 20.2 bar (≈ 300 psig) while accommodating a gas flow rate of approximately ≈ 44,000 m3/h (26,000 CFM), ensuring reliable performance under the given operating conditions. The 46M frame is selected for the estimation of compressor C-102,

which is expected to operate in a polytropic approach, representing real-world conditions with efficiency of 80% and nominal rotational speed of 6,300 rpm (as indicated in the Appendix B.3, Table B.3.1).

This compressor delivers a calculated discharge temperature of 354℃, with the polytropic head of 98 kJ/kg. The associated power output is 5,437 kW, while the brake horsepower is estimated as 7,291 bhp, accounting for 2.5% mechanical losses (Appendix B.3, Table B.3.2), showing close aligning with the Aspen Plus simulation results. For compressor C-102, evaluations indicate that five impellers per rotor are most suitable, with each impeller consisting of 18 blades. The type of impellers is a 3D-shrouded type arranged in-line and equipped with a vaneless diffuser (the reasoning is explained in Appendix B.3, Compressor characteristics and dimensions). Additionally, according to Lüdtke's design guidelines [36], assumptions for calculating various impeller components are applied to determine the impeller parameters (can be seen in Appendix B.3, Compressor characteristics and dimensions). The detailed estimations and applied equations are demonstrated in Excel of C-102, Appendix B.3.

3.3.3 Compressor C-102 Design Specifications

Table 3.3.1. Compressor C-102 Design Specifications

Compressor C-102 Specification Sheet				
1	Equipment name: Process Gas Compressor C-102			
2	Type: Centrifugal Compressor			
№	Description	Units	Data	
Operating Conditions				
1	Suction pressure	bar	4.50	
2	Discharge pressure	bar	9.53	
3	Suction temperature	°C	354.27	
4	Discharge temperature	°C	397.81	
5	Mass flow	kg/h	156,109.5	
Compressor Conditions			**At suction**	**At discharge**
6	Heat capacity ratio	-	1.080	1.079
7	Compressibility factor	-	0.995	0.992
8	Volumetric flow rate	m^3/h	43,738.3	22,022.9
9	Density of a mixture	kg/m^3	3.569	7.088

10	Mach number	-	0.943	0.914
Work and Head				
11	Euler head	kJ/kg	122.3	
12	Actual work (including losses)	kJ/kg	125.3	
13	Adiabatic work	kJ/kg	97.15	
14	Adiabatic head	kJ/kg	97.03	
15	Adiabatic efficiency	%	79	
16	Polytropic work	kJ/kg	97.79	
17	Polytropic head	kJ/kg	97.67	
18	Polytropic efficiency	%	80	
19	Polytropic head per stage	kJ/kg	24.42	
Power				
20	Power	kW	5,433.1	
21	Mechanical losses	kW	177.7	
23	Brake Horsepower	hp	7,285.9	
Compressor Parameters				
24	Sonic velocity	m/s	235.1	
25	Peripheral velocity of tip speed	m/s	221.77	
26	Rotative speed	rpm	5,984	
Casing				
27	Casing type	-	Horizontally split	
28	Number of impellers per rotor	-	5	
29	Overall number of impellers	-	20	
30	Length of 1-casing stage	m	1.0	
31	Height of compressor	m	1.8	
32	Number of casing stages	-	4	

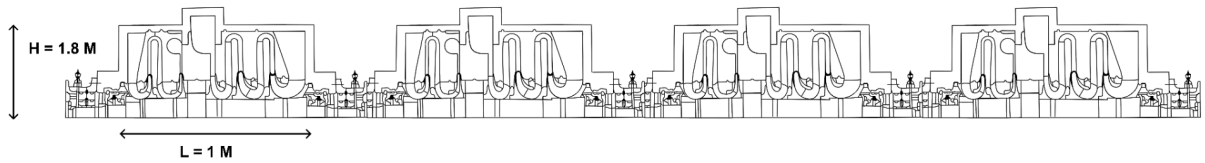

Four-casing horizontally split compressor with 5 impellers per rotor [36]

Impeller dimensions			
33	Impeller type	-	3D-shrouded
34	Number of blades	-	18
35	Disk radius	mm	369.4
36	Blade outlet radius	mm	353.9
37	Blade inlet radius	mm	193.2
38	Blade thickness	mm	7.39
39	Eye root radius	mm	114.1
40	Eye radius	mm	227.3
41	Impeller outlet width	mm	49.54
42	Impeller inlet width	mm	96.05
43	Leading-edge hub radius	mm	116.8
44	Outflow section after blades	mm	15.57
45	Blade inlet angle	deg.	38
46	Blade exit angle	deg.	50
47	Diffuser type	-	Vaneless
48	Diffuser outlet radius	mm	609.6
49	Diffuser inlet radius	mm	369.4
50	Volute outer diameter	mm	1,493.3

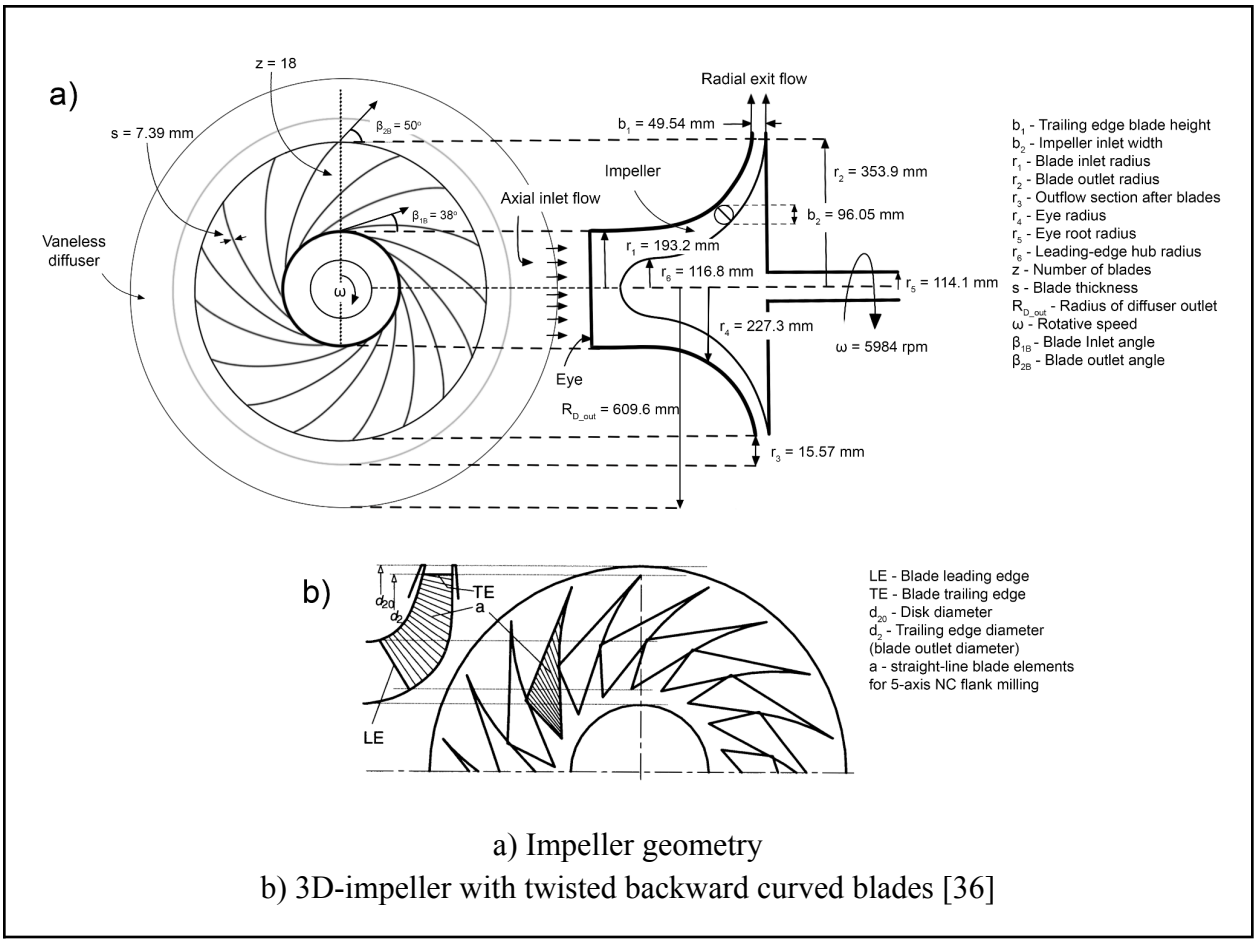

a) Impeller geometry
b) 3D-impeller with twisted backward curved blades [36]

3.3.4 Material selection

The selection of materials for centrifugal compressors requires consideration of many factors, including their properties and the operating conditions of the equipment. It is of particular importance when building the main parts of the compressor, such as the rotor, which consists of a number of impellers and shafts. The correct selection of materials directly affects the reliability, efficiency and longevity of the compressor.

Centrifugal compressors use high-strength steels and nickel alloys for durability, corrosion resistance, and thermal stability. The table 3.3.2 below shows the materials used for each part of the centrifugal compressor along with a brief explanation of their application.

Table 3.3.2. Materials for centrifugal compressor

Compressor Part	Material	Properties
Impeller	AISI 4330/4340	High strength and resistance to mechanical loads, ensuring durability in high-speed rotation [38]

	AISI 4130/4140	Ultrahigh-strength steels, high heat treatment capabilities [37, 39, 40]
	AISI 410/17-4PH	Excellent corrosion resistance, thermal stability, good mechanical properties under high pressure, good hardenability [37, 41]
	13Cr4Ni and nickel alloys	High strength, superior resistance to hydrogen sulfide, corrosion, ensuring longevity in sour gas environments, better weldability [37]
	AISI 4320 (UNS G43200)	High yield strength (90 ksi), suitable for applications requiring superior mechanical performance [37]
Rotor Shaft	AISI 4330/4340	Exceptional strength at low temperatures, with high impact toughness to withstand stress [37, 38]
	ASTM A470 Class 7	Ensures structural stability in extreme conditions [37]
Casing	Carbon steel	High tensile strength, which ensures the casing can withstand high pressures and mechanical loads [42]
	High alloy steels	Utilized in aggressive corrosion environments, provides high durability and resistance [37, 42]
Diaphragms	Mild steel	Preferred due to easy weldability and higher strength compared to gray cast iron [37]

3.3.5 Compressor cost estimation

The cost estimation for the compressor was carried out using the guidelines outlined in Chemical Engineering Design by G. Towler [31]. The calculations took into account driver power (kW) of the centrifugal compressor and resulted in 4.0 millions USD according to the cost correlations (Eq. 42. Appendix B.3). With a Lang installation factor of 2.5 for compressors and material factor for high alloy steel (≈1.3), the evaluated cost amounted to 13.2 million USD. To determine the cost adjustment based on location of the plant, the location factor was set at 0.732, accounting for China's base factor (0.61) and a 20% increase for the 2,000-mile transport to Taraz. Cost escalation, based on the CEPCI index (532.9 in 2010 to 800 in 2024), estimates the compressor cost at 14.5 million USD (Eq. 45. Appendix B.3). The detailed calculations are presented in Excel for CapCost of the compressor C-102 and Appendix B.3.

Table 3.3.3. The cost estimates for compressor

Cost estimation	Cost (USD)
Purchased equipment cost	4,063,847
Lang estimation	13,207,501
Location	9,667,891
Cost Escalation	14,513,629

3.4 Heat Exchanger E-103 Design

Heat Exchanger E-103 is used to cool down hot mixture after the compressor C-101 in order to provide suitable temperature for Phase separator (Flash drum). Cooling water is going to be used as a cooling stream in the shell side, and hot fluid will flow in the tubes, as we follow heat exchanger heuristics, which states that low viscosity gases can be placed in the tube side.

Whole process of designing Heat Exchanger E-103 is according to the procedure for designing a 1 shell-2 pass heat exchanger from Chapter 12 of the Chemical Engineering Design book by Towler and Sinnott [30].

Initially the heat transfer coefficient was assumed to be 400 W/(m^2 K). After several iterations and simulations, the resulting heat transfer coefficient is slightly above the initially assumed value (424 W/(m^2 K)) , meaning assumption was approved. All the calculations during the process of designing a Heat Exchanger E-103 are provided in “Heat Exchanger E-103” excel file and Appendix B.4.

For tube side 2 passes was identified as the most suitable as usage of 4 or more passes resulted in the temperature crossover in Aspen Plus, making the design unacceptable. The same method provided us with an optimal value of 1 shell pass.

Material for the heat exchanger parts is chosen as Carbon Steel as it has good balance in strength, durability (suitable for relatively high pressure and temperature inside equipment), as well as slightly better thermal conductivity than Stainless steel and lower price [43]. All values such as inside and outside diameter, tube lengths are in accordance with TEMA standards [30].

3.4.1 Heat exchanger E-103 Design Specifications

Table 3.4.1. Heat exchanger E-103 Design Specifications

Heat exchanger, E-101		Type: BEM, 1-2 shell and tube, horizontal			
Performance					
Fluid location		Tube Side		Shell Side	
Fluid type		Hot fluid		Cold fluid	
Fluid		Compressor outlet		Cold water	
Mass flow rate, kg/s		36.9		500	
Stream		In Stream	Out Stream	In Stream	Out Stream
T, °C		397.81	166.04	20	29.81
P, bar		9.534	9.459	1	0.47
Pressure drop, bar		0.075		0.53	
Velocity, m/s		16.79		1.01	
Heat Exchanged, kW		22,187.4			
LMTD (corrected), °C		242.48			
Heat transfer rate, $W/m^2°C$	Service	427.8			
	Dirty	428.2			
	Clean	618.5			
Design Specifications					

Area total, m^2	213.9
Area total overdesigned, m^2	256.68
N_{tubes}	300
$N_{tube\ passes}$	2
Tube OD, m	0.050
Tube thickness, m	0.00211
Tube length, m	4.65
Pitch, m	0.0625
Pitch type	Square
Construction material	Carbon Steel
Shell ID, m	3
Shell OD, m	3.026
Baffle type	Single segmental Horizontal cut (30.49%)
Baffle spacing, m	0.450

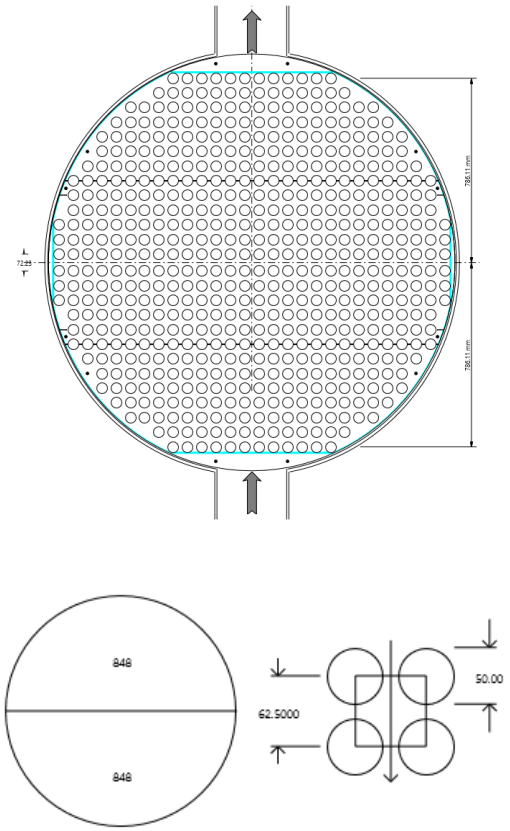

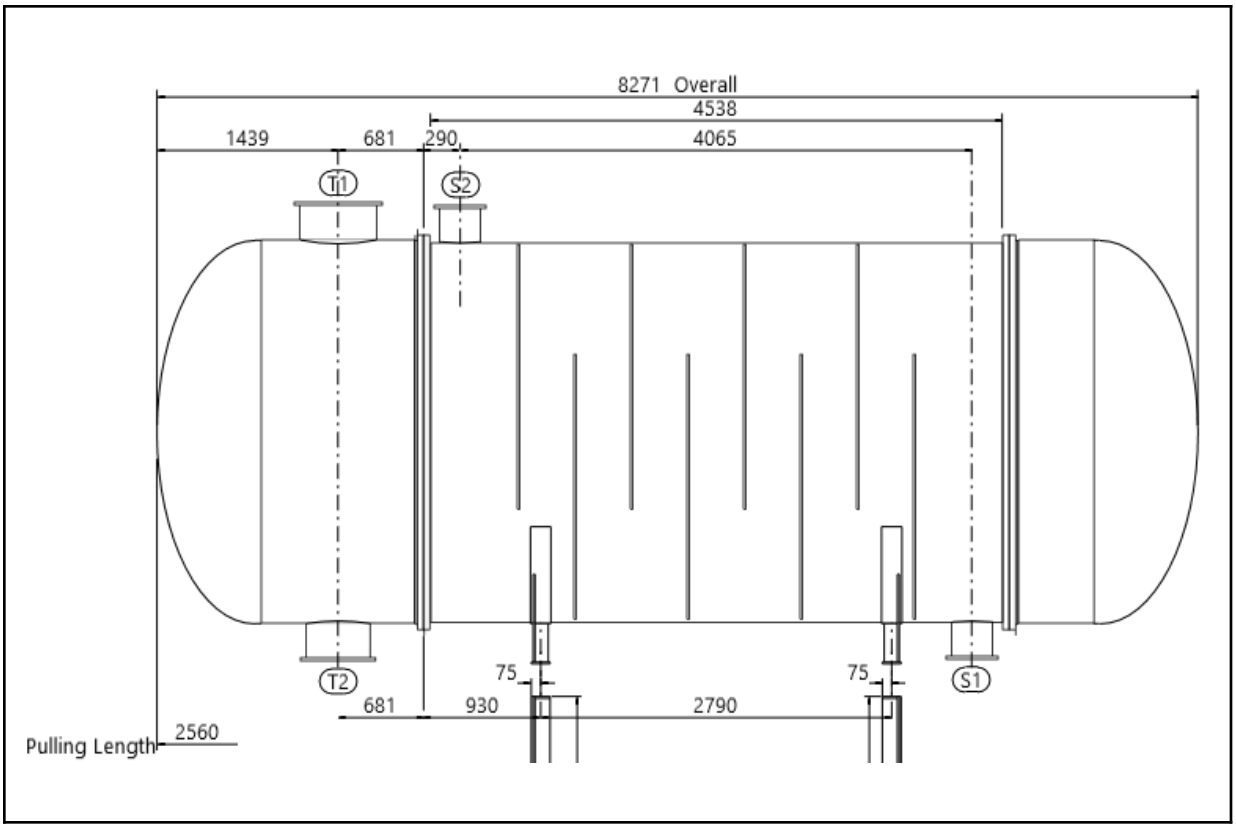

3.4.2 Heat Exchanger E-103 Cost Estimation.

Base equipment cost of the Heat Exchanger E-103 can be calculated using the cost constants a and b for U-tube shell and tube heat exchanger are given as 28,000 and 54 respectively. Scaling factor is taken as 1.2 and the area is 256.68 m^2. All the calculations according to Towler and Sinnott's "Capital Cost Estimating" [31] are in Appendix B.4, E-103 Cost estimation. Results are shown in the table below:

Table 3.4.2. Cost estimation of Heat Exchanger E-103

Cost estimation	Cost Estimation, USD	Location factor applied, USD	Cost escalation, USD
Lang	245,140	179,442	269,383
Material	224,128	164,062	246,293

As a result, it can be seen that the approximate cost of the Heat exchanger E-103 is about 250,000 USD.

3.5 Depropanizer Distillation Column T-101 Design

Depropanizer T-101 is a distillation column with the main purpose of separating propane and lighter components from the bottom feed of Flash F-101 in order to increase purity of the final 1,3-butadiene product. The separation is done based on components boiling points and their relative volatility.

Overall, the working principle of the distillation column is separating a mixture of two or more components with different boiling points. The component with lower boiling point will evaporate more readily and come as the top product, while the component with higher boiling point will mostly come at the bottom stream. The liquid feed is partially vaporized in the reboiler and temperatures across the column separates the components from the mixture. In the condenser some of the top stream can be withdrawn in liquid or vapor phase as distillate product, while a part of the top mixture is condensed and returned back to the column for increasing separation efficiency. This returned mixture is called reflux.

3.5.1 Choice of type design and operating conditions

Distillation columns can be 2 types: packed and tray column. Tray type column was chosen for depropanizer based on available papers on optimizing depropanizer columns or which are used in industry. For instance, Listijorini et al in their work "Optimization of Depropanizer Column" [44] used depropanizer as tray type distillation column and simulated it in Aspen HYSYS. (More details in Appendix B.5). Bubble cup trays were chosen as they provide excellent vapor-liquid mixing and minimize weeping, ensuring efficient separation. In contrast to them, more simple and cost-effective sieve trays can lead to liquid seeping at low flow rates or vertically exiting vapors can cause liquid entrainment, which results in lower efficiency of the column [45].

The operating conditions of the T-101 units are based on a benchmark process offered by Brencio [25]. The operating pressure is 20.2 bars and temperature range is from 3 to 104 °C [25]. In the benchmark process the distillate is taken out as liquid of 2.8 °C at 20 bars [25]. Thus, the pressure drop is taken as 0.2 bars and condenser temperature 2.8°C.

3.5.2 T-101 column design

In the process this column is required to increase purity of the final product by removing impurities. In order to establish proper separation light and heavy key components must be chosen. Main criteria is their boiling points under normal conditions or it can be their relative volatilities under column operating conditions. Boiling points are -0.49 °C for butane, -6.24 °C for butene, -4.41°C for butadiene, -10.74 °C for ethylene, -47.7°C for propylene, -42.11 °C for propane, -252.76 for hydrogen gas, 204.27 °C for NMP and 100°C for water. Since the main aim of depropanizer is to separate undesired products from the feed the light key is propane, since hydrogen, ethylene, propylene, have lower boiling points and will evaporate easily. The heavy

key is butene, as while butane, butadiene, water, NMP have higher boiling point and will go in the bottom stream.

The relative volatilities are calculated by using K values from Aspen Plus v14 simulation [46].

$$\alpha_i = K_i/K_r \tag{3.5.1}$$

where,

α_i - relative volatility of component i to respect to reference component

K_i and K_r - K values of i and reference components

The heavy key component is chosen as the reference for calculation. For more accurate value of α_i, it is estimated from[30]:

$$\alpha_i=(\alpha_{top}\alpha_{bottom})^{1/2} \tag{3.5.2}$$

$$\alpha_i=(\alpha_{top}\alpha_{middle}\alpha_{bottom})^{1/3} \tag{3.5.3}$$

For the primary design of column Fenske-Underwood-Gilliland (FUG) method was used, as feed to the column is a multicomponent stream. By using this method, minimum and actual number of stages, reflux ratio and feed stage location in the column were calculated.

The Fenske equation is used to estimate the minimum required stages at total reflux [30]:

$$N_m = \frac{log(\left[\frac{x_{LK}}{x_{HK}}\right]_d\left[\frac{x_{HK}}{x_{LK}}\right]_b)}{log(\alpha_{LK})} \tag{3.5.4}$$

where,

α_{LK} - the average relative volatility of the light key with respect to the heavy key

x_{LK} and x_{HK} - the light and heavy key molar fractions, and subscripts d refer to distillate product and b to bottom product

The Underwood correlation is used to calculate the minimum reflux ratio. In order to do that the θ value is estimated from following equation[46]:

$$\sum\frac{\alpha_i x_{i,f}}{\alpha_i-\theta} = 1 - q \tag{3.5.5}$$

where,

α_i is the relative volatility of component i with respect to the heavy key component

$x_{i,f}$ is molar ratio of component i in the feed stream and q is feed quality

The θ value usually lies between values of the relative volatility of the light and heavy keys and can be found by trial and error. The feed quality depends on feed conditions and is calculated by the following formula [47]:

$$q = \frac{-H_F + H_V}{H_V - H_L} \tag{3.5.6}$$

where,
H_F - enthalpy flow of feed stream, kJ/hr
H_v - enthalpy flow of vapor stream, kJ/hr
H_L - enthalpy flow of liquid stream, kJ/hr

These values were obtained from Aspen Plus v14 using flash simulation, keeping feed temperature and changing vapor fraction. With obtained value of θ, the minimum reflux ratio R_m can be found by this Underwood correlation [46]:

$$\sum \frac{\alpha_i x_{i,d}}{\alpha_i - \theta} = R_m + 1 \tag{3.5.7}$$

where,
$x_{i,d}$ - molar ratio of component i in the distillate stream at minimum reflux

Feed point location is calculated using empirical equation given by Kirkbride [19]:

$$log[\frac{N_r}{N_s}] = 0.206\, log\,[(\frac{B}{D})(\frac{x_{HK,f}}{x_{LK,f}})(\frac{x_{LK,b}}{x_{HK,d}})^2] \tag{3.5.8}$$

where,
N_r - number of stages above the feed, including any partial condenser
N_s - number of stages below the feed, including the reboiler
B - molar flow bottom product, kmol/hr, D- molar flow top product, kmol/hr

The limitation of the FUG method is that it is best applied to mixtures that form ideal or nearly ideal solutions and for the Fenske equation total reflux is used. This approach can not be used for the feed to T-101, as it is in high pressure and cannot be totally condensed to ensure total reflux. The reason is that there is the presence of hydrogen gas, which is considered a Henry component and can not be in liquid phase under 2.8°C and 20 bars. Also, NMP is not condensable solvent [25] and with water, these compounds affect calculation, resulting in negative values. Thus these 3 components were taken out from the feed stream to ensure hand calculation and proper work of the DSTWU column. Simulation with this column in Aspen Plus v14 is used in order to compare calculated values from FUG approach with obtained values from simulation. Assumption of 40 stages and recovery of propane of 0.999 and 0.001 of butene in the distillate was taken. The NRTL property method is used for T-101, both for DSTWU and RadFrac columns due to the presence of the Henry component in the stream. Original feed is taken for calculating q. The Excel file can be seen in ESI.

Table 3.5.1. Relative volatilities of compounds in assumed feed

Compound	Estimated relative volatility
Butane	0.83
Butene	1
Butadiene	0.976
Ethylene	0
Propylene	3.436
Propane	2.940

Table 3.5.2. Comparison of calculated and obtained values

Value	Calculated	Taken from DSTWU
Minimum number of stages	12.808	14.49
Actual reflux ratio	252	0.226
Total number of stages	26.09	40
Feed stage	2	20.87

The values from table 3.5.2 are not the same due to the reason of feed quality being less than 1. In reality, q should be more than 1, as the original feed is subcooled. However, the simulation stream for feed is taken separately, while originally it is the bottom stream of the flash unit. The properties are not calculated correctly, which resulted in wrong values. Another major problem is that there is no sufficient data in data banks for any of the methods for calculation, especially for molecular interaction for the Henry component (hydrogen gas). Because of insufficient data, Aspen takes other components as Henry components, which is the wrong approach. The high pressure conditions also complicates the calculation. The property estimations were done incorrectly, leading to possibly wrong values, consequently influencing the design. In order to obtain correct values and design, a detailed research should be done on how molecules interact with each other under high pressure and taking hydrogen as a Henry component and not other compounds.

For the designing of a column, a RadFrac model was used. Initially, detailed analysis was done on optimal number of stages, reflux ratio, distillate rate and feed stage using shortcut method. This analysis can be seen in Appendix B.5. Then it was designed in equilibrium calculation type and later on in rate-based. The design specifications for the column can be seen in table 3.5.3.

3.5.3 Depropanizer Distillation Column T-101 Design Specifications

Table 3.5.3. Equipment specification sheet for T-101

<table>
<tr><td colspan="2">Unit</td><td colspan="2">Depropanizer Distillation Column T-101</td></tr>
<tr><td colspan="2">Sketch</td><td colspan="2">Operating Parameters</td></tr>
<tr><td colspan="2" rowspan="10"> 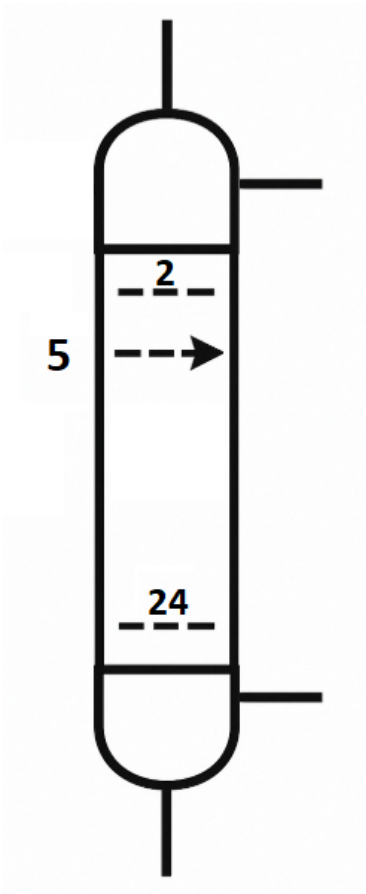
</td><td>Calculation type</td><td>Rate-Base</td></tr>
<tr><td>Condenser type</td><td>Partial-Vapor</td></tr>
<tr><td>Reboiler type</td><td>Kettle</td></tr>
<tr><td>Phase</td><td>Vapor and Liquid</td></tr>
<tr><td>Number of stages</td><td>25</td></tr>
<tr><td>Reflux ratio</td><td>16</td></tr>
<tr><td>Feed stage</td><td>5 Above-stage</td></tr>
<tr><td>Column total height (m)</td><td>20.1</td></tr>
<tr><td>Column design</td><td>Tray</td></tr>
<tr><td>Tray type</td><td>Bubble-cup</td></tr>
<tr><td>Material</td><td>Stainless steel 316L</td></tr>
<tr><td colspan="4">Operating conditions</td></tr>
<tr><td>Stream</td><td>Feed (Stream 15)</td><td>Top
(Stream“By-products”)</td><td>Bottom (Stream 16)</td></tr>
<tr><td>Temperature (°C)</td><td>14</td><td>92.30</td><td>103.83</td></tr>
<tr><td>Pressure (bar)</td><td>20.2</td><td>20</td><td>20.2</td></tr>
<tr><td colspan="4">Section 1 (2-4 stage)</td></tr>
</table>

<table>
<tr><td rowspan="7"> 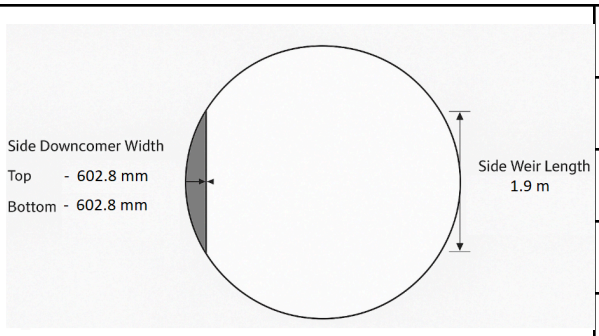

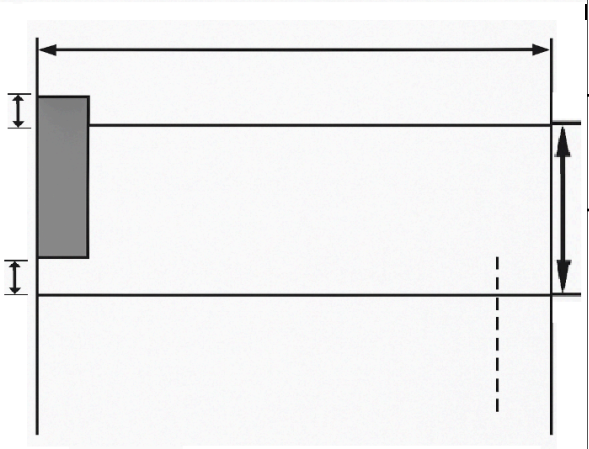 </td><td>Number of passes</td><td>1</td></tr>
<tr><td>Tray spacing (m)</td><td>0.7</td></tr>
<tr><td>Diameter (m)</td><td>2.1</td></tr>
<tr><td>Cap diameter (mm)</td><td>76.2</td></tr>
<tr><td>Number of caps per active area $1/m^2$</td><td>50</td></tr>
<tr><td>Downcomer clearance (mm)</td><td>45.63</td></tr>
<tr><td>Side Downcomer width (mm)</td><td>Top - 687.8
Bottom - 687.8</td></tr>
<tr><td colspan="3">Section 2 (5-24 stage)</td></tr>
<tr><td rowspan="8"> 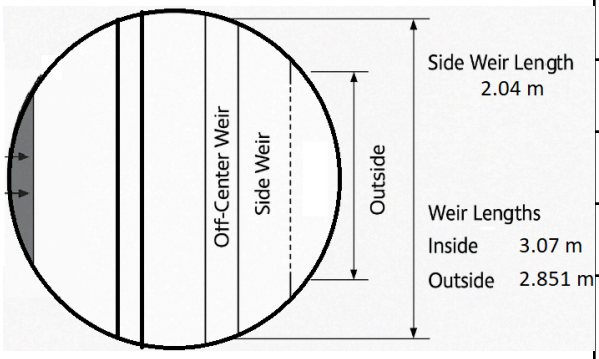
</td><td>Number of passes</td><td>3</td></tr>
<tr><td>Tray spacing (m)</td><td>0.9</td></tr>
<tr><td>Diameter (m)</td><td>4</td></tr>
<tr><td>Cap diameter (mm)</td><td>76.2</td></tr>
<tr><td>Number of caps per active area $1/m^2$</td><td>50</td></tr>
<tr><td>Downcomer clearance (mm)</td><td>80</td></tr>
<tr><td>Side Downcomer width (mm)</td><td>Top - 380.1
Bottom - 380.1</td></tr>
<tr><td>Off-Center Downcomer width (mm)</td><td>Top - 357
Bottom - 357</td></tr>
</table>

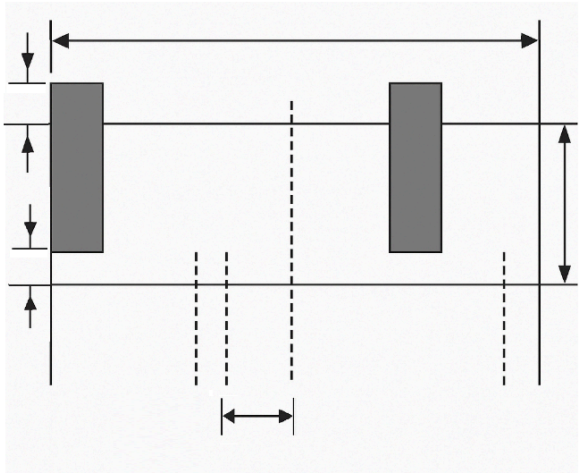			
Condenser conditions		Reboiler conditions	
Heat duty, MW	-1.1522	Heat duty, MW	13.2315

Material for the column is selected to be stainless steel 316 [48], as the feed contains water and the material is required to be corrosion protective to ensure longer working time for the depropanizer. Base equipment cost of the column can be calculated considering it as a pressure vessel and for each section mass of steel required is found. Cost for the trays are also estimated for both sections by using cost estimation for bubble trays. All the calculations according to Towler and Sinnott's "Capital Cost Estimating" [31] are in the Excel file in ESI . Results are shown in the table below:

Table 3.5.4. Cost estimation of Depropanizer Column T-101

Cost estimation	Cost Estimation, thousand USD	Location factor applied, thousand USD	Cost escalation, thousand USD
Lang	1372.83	1004.91	1508.59
Material	987.38.	722.76	1085.03

Cost is estimated to be between 1.08 million USD and 1.50 million USD.

Chapter 4. Minor Equipment Design

4.1 Heaters

4.1.1 Heater E-100

The heat duty was calculated using:

$$Q = \Delta H * n \quad (4.1.1)$$

Heater E-100 is located after the mixture M-102 and before the heat exchanger E-101. E-100 heats the stream H at -10.54°C until 85.43°C. The operating pressure of E-102 is 1 bar.

Table 4.1.1. Input data for heat duty calculations

Inlet T, °C	Outlet T, °C	n, kmol/s	ΔH at T = -10.54°C, kJ/kmol	ΔH T = 85.43°C, kJ/kmol
-10.54	85.43	0.905	-38,182.2	-16,184.6

Table 4.1.2. The comparison of calculated and Aspen Plus data

E-102	Calculated	Aspen Plus
Q, kW	19,914.54	19,914.6

4.1.2 Heater E-102

The heat duty was calculated using the following equation:

$$Q = nCp\Delta T \quad (4.1.2)$$

where,
n - molar flow rate, kmol/s
C_p - heat capacity of mixture, J/kmol°C
ΔT - temperature difference, °C

Heater E-102 is located after heat exchanger E-101. E-102 is used to heat the E-101 outlet at 268.87°C to the operating temperature (625°C) of the reactor. The operating pressure of E-102 is 1 bar.

Table 4.1.3. Input data for heat duty calculations

Inlet T, °C	Outlet T, °C	n, kmol/s	C_p at T = 446.94°C, kJ/kmol°C
268.87	625	0.9052	144.426

Table 4.1.4. The comparison of calculated and Aspen Plus data

E-102	Calculated	Aspen Plus
Q, kW	46,558.45	46,118.8

4.1.3 Heater E-104

Heater E-104 is located after compressor C-103 is used to heat the outlet to 14°C for further separation in the flash drum. The operating pressure of E-104 is 20.2 bar. Heat duty was found as difference of molar enthalpies multiplied to mole flow:

$$Q = \Delta H * n \tag{4.1.3}$$

Table 4.1.5. Input data for heat duty calculations

Inlet T, °C	Outlet T, °C	n, kmol/s	ΔH at T = 189.67°C, kJ/mol	ΔH at T = 14°C, kJ/mol
189.67	14	1.0534	11.08	-19.03

Table 4.1.6. The comparison of calculated and Aspen Plus data

E-104	Calculated	Aspen Plus
Q, kW	31,717.9	31,720.2

4.2 Compressors C-101, C-102

Since the operating pressure of the reactor is 6 bar, a compressor (C-101) must be installed upstream to increase the pressure from 1 to 6 bar. This will ensure a stable gas supply to the reactor under the required conditions.

As stated above, the second compressor C-103 of the multistage compressor system increases the pressure to 20.2 bar, prior to entering the second heat exchanger.

Both C-101 and C-103 compressors are considered to function under polytropic condition, with efficiencies of 80% (implemented as an industry standard practice) and 80% (from Table B.3.1, Appendix B.3), respectively. Mechanical losses of 2% (Table B.3.2 in

Appendix B.3) for both compressors C-101 and C-103 are included in power estimations, ensuring accurate performance evaluation. The design specifications for these compressors are estimated using Equation 7, 9, 13 (Appendix B.3) and presented in Table 4.1.7.

Table 4.2.1. Compressors design specifications

Compressor		C-101	C-103
Suction pressure, bar		1	9.46
Discharge pressure, bar		6	20.2
Polytropic efficiency, %		80	80
Mechanical losses, %		2	2.5
Temperature at outlet, °C	Hand calculated	610.90	200.23
	Aspen Plus	611.37	211.80
Power, kW	Hand calculated	14,316.2	3,743.1
	Aspen Plus	14,326.9	3,749.0
Polytropic head, kJ/kg	Hand calculated	258.87	66.57
	Aspen Plus	259.03	67.43

4.3 Storage Tanks

4.3.1 Butane storage tank

The n-butane is used as the feed in the butadiene production. It is a gas fluid. The storage tank should be able to store butane for a month. The butane will be stored at 20°C on average and 4 bars to ensure liquid phase. Therefore the storage tank will have a smaller volume. The density of the butane at these conditions is assumed to be 582 kg/m^3 with the compressibility factor of 0.95. The 5000 m^3 LPG Propylene Spherical Sphere Storage Tank [49] will be used for the storage of butane as it has high capacity for volume to store all compounds as well as it can withstand pressure up to 100 bar (much higher than our 5 bar). The tank is constructed by the ASME standard.

The volume of the storage tank can be calculated using the following equation:

$$V = \frac{Mass}{Density} = \frac{30\ days * (24h/day) * (17542.924\ kg/h)}{582\ kg/m^3} = 21{,}702.59\ m^3 \quad (4.3.1)$$

Table 4.3.1. Specifications of butane storage tank

Storage tank type	ASME BPVC
Material of construction	Carbon steel
Temperature, °C	20
Operating temperature range, °C	max 50
Pressure, bar	4
Operating pressure range, bar	100
Nominal capacity, m^3	5,000
Number of tanks	5
Shell plate thickness, mm	75
Corrosion allowance, mm	1

4.3.2 Hydrogen storage tank

The hydrogen in the gas phase is removed from the stream using the splitter and then will be sold. The stream conditions are 14°C and 20.2 bars. The storage tank should store the hydrogen for a month. The calculated volume of the tank:

$$V = \frac{Mass}{Density} = \frac{30\ days * (24h/day) * (1072.97\ kg/h)}{0.0813\ kg/m^3} = 9{,}502{,}317.34\ m^3 \quad (4.3.2)$$

In order to decrease the volume for the storage the hydrogen should be stored in the liquid form. However, it requires an extremely low temperature (-259°C) and therefore hydrogen will not be stored. It was decided to directly transport the hydrogen via pipelines.

4.3.3 NMP storage tank

NMP solvent is introduced into the extractive distillation column T-102. NMP is in the liquid phase. It will be stored at conditions at 25°C and 5 bars, at these conditions it enters the process. The solvent is introduced into the process and then recycled through the units, not produced. Therefore it is not required to be stored for a month as butane, H_2 and butadiene. The time parameter is eliminated from the calculations. The volume of the storage according to the calculations:

$$V = \frac{Mass}{Density} = \frac{1414823.79\ kg/h}{1028\ kg/m^3} = 1{,}376.29\ m^3 \quad (4.3.3)$$

Table 4.3.2. Specifications of NMP storage tank

Storage tank type	ASME BPVC
Material of construction	Carbon steel
Temperature, °C	25
Operating temperature range, °C	max 50
Pressure, bar	5
Operating pressure range, bar	100
Nominal capacity, m^3	5,000
Number of tanks	1
Shell plate thickness, mm	75
Corrosion allowance, mm	1

4.3.4 Butadiene storage tank

The desired product butadiene in gas form is produced at the rate of 11411.45 kg/h. It will leave the extractive distillation column at 36.4°C and 5 bars. From the economic point of view it was decided to store the butadiene in liquid phase under 2.5 bar pressure.

$$V = \frac{Mass}{Density} = \frac{30\ days * (24h/day) * (11411.45119\ kg/h)}{610\ kg/m^3} = 13{,}469.25\ m^3 \quad (4.3.4)$$

Table 4.3.3. Specifications of butadiene storage tank

Storage tank type	ASME BPVC
Material of construction	Carbon steel
Temperature, °C	25
Operating temperature range, °C	max 50
Pressure, bar	5
Operating pressure range, bar	100
Nominal capacity, m^3	5,000

Number of tanks	3
Shell plate thickness, mm	75
Corrosion allowance, mm	1

4.4 Extractive distillation column (T-102)

The T-102 unit was designed using the RadFrac unit in Aspen PLUS. The feed values were obtained from PFD and put into tests. The distillate of the columns must primarily consist of butane and butene because of purification using NMP. The bottom product consists of more pure butadiene with water and NMP. The series of simulations were done to obtain optimal values for number of stages, reflux ratio, feed streams and distillate temperature. Simulation results suggest the following:

Table 4.4.1. T-102 specification.

Number of stages	25	Split fractions (Top product)	
Reflux ratio	1	Butane	0.988
Condenser	Total	Butene	0.988
Condenser Temperature	23.76°C	Butadiene	0.788
NMP stream feed stage	2	NMP	≈ 0
Main feed stage	15	H2O	0.017

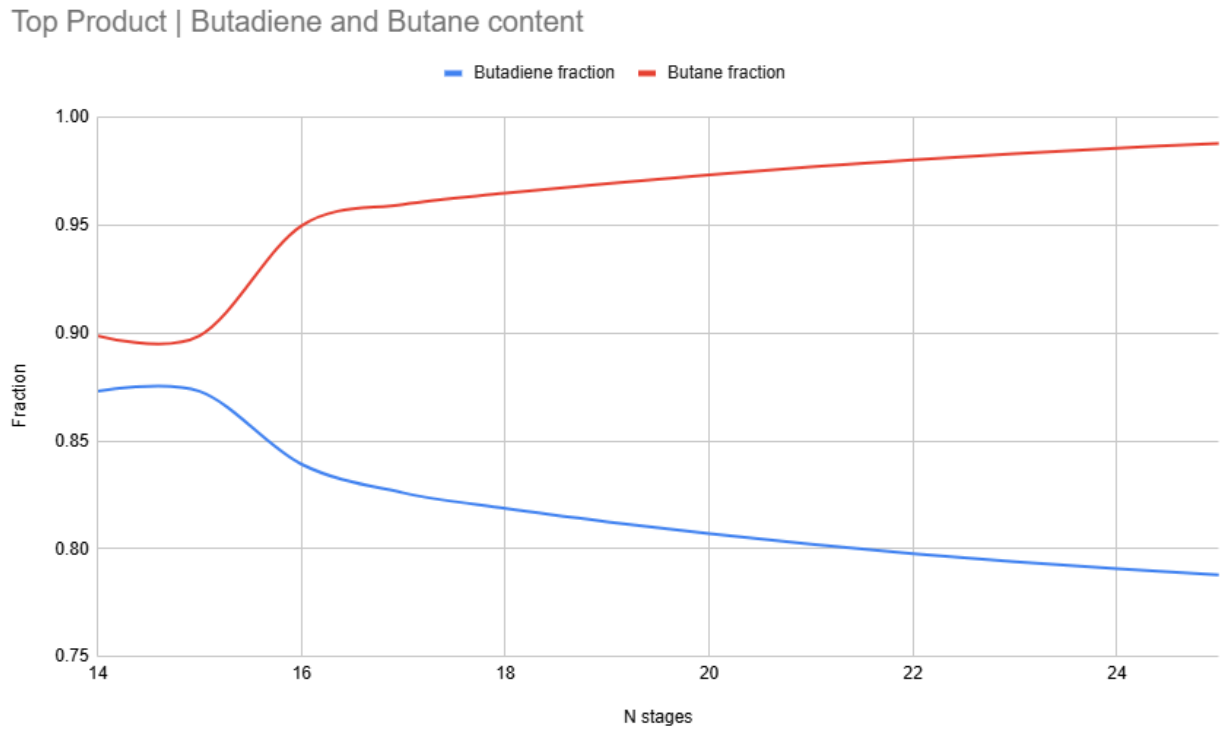

Figure 4.4.1. Butadiene and Butene content at distillate of T-102

4.5 Second Extractive Distillation Column (T-103)

The second extractive distillation column was designed as a minor unit using the RadFrac block in Aspen Plus. It is located at the end of the production process and its objective is to increase the purity of the product. The feed values were taken from main PFD and optimal values of distillate rate, number of stages, reflux ratio and feed stages were found using Sensitivity analysis tool. The required product purity was achieved and the obtained values are presented in Table 4.5.1.

Table 4.5.1. T-103 specification

Number of stages	11	Split fractions (Top product)	
Reflux ratio	3	Butane	0.0001
Condenser	Total	Butene	0.0003
Condenser Temperature	43.91°C	Butadiene	0.9757
NMP stream feed stage	3	NMP	0
Main feed stage	8	H2O	0.0002

As a result, this design achieves desired purity of 99.5% and even slightly outperforms, which is needed to ensure there is a margin to allow for error.

4.6 Rectification column (RC-101)

Rectification column was designed as a minor unit using the RadFrac unit. Applying feed values from the main PFD, we used Sensitivity analysis to obtain optimal values for Reflux Ratio, Feed stage number and Subcooled temperature of the condenser in order to preserve desired split fraction values (Butane, Butene and Butadiene to the top and NMP, Water to the bottom). As a result of sensitivity analysis, we identified that the most suitable values are:

Table 4.6.1. RC-101 specification

Number of stages	50	Split fractions (Top product)	
Reflux ratio	16	Butane	0.999
Condenser	Total	Butene	0.999
Condenser Temperature	1°C	Butadiene	0.814
NMP stream feed stage	4	NMP	0
Main feed stage	4	H2O	0

In the end, the current rectification column provides acceptable splitting of hydrocarbons from NMP and water that will be sent to the second extractive distillation column.

4.7 Phase separator F-101

The phase separator is a unit that is used to separate different phases of a mixture. This unit works without phase change as the feed conditions are already sufficient and the feed stream contains both vapor and liquid phases that should be separated. In this process a vertical separator is used and its design method is similar to a flash drum.

In order to calculate the dimensions of the phase separator, it is necessary to find maximum vapor velocity using the formula below:

$$U_{vapor,max} = K[(\rho_l - \rho_v)/\rho_v]^{0.5} \quad (4.7.1)$$

K is a system constant and in order to find it we need to find value of another constant X:

$$X = ln(W_l/W_v(\rho_v/\rho_l)^{0.5}) \quad (4.7.2)$$

where,
W - liquid or vapor flow rate

Then K constant can be calculated using the formula below:

$$K = Exp(A + BX + CX^2 + DX^3 + EX^4 + FX^5) \quad (4.7.3)$$

where,
A = - 1.942936
B = - 0.814894
C = - 0.179390
D = - 0.0123790
E = 0.000386235
F = 0.000259550

When maximum vapor velocity is known, cross sectional area can be calculated by dividing vapor flow rate by maximum vapor velocity. The diameter can be found from cross sectional area, and the length is usually in the range of 3 to 5 diameters. All calculations were done in excel sheet and the results are: the diameter is equal to 0.761 m and the length is equal to 2.283 m.

Chapter 5. Plant Site Location

5.1 Location of the Plant

The selection of a suitable plant location depends on a combination of critical factors, including: (1) plant siting options in Kazakhstan, (2) service tariffs, (3) weather conditions, (4) transportation, and (5) political and strategic considerations. These aspects are examined in the following discussion to determine the most appropriate site for the plant.

5.1.1 Plant siting options in Kazakhstan

In the long term, it will be necessary to choose a suitable location for the extraction and processing of raw materials within Kazakhstan. Kazakhstan has large reserves of hydrocarbons, especially in the western regions (Atyrau, Mangystau, and West Kazakhstan), making these regions promising for the construction of new oil and gas processing facilities for butadiene production. Atyrau region is included in the Special Economic Zones (SEZ) with exclusive opportunities for the plant construction and operation. As another option for the plant location Taraz city is favorable for chemical plants. The region is also one of the SEZ, which are economically attractive for the production. Including the absence of tax obligations, “Chemical park” in Taraz encourages the production of rubber materials, which is one of the products of butadiene [50]. Therefore, these two options for locating the plant will be analyzed.

5.1.2 Service Tariffs

The comparison of service tariffs in Atyrau and Taraz cities is presented in Table 5.1.1. These particular services are important because they are included in the plant operation. The most important service is electricity supply, which will be used for the work of all the operating units. Even though water is not directly included in the reaction itself, water plays a crucial role in the cooling and product recovery process. High costs for heat supply services are expected in winter to keep the plant at an acceptable temperature for workers and operating units.

Table 5.1.1. Service tariffs for Atyrau and Taraz cities

City	Water supply services (tg/m^3)	Electricity supply services (tg/kW*h)	Heat supply services (tg/Gcal)
Atyrau	333 [51]	19.15 [51]	19.6 [51]
Taraz	114 [51]	27 [51]	71 [51]

5.1.3 Weather conditions

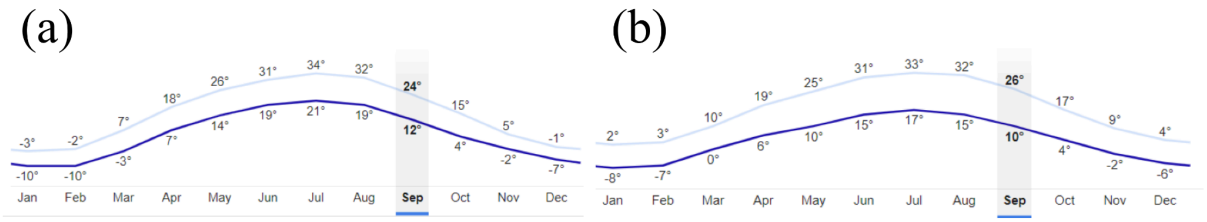

Figure 5.1.1. Temperature vs months a) Atyrau city b) Taraz city [52].

Weather conditions for Atyrau (Atyrau region, West Kazakhstan) and Taraz (Jambyl region, South Kazakhstan) cities are similar for a whole year, which can be seen in Figure 5.1.1. In comparison with other regions and cities in Kazakhstan, Atyrau and Taraz have milder weather conditions, which allow the industry to work in winter. This is because comparably high temperatures in winters that make up about -10°C in average prevent operating units and pipes from freezing. This fact increases the number of days of production and minimizes the costs of repair and replacement for the units.

5.1.4 Transportation

If the plant is located in Taraz, its proximity to China allows us to purchase the raw material (n-butane) from China and economize on transportation. In addition, the SEZ provides the opportunity to cooperate with Chinese companies such as IDAN [50]. In the case of Atyrau city, raw materials can be purchased from neighboring plants. For example, “TCO” oil refinery located in Atyrau region sells butane at bargain prices to “LLP Butadiene” company, this considerably reduces transportation costs [53]. However, prices for n-butane for China and Kazakhstan significantly differ. The prices for n-butane in the China and Kazakhstan market account for 5 USD/ton and 79,680.28 tg/ton (165 USD/ton), respectively [54, 55]. The price for transportation from China to Taraz city is compiled from the price 300 tg for 1 km and the distance between the destinations (2900 km).

5.1.5 Political and strategic considerations

Table 5.1.2 compares the taxation and tax benefits for industries operating in Kazakhstan's standard taxation system versus two Special Economic Zones (SEZs): "National industrial petrochemical technopark" in Atyrau and "Chemical Park" in Taraz. Because SEZs offer substantial tax benefits, they are perfect for industrial operations. These exclude some taxes, which makes them very advantageous compared to the standard tax system.

Table 5.1.2. Standard taxation and taxes for the Special Economic Zone (SEZ) in Kazakhstan

Tax Obligations	**Standard taxation in**	**SEZ “National industrial**	**SEZ “Chemical**

	Kazakhstan	petrochemical technopark" in Atyrau region [56, 57]	Park" in Taraz [50]
Corporate income tax	Basic rate 20% [58]	0% [59]	0% [50]
Export and Import tax	Import custom duty - 5%, Import VAT - 6.4% [60, 61] Export custom duty - 21 USD/ton[a], Export VAT - 0% [62,63].		
Land tax	The tax amount varies based on the land plot parameters [58]	0% [59]	0% [50]
Property tax	1.5% [64]	0% [59]	0% [50]
Value added tax (VAT)	12%, paid 4 times a year [58]	0% [59]	0% [50]

[a]Since the average price of oil for April 2024 was 73 US dollars per barrel, it falls into the range "from 70 to 75 US dollars per barrel" (item 11 in table "Export Customs Duty Rates on Crude Oil and Light Petroleum Products" according to adilet.zan) [63, 65].

By considering factors such as weather conditions, service tariffs, purchase and transportation of raw materials, political and strategic considerations it was concluded that Taraz city is suitable as the plant location.

5.2 Plant Layout

5.2.1 Infrastructure and strategic location advantages of SEZ in Taraz city

The city of Taraz benefits from a strategically located Special Economic Zone (SEZ), positioned 15 km from Chu and 242 km from Taraz. As illustrated in Figure 5.2.1, the facility gains several advantages from this location:

- A well-developed transport network (roads and railways), ensuring efficient logistics
- Proximity to a river, enabling reliable water supply and additional transport options
- Institutional backing from the SEZ and Chemical Park, fostering long-term growth in the sector

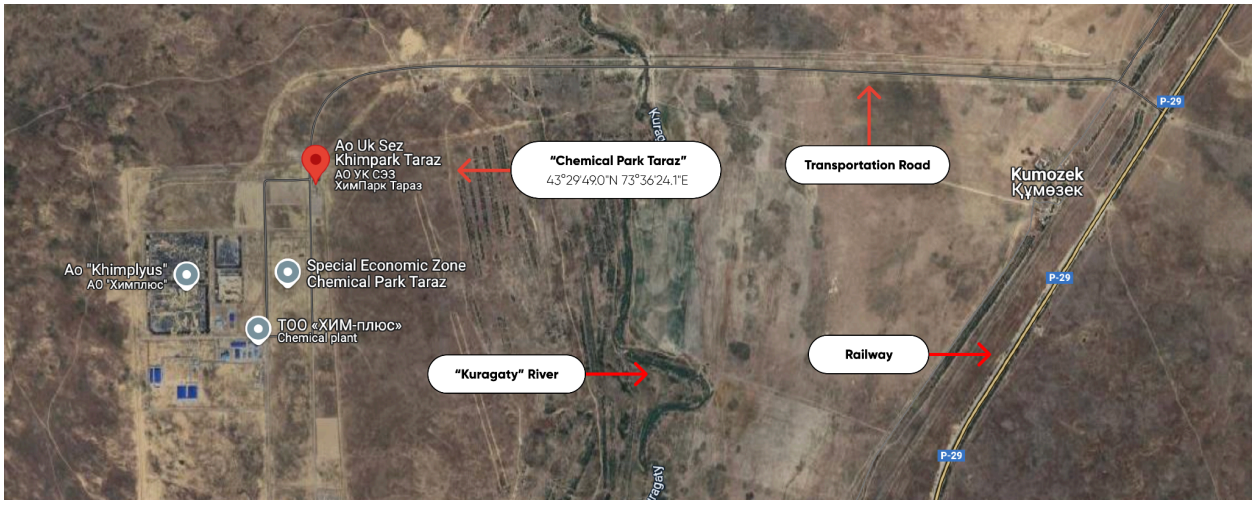

Figure 5.2.1. Plant location (Google Earth screenshot)

The "Taraz Chemical Park" has large land areas that are a great fit for setting up a butadiene production facility. Since a capacity of 90,000 tons per year is considered quite large in the industry, having access to a site with a perimeter of about 3,000 meters and an area of roughly 60 hectares, it provides a solid foundation for such a project (Figure 5.2.2). This designated area already allows for the implementation of a full-scale production complex.

Moreover, the park still has additional undeveloped land, offering further expansion potential if needed, therefore, the site provides the flexibility and scale required for a project of this size.

Figure 5.2.2. Plant location sizing (Google Earth screenshot)

5.2.2 Plant Layout Design

The plant layout has been developed in accordance with the general principles outlined by Moran [66], along with key considerations driven by process safety requirements. The layout

(Figure 5.2.3) is divided into several functional zones according to their risk level and operational purpose:

- Red zone represents the core production area and storage tanks, which are associated with the highest safety risks due to the presence of reactive chemicals and high-temperature processes.
- Orange zones indicate areas that involve machinery operations, utilities, laboratories, control rooms and fire station.
- Green zones mark the safe areas, these include administrative buildings, canteen, parking, and other auxiliary facilities such as hospital, first aid stations, changing rooms, washrooms and restrooms. These zones are located farther from the high-risk operations to minimize personnel exposure.

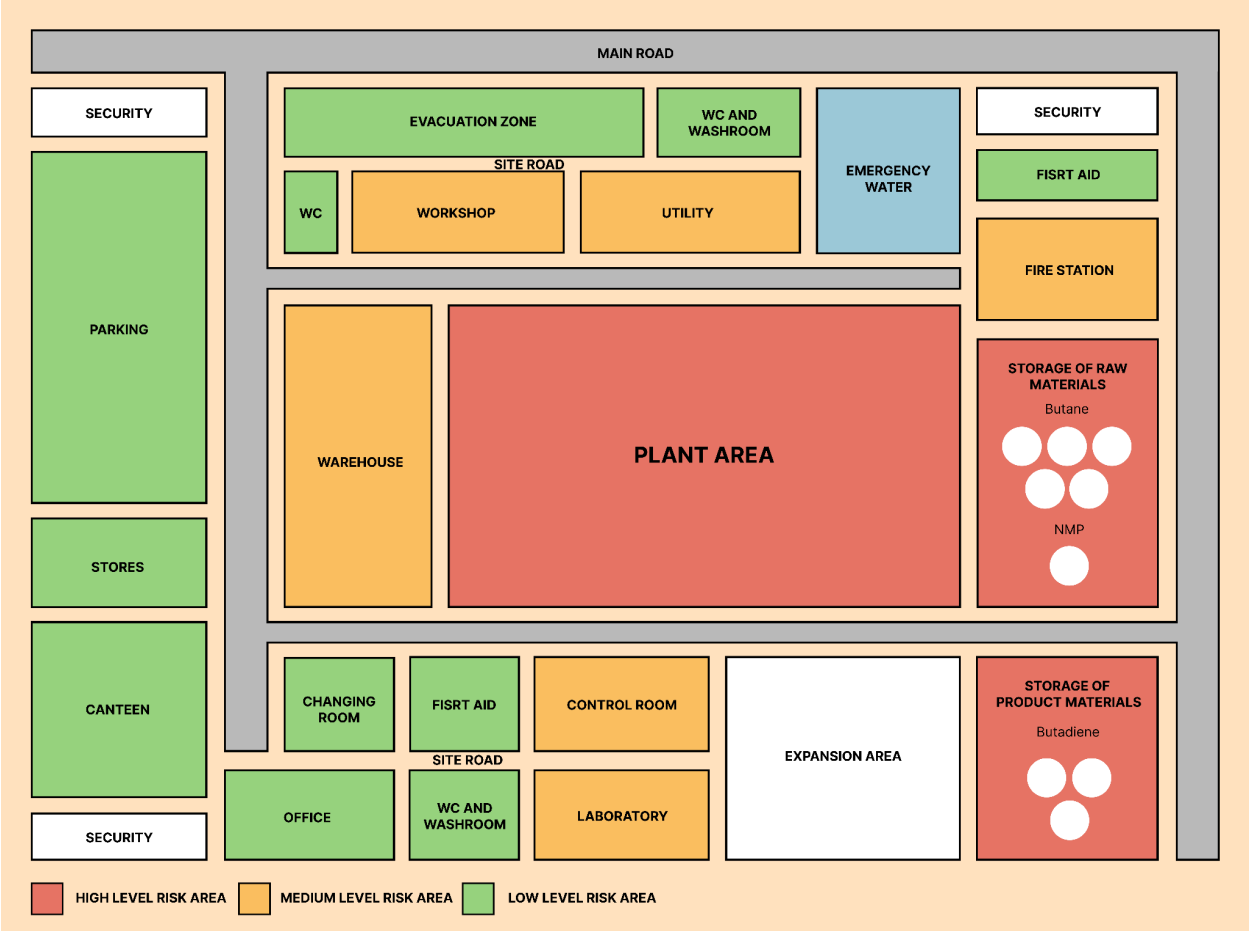

Figure 5.2.3. Butadiene production plant layout

Storage and production area

Raw materials and product storage zones are located separately from the main production area to reduce the risk of cross-contamination and improve overall safety. Additionally, the

storage tanks were placed closer to the main road within the Chemical Park Taraz. This strategic positioning allows for faster loading and unloading of raw materials and final products, improving overall logistics efficiency and minimizing transportation time. The layout also specifies the number of storage tanks for each substance. There are 5 tanks designated for butane, 1 tank for NMP, and 3 tanks for the final product butadiene.

Safety and emergency zones

Emergency zones, such as the fire station, first aid, emergency water and evacuation area are purposely placed nearby to ensure a fast response in case of incidents. In terms of security, the plant has three checkpoints at the borders of the industrial area, which improves access control and reduces the risk of unauthorized entry.

Human-oriented zoning

To ensure both safety and comfort, parking areas, the canteen, and office buildings are positioned away from the main production zones, reducing exposure to high-risk operations. At the same time, washrooms and changing rooms are placed near work areas, providing convenience for employees and supporting hygiene. These design choices contribute to a safer and more comfortable working environment.

Future expansion

The layout includes reserved space near both the plant area and the storage area, allowing for potential future expansion. This provides flexibility for scaling up operations or adding new units without disrupting the current workflow.

Chapter 6. Environment and Waste Streams

The process of production of 1,3-butadiene involves hazardous compounds such as n-butane, 1-butene, 1,3-butadiene, and hydrogen, which present significant fire, explosion, and toxicity risks, especially under high-temperature or pressurized conditions. Hydrogen and 1,3-butadiene gases exhibit wide flammability ranges and high reactivity, requiring strict control of ignition sources and exposure limits. Additional hazards include the carcinogenic potential of butadiene and the toxicity of certain metal oxide catalysts. A detailed assessment of properties, hazards, and safety measures is provided in Appendix C. In order to avoid any potential emergency cases, governmental law, fire safety standards and waste stream treatment should be taken into consideration.

6.1 Overview of Waste Streams

In the production of 1,3-butadiene from n-butane, two primary gaseous waste streams are generated: the "H_2 stream," which is the top product stream of the splitter (F-101) and the "By-products stream," which is the top stream of the distillation column (T-101).

These waste streams predominantly consist of hydrogen and hydrocarbon gases, making them ideal candidates for thermal oxidation. Rather than venting these streams, they are directed to an incineration system to recover energy and reduce environmental impact. Table 6.1.1 summarizes the composition and thermodynamic properties of each waste stream and combustion reactions.

Table 6.1.1. Composition and properties of waste streams

Mole Flows (mol/hour)	H_2	By-products	Burning Reactions
T [C]	14	92.3	-
P [bar]	20.2	20.2	-
Vapor fraction	1	0.74	-
n-butane (C4H10)	6,743.74	1,484.28	$C_4H_{10}+6.5O_2 \rightarrow 4CO_2 + 5H_2O$
Butene (C4H8)	22,531.60	3,559.05	$C_4H_8+6O_2 \rightarrow 4CO_2 + 4H_2O$
Butadiene (C4H6)	26,090.46	4,899.92	$C_4H_6+5.5O_2 \rightarrow 4CO_2 + 3H_2O$
Ethylene	155.11	313.75	$C_2H_4+3O_2 \rightarrow 2CO_2 + 2H_2O$
Propylene	73.99	863.71	$C_3H_6+4.5O_2 \rightarrow 3CO_2 + 3H_2O$
Propane (C3H8)	121.64	1,867.52	$C_3H_8+5O_2 \rightarrow 3CO_2 + 4H_2O$

H2	532,258.77	902.38	$2H_2+O_2 \rightarrow 2H_2O$
NMP	0.002	0.000001	C_5H_9NO+ $7.5O_2 \rightarrow 5CO_2 + 4.5H_2O + NO_2$
H2O	107.09	1,104.27	-
Total	588,082.39	14,994.88	-

Full combustion will take place as the plant will provide enough oxygen. Since the amount NMP in both streams is very low and it will undergo high-temperature combustion with excess air, complete oxidation is assumed. Any risk of incomplete combustion is negligible under standard operating conditions.

6.2 Law Regulations

Water vapor (H_2O) is not strictly regulated as an air pollutant under Kazakhstan's environmental legislation. According to the official *List of pollutants subject to regulation and accounting* approved by the Order of the Minister of Energy of the Republic of Kazakhstan No. 436 (dated December 28, 2015), water vapor is not included among the substances subject to emission limits or environmental permits [67].

However, combustion units must comply with emissions regulations for actual pollutants like CO_2, NO_2, and volatile organics (if present in trace amounts). Proper burner design, temperature control, and excess oxygen ensure regulatory compliance and environmental safety.

In order to safely burn the waste streams, a thermal oxidizer can be used with typical operating temperature range from 850 and 1,100 °C. It will provide complete combustion of hydrocarbons and hydrogen, while minimizing the formation of harmful by-products such as carbon monoxide or unburned volatile organic compounds. The hot streams of CO_2 and water can be used for heat exchangers in order to maximize energy recovery. Then to reduce the carbon footprint of the process, a CO_2 absorption unit can be installed [68].

6.3 Safety Measures for Incinerating Hydrogen Stream

- Oxygen Supply: Ensure 110% of stoichiometric air to avoid flammable mixtures.
- Ignition Control: Use pilot burners or spark igniters rated for hydrogen [69].
- Mixing: Achieve uniform H_2-air mixing to prevent hotspots or incomplete combustion.
- Combustor Design: Equip with flame arrestors and check valves to prevent flashbacks [70].
- Temperature Control: Design for high combustion temperatures with appropriate refractory materials.

- Instrumentation: Install gas detectors for H_2 leaks and automatic shutdown systems [71].
- Ventilation: Ensure effective ventilation around combustion units.

6.4 Energy Recovery from Waste Stream Combustion

The amount of energy which will be produced by burning these streams was found using a special property named “Higher Heating Value” at 15 °C for both streams in Aspen Plus v14:

Table 6.4.1. Energy saved by burning waste streams

	H_2	By-products
Higher Heating Value, kJ/mol	510.06	2208.66
Higher Heating Value, MW	83.32	9.20

The combustion of waste streams, particularly hydrogen and process by-products, presents a significant opportunity for energy recovery in the butadiene production process. As shown in Table 6.1.2, the higher heating value (HHV) of hydrogen reaches approximately 510.06 kJ/mol, which translates to an impressive 83.32 MW of recoverable energy. Similarly, the by-product stream contributes an additional 9.20 MW of thermal energy. This substantial energy output can be effectively utilized for steam generation, process heating, or power recovery, thereby reducing the overall energy demand from external utilities. Such integration not only improves the energy efficiency of the plant but also contributes to sustainable waste management, aligning with industrial best practices for resource optimization.

The substantial energy recovered from the combustion of hydrogen (83.32 MW) and process by-products (9.20 MW) can be strategically integrated into various thermal and utility demands within the butadiene production plant. However, combustion gases from H_2 and by-products can reach temperatures above 2000 °C, but practical recovery is limited by materials of construction and downstream equipment tolerance. Most waste heat boilers and piping systems are designed for exhaust gas temperatures below 650–700 °C to avoid [72]:

- Tube scaling and thermal stress
- Damage to insulation and protective linings
- Equipment degradation

Thus, dampers and dilution air may be used to control the temperature before heat exchange.

6.5 Water Stream Outlet

The plant's operation includes a water stream utilized in heat exchangers, serving as a cooling medium. This water stream enters the heat exchanger at an initial temperature of 20 °C and exits at 29.8 °C, with a continuous flow rate of 500 kg/s. The temperature increase of 9.8 °C ensures that the discharged water remains below 30 °C, aligning with Kazakhstan's environmental regulations for thermal discharges into surface water bodies:

According to Kazakhstan's environmental standards, the permissible temperature of wastewater discharged into natural water bodies should not exceed 30 °C in order to prevent thermal pollution and protect aquatic ecosystems [73]. The current discharge temperature of 29.8 °C complies with this regulation, ensuring minimal thermal impact on the receiving water body.

Regarding the flow rate, a discharge of 500 kg/s is substantial and necessitates obtaining the appropriate permits from Kazakhstan's environmental authorities [73]. The permitting process involves assessing the potential impact on the local water body, ensuring that the discharge does not adversely affect water quality or aquatic life. By adhering to the regulatory framework and securing the necessary permissions, the plant demonstrates its commitment to environmental compliance and sustainable operations.

6.6 Catalysts Usage and Disposal

The 10Ni–5Fe–5Co–30Bi catalyst on γ-Al_2O_3 contains toxic heavy metals that pose significant health hazards. Inhalation of fine catalyst dust is dangerous: nickel and cobalt compounds are harmful and suspected carcinogens when inhaled, and nickel can cause skin sensitization upon contact [74]. Safety measures are listed below:

- Proper handling requires avoiding dust generation and using protective equipment to prevent inhalation or skin exposure.
- The fresh catalyst should be stored in tightly sealed containers in a cool, dry, well-ventilated area restricted to trained personnel [75].
- Contact with moisture or incompatible chemicals (e.g. strong acids) should be minimized to prevent reactions or leaching of metals.
- Spent catalyst must be handled cautiously: it may remain hot and could become pyrophoric upon exposure to air if it contains residual hydrocarbons or reduced metals [76].

Therefore, used catalysts should be cooled under inert conditions and stored similarly in closed, labeled containers (on impermeable surfaces) to avoid dust release and environmental contamination. For disposal or regeneration, specialized procedures are recommended – spent catalysts are often treated as hazardous waste, with disposal via controlled landfill (with leachate

precautions) or sent for metal recovery [77]. Alternatively, controlled oxidative regeneration can be used to remove carbon deposits and restore catalyst activity, reducing waste generation.

6.7 Fire safety

Since the plant involves the presence of highly flammable organic compounds and combustion units, the plant should implement a fire safety strategy such as european fire safety standards (CFPA-E Guideline No. 18.) [78]. The buildings should be constructed with non-combustible materials, such as reinforced concrete. Hydrants are required to be installed every 50–75 m, with pressure maintained across the site for easy access in case of emergency. Additionally, explosion-proof electrical fittings, adequate ventilation, and proper grounding of equipment are crucial to prevent ignition in areas with flammable vapors. A clear fire safety organization, preventive maintenance program, and staff training should also be incorporated to prevent and handle any emergency cases.

In order to minimize the risk of leakage, all pipelines, plant units and storage vessels should be fully sealed and frequently inspected. Gas detectors must be installed near potential release points, with automatic shutdown systems in case of detection of any gases. Despite the fact NMP has low flammability, it poses health and environmental risks, so its storage and transfer must be carefully controlled using closed systems, proper ventilation, and spill containment protocols. All hazard identification tables for potentially hazardous substances (including catalyst) on the plant can be seen in Appendix C4.

Chapter 7. Total Investment and Profitability

Economic analysis were conducted based on the Chapter 16&17 of the fourth edition of "Product and process design principles: synthesis, analysis, and evaluation" textbook by Seider and Chapter 7 of second edition of "|Chemical Engineering Design" textbook by Towler [31]. Inside battery limit (ISBL) was calculated using Capital costs of equipment, which in turn was obtained using Aspen Process Economic Analyzer (APEA) and Towler textbook [31]. Detailed calculations are shown in the 'economic_analysis.xlsx' file. Offsite battery limits (OSBL) was estimated to be 20% of ISBL which is reasonable estimation for our plant. The cost of equipment can be seen in Table 7.1.

Table 7.1. Equipment Cost

Equipment name	Equipment Cost	Capital cost (including Lang factor, cost escalation)
E-100	$78,500	$201,117
E-101	$816,780*	$816,780
E-102	$2,655,256*	$9,293,396
E-103	$269,383*	$269,383
E-104	$126,900	$325,118
C-101	$7,487,142*	$18,717,854
C-102	$14,513,629*	$14,513,629
C-103	$4,381,213*	$10,953,032
R-101	$437,949*	$437,949
T-101	$1,508,593*	$1,508,593
T-102		
RC-101	$8,938,300	$26,171,342
F-101	$118,000	$345,504
T-103	$1,717,500	$5,028,840
Storage Tanks	$9,000,000	$9,000,000
Total Cost	$51,544,552	$97,582,538

* - unit cost was estimated using a textbook, hence Lang and location factors with cost escalation were already taken into account.

After the cost of equipment was obtained, the ones taken from APEA were multiplied by their respective Lang factors and location factor of 0.732. Location factors accounted for indigenous production in China with a 20% increase due to the distance between China and

Taraz. Cost escalation was done based on CEPCI factors of book (532.9) and of June 2024 (800). The resultant value is around $97.6MM which roughly describes our ISBL. Including OSBL, engineering costs and contingency charges, the total fixed capital investment (FCI) was estimated to be around $140.5MM. By adding working capital cost (10% of FCI) Total Capital Investment (TCI) of $154.6MM was obtained.

Table 7.2. Total Capital Investment

Cost type	Capital cost (including Lang factor, cost escalation)
ISBL	$97,582,538
OSBL	$19,516,508
Engineering cost	$11,709,905
Contingency Charges	$11,709,905
Total Fixed Capital Investment (FCI)	$140,518,854
Working Capital	$14,051,885
Total Capital Investment (TCI)	$154,570,740

Cost of production per year included utility, labor related operations, maintenance, overheads, transportation and general expenses. Estimated cost of production is around $39.4MM per year. To account for the number of operators, Alkhayat and Gerrard correlation was obtained for 28 fluid processing units (including reboiler and condenser in each distillation column). Correlation shows 13 operators per shift and overall 65 operators are required (multiplied by 5 to consider day offs, sick leaves and training). Values for utilities, except electricity was taken from APEA. Electricity expenditures were based on the Taraz region's cost. Utilities alone contribute $19.8MM, reflecting the high energy and material demands of the process-particularly steam ($6.7MM), refrigerants ($3MM), and cooling water ($1.3MM). Labor-related operations, including operator wages, benefits, technical assistance, and control laboratory support, total $1.3MM, while maintenance and operational reliability efforts contribute another $3.2MM.

Operating overhead, which includes expenses like general plant oversight, mechanical department services, and business services, adds a further layer of cost, along with depreciation and transportation costs. Depreciation was determined using the Straight-Line method. Beyond the manufacturing floor, General Expenses play a significant role, amounting to $9.5MM. These include selling expenses, research and development ($4.8MM), administrative costs ($2MM), and management incentive compensation, indicating investment into both business growth and operational sustainability.

Table 7.3. Total General Expenses

Cost type	Capital cost (including Lang factor, cost escalation)
Utilities	$19,872,235
Total labor-related operations	$1,325,088
Total maintenance	$3,231,934
Operating overhead	$528,685
Depreciation	$2,209,802
Transportation	$4,321,000
Research and development	$4,752,000
Administrative expense	$1,980,000
Management incentive compensation	$1,237,500
Total General Expenses (GE)	$9,454,500

Market analysis showed that the butadiene price ranges for Europe (1026-1060 USD/metric ton) and for Asia Pacific regions (1265-1926 USD/metric ton). Since the information on the butadiene price for CIS regions is unavailable, the price of 1100 USD/metric ton was assumed. Revenue from selling the final product is $99MM ($1100/ton), yielding $59.6MM of constant gross profit.

Table 7.4. Production vs Selling Price

	Unit cost	Annual Cost
Production cost	$438/ton	$39,431,642
Selling price	$1100/ton	$99,000,000

Accounting for depreciation (considering 20 years of service life) of $4.4MM, it was calculated that Net Present Value (NPV) of the plant will be positive in 9 years as can be seen from Figure 7.1. Interest rate was taken as 15%. Positive value of NPV after 9th year justifies the profitability of the project - investment will give benefit.

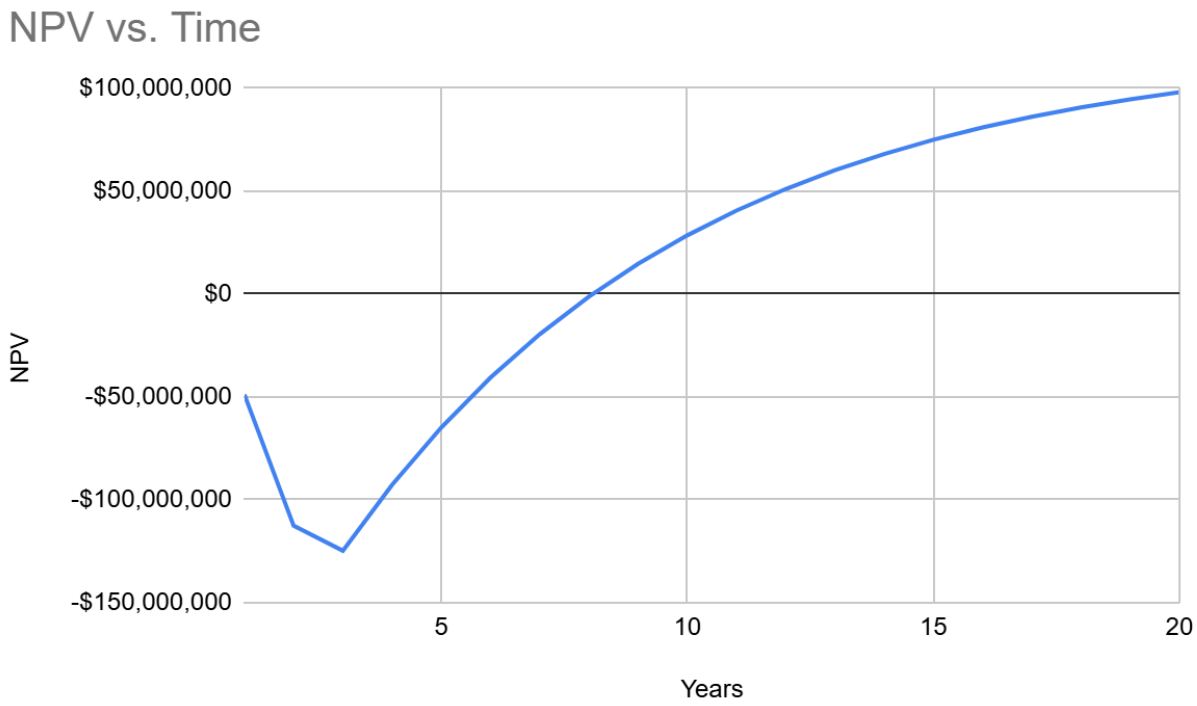

Figure 7.1. NPV over 20 years

Return on investment (ROI) is calculated to be 39.09% while payback period (PBP) based on constant annual cash flows is 2.4 years. Internal rate of return (IRR) was obtained for a 5, 10 and 20 years period. Table 7.2 reveals that in 20 years IRR will be 26%.

Table 7.5. IRR values.

IRR in 5 years	-12%
IRR in 10 years	20%
IRR in 20 years	26%

The butadiene production in Kazakhstan has medium risk level with 16-24% Minimum Acceptable Rate of Return (MARR%) [Bidar & Shahraki, 2018, Energy and Exergo-Economic Assessments of Gas Turbine Based CHP Systems: A Case Study of SPGC Utility Plant, Iran. J. Chem. Chem. Eng., Vol.37, No.5]. IRR for 20 years is higher than the MARR, which means that the project is financially attractive, exceeding an investor's expectations.

The total capital investment required for the butadiene plant is $154.6MM. The economic analysis for 20 years of service life shows that the project is financially viable and initial investments will be recovered after 2.4 years.

Chapter 8. Conclusions and future work

This Capstone project presented a comprehensive design of an industrial-scale chemical plant for the production of 1,3-butadiene from n-butane, with an estimated capacity of 90,000 tons per year. The design was developed considering both the technological feasibility and the regional demand in the Commonwealth of Independent States (CIS), excluding Russia. Given Kazakhstan's strategic location and growing chemical sector, the proposed site in Taraz offers favorable infrastructure, climate conditions, and access to raw materials from China.

Through comparative analysis of multiple production methods, catalytic dehydrogenation (CDH) of n-butane was selected as the most suitable route due to its lower environmental impact, moderate energy demands, and competitive selectivity towards 1,3-butadiene. Catalyst screening and economic evaluation identified 10Ni–5Fe–5Co–30Bi catalyst on γ-Al_2O_3 as the most effective and cost-efficient catalyst. A fixed-bed adiabatic reactor was chosen for its simplicity, robust performance, and scalability.

The downstream separation system was optimized to meet the 99.5% purity specification of butadiene required for polymer applications. Aspen Plus simulations were employed for heat exchanger sizing, distillation column design, and pressure drop estimation, ensuring accurate process modeling. Special emphasis was placed on waste heat recovery, where over 90 MW of thermal energy from waste hydrogen and hydrocarbon combustion can be recovered and redirected to key utility units, such as reboilers and preheaters. Environmental considerations were addressed by incorporating an incinerator and wastewater control systems to comply with Kazakhstan's environmental regulations, particularly concerning thermal discharge and pollutant emissions.

While the current project successfully outlines a feasible and efficient plant design, several areas warrant further investigation:

- Pilot plant development: construction and testing of a small-scale pilot unit is recommended to validate the reactor performance, catalyst stability, and process yields under real operating conditions.
- Process control and automation: development of a dynamic process control strategy and integration of advanced automation systems to ensure safety, optimize energy use, and minimize downtime.
- Thermodynamic modeling limitations: since molecular interactions with Henry components are missing in data banks and cannot be estimated properly in Aspen Plus v14, future research should focus on improving thermodynamic models for such systems. With more accurate data, the design of the T-101 depropanizer column will become more precise and realistic.

- Catalyst longevity and regeneration: long-term catalyst testing should be conducted to evaluate deactivation mechanisms and develop on-site regeneration protocols to reduce operating costs.
- CO_2 and emissions utilization: explore carbon capture or chemical conversion of CO_2 generated during combustion to further enhance the plant's sustainability profile.
- Economic sensitivity analysis: a more detailed techno-economic analysis considering fluctuating market prices of butane, utilities, and butadiene is necessary for investment decisions.

Reference list

1. White, W.C.J.C.-b.i., *Butadiene production process overview.* 200**7. 166(1-3**): p. 10-14.
2. PubChem. *1,3-Butadiene*. 2024; Available from: https://pubchem.ncbi.nlm.nih.gov/compound/1_3-Butadiene.
3. Kirk-Othmer, *Kirk-Othmer Encyclopedia of Chemical Technology, Volume 23.* 2006.
4. Humans, I.W.G.o.t.E.o.C.R.t., *1, 3-Butadiene*, in *Re-evaluation of Some Organic Chemicals, Hydrazine and Hydrogen Peroxide*. 1999, International Agency for Research on Cancer.
5. *Бутадиен-1,3 Технические условия*. 2012 ГОСТ Р 55066-2012].
6. Titan Group, "Butadiene," *Product Catalog – Petrochemical Products*, [Online]. Available: https://titan-group.ru/catalog/neftekhimicheskaya-produktsiya/produktsiya-orgsinteza/butadien/
7. Tatneft-Togliatti, *Technical Specifications for Butadiene Production*, [Online]. Available: https://togliatti.tatneft.ru/storage/block_editor/files/ad40b6700e205f3ab52bcf43904065b2b7cf063d.pdf
8. Saratov Petroleum Chemical Plant (SNHZ), Butadiene-1,3 TU 38.103658-88 with Amendments 1–9, [Online]. Available: https://snhz.ru/kp/?event=pages&page=butadien-13-tu-38.103658-88-s-izm.-1-9-5afe5849ae69f
9. *1.3 Бутадиен (C4H6)*. Available from: https://www.bk-group.org/chistye-gazy/1-3-butadien.
10. LG Chem, *1,3-Butadiene Product Specifications*, Issued Feb. 16, 2022. [Online]. Available: https://www.lgchem.com
11. *Выбрана технология для завода бутадиена и синтетического каучука в Казахстане*. 2023; Available from: https://plastinfo.ru/information/news/51071_14.03.2023/.
12. Gholami, Z., et al., *A review on the production of light olefins using steam cracking of hydrocarbons.* 2021. 14(23): p. 8190.
13. Rischard, J., et al., *Oxidative dehydrogenation of n-butane to butadiene with Mo-V-MgO catalysts in a two-zone fluidized bed reactor.* 2016. 511: p. 23-30.
14. Schindler, G.-P., et al., *Method for the production of butadiene from n-butane*. 2006, Google Patents.
15. *BUTADIENE: PRODUCT STEWARDSHIP GUIDANCE MANUAL*. 2024.
16. Yan, W., et al., *Catalytic oxidative dehydrogenation of 1-butene to 1, 3-butadiene using CO2.* 2014. 46: p. 208-212.
17. Young, B., et al., *Environmental life cycle assessment of olefins and by-product hydrogen from steam cracking of natural gas liquids, naphtha, and gas oil.* 2022. 359: p. 131884.
18. Van Goethem, M.W.M., *Next generation steam cracking reactor concept.* 2010.

19. Ntola, P. and M.J.C. Shozi, *Gas-Phase Oxidative Dehydrogenation of n-Octane over Metal Oxide Catalysts: A Review.* 2024. 14(2): p. 100.
20. Milne, D., et al., *The Oxidative Dehydrogenation of n-Butane in a Fixed-Bed Reactor and in an Inert Porous Membrane Reactor Maximizing the Production of Butenes and Butadiene.* 2006. 45(8): p. 2661-2671.
21. Chu, M., et al., *Suppressing Dehydroisomerization Boosts n‐Butane Dehydrogenation with High Butadiene Selectivity.* 2021. 27(45): p. 11643-11648.
22. Kurokawa, H.J.J.o.M.S. and C. Engineering, *Dehydrogenation of n-butane to butenes and 1, 3-butadiene over PtAg/Al 2 O 3 catalysts in the presence of H 2.* 2018. 6(07): p. 16.
23. Akhairi, M. and S.K.J.I.j.o.h.e. Kamarudin, *Catalysts in direct ethanol fuel cell (DEFC): An overview.* 2016. 41(7): p. 4214-4228.
24. Zhang, Y., et al., *Mechanism and kinetics of n-butane dehydrogenation to 1, 3-butadiene catalyzed by isolated Pt sites grafted onto≡ SiOZn–OH nests in dealuminated zeolite Beta.* 2022. 12(6): p. 3333-3345.
25. Brencio, C., et al., *Butadiene production in membrane reactors: A techno-economic analysis.* 2022. 47(50): p. 21375-21390.
26. Jermy, B.R., et al., *Oxidative dehydrogenation of n-butane to butadiene over Bi–Ni–O/γ-alumina catalyst.* 2015. 400: p. 121-131.
27. *BUTADIENE: PRODUCT STEWARDSHIP GUIDANCE MANUAL*. 2024.
28. *Butadiene Production from n-Butane*. 2021; Available from: https://cdn.intratec.us/docs/reports/previews/butadiene-e11a-b.pdf.
29. G. Tanimu, et al. “Kinetic Study on *N*-Butane Oxidative Dehydrogenation over the (Ni, Fe, Co)–Bi–O/γ-al_2O_3 Catalyst.” *Industrial & Engineering Chemistry Research*, vol. 59, no. 7, 27 Jan. 2020, pp. 2773–2780, https://doi.org/10.1021/acs.iecr.9b06121. Accessed 15 Mar. 2025.
30. G. Towler.&Sinnott,R. (2008). Chemical Engineering Design. Elsevier Inc.
31. G. Towler and R. Sinnott, “Capital Cost Estimating,” *Chemical Engineering Design*, pp. 307–354, 2013, doi: https://doi.org/10.1016/b978-0-08-096659-5.00007-9.
32. BPVC.II.D.C - BPVC Section II-Materials-Part D-Properties-(Mertric). ASME, 201
33. Coker, A. Kayode. (2015). Ludwig's Applied Process Design for Chemical and Petrochemical Plants, Volume 3 (4th Edition). Elsevier. Retrieved from https://app.knovel.com/hotlink/toc/id:kpLAPDCP12/ludwigs-applied-process/ludwigs-applied-process
34. Darazz, Ahmed Refaee, and Abdul Aziz Al-Obaidan. "What is the Best Compressor for Our Applications, Centrifugal or Reciprocating." Paper presented at the SPE Kuwait Oil and Gas Show and Conference, Kuwait City, Kuwait, October 2013. doi: https://doi.org/10.2118/167292-MS
35. M. S. Peters, K. D. Timmerhaus, and R. E. West, *Plant Design and Economics for Chemical Engineers*, 5th ed. New York, NY, USA: McGraw-Hill Professional, 2002.

36. K. H. Lüdtke, *Process centrifugal compressors* : basics, function, operation, design, application /. Berlin ; London: Springer, 2010.
37. Dowson, P., Bauer, D., & Laney, S. (2008). Selection of Materials and Material Related Processes for Centrifugal Compressors and Steam Turbines in the Oil and Petrochemical Industry. *Texas A&M University. Turbomachinery Laboratories*. https://oaktrust.library.tamu.edu/items/89eb3b66-2a0e-4440-9cdf-de3808868556
38. "4330 Steel vs 4340 Steel: What's the Difference?" *MachineMFG*. Available: https://shop.machinemfg.com/4330-steel-vs-4340-steel-whats-the-difference/
39. "4140 vs 4130: What's the Difference?" *Fushun Special Steel*. Available: https://www.fushunspecialsteel.com/4140-vs-4130/
40. "AISI Alloy 4140 Steel Bar," ASTM Steel. Available: https://www.astmsteel.com/product/aisi-alloy-4140-steel-bar/
41. "17-4 PH vs 410 Stainless Steel: What's the Difference?" The Piping Mart Blog. Available: https://blog.thepipingmart.com/metals/17-4-ph-vs-410-stainless-steel-whats-the-difference/
42. "Low, Medium & High Carbon Steel," Essentra Components. Available: https://www.essentracomponents.com/en-us/news/solutions/access-hardware/low-medium-high-carbon-steel.
43. P. Flenner, "Carbon Steel Handbook," Electric Power Research Institute (EPRI), Palo Alto, CA, USA, Rep. 1014670, Mar. 2007. [Online]. Available: https://www.uobabylon.edu.iq/eprints/publication_12_18692_70.pdf
44. E. Listijorini, N. D. Pratama, M. A. Vianda and T. R. Biyanto, "Optimization of depropanizer column quality product by changing controller set points of reflux flow and reboiler heat rate," 2016 6th International Annual Engineering Seminar (InAES), Yogyakarta, Indonesia, 2016, pp. 116-120, doi: 10.1109/INAES.2016.7821918.
45. *Distillation Column Trays and Packing: A Comprehensive Overview*. (n.d.). https://www.chemicalpackings.com/article/distillation-column-tray.html
46. Perry, R.H., Green, D.W. and Southard, M.Z. (2018) Perry's Chemical Engineers' Handbook. 9th Edition, McGraw-Hill Education, New York, 2272.
47. André B., Burak E., Boelo S., (2020).Industrial Separation Processes: Fundamentals. pKnovel - Industrial Separation Processes - Fundamentals
48. *316 / 316L Stainless Steel - AMS 5524, AMS 5507 - Sheet, Coil & bar*. (n.d.). https://www.upmet.com/products/stainless-steel/316316l
49. "life-long service 6000m3 round LPG Propane Gas Spherical Tank Project Terminal," Made, https://cimchonto.en.made-in-china.com/product/lswALpDMCFUm/China-Life-Long-Service-6000m3-Round-LPG-Propane-Gas-Spherical-Tank-Project-Terminal.html?pv_id=1ip91uo0709c&faw_id=1ip91vru4b79&bv_id=1ip9234f9021&pbv_id=1ip91uncbc62 (accessed Apr. 20, 2025).

50. *Специальная Экономическая Зона «Химический Парк Тараз»*. Available from: http://sezunion.kz/kz/component/k2/item/38-spetsialnaya-ekonomicheskaya-zona-khimicheskij-park-taraz.html.
51. *Специальные экономические зоны*. 2024; Available from: https://invest.gov.kz/ru/doing-business-here/fez-and/the-list-of-sez-and/.
52. *National Centers for Environmental Information.*
53. *Tengizchevroil supports development of Kazakhstan's Petrochemical Industry*. 2024; Available from: https://www.tengizchevroil.com/tco-news/detail/2024/02/20/tengizchevroil-supports-development-of-kazakhstan-s-petrochemical-industry.
54. *Butane CAS NO.106-97-8*. Available from: https://chemwill.lookchem.com/products/CasNo-106-97-8-Butane-22647041.html.
55. *LPG.СНГ. NG. ПГТ. Средневзвешенная цена на пропан-бутан технический в Казахстане составила 60 466,44 тенге за 1 метрическую тонну*. 2021; Available from: https://ets.kz/press_centre/indices/lpg-sng-ng-pgg-srednevzveshennaya-tsena-na-propan-butan-tekhnicheskiy-v-kazakhstane-sostavila-60-466/#:~:text=%D0%A1%D1%80%D0%B5%D0%B4%D0%BD%D0%B5%D0%B2%D0%B7%D0%B2%D0%B5%D1%88%D0%B5%D0%BD%D0%BD%D0%B0%D1%8F%20%D1%86%D0%B5%D0%BD%D0%B0%20%D0%BD%D0%B0%20%D0%B1%D1%83%D1%82%D0%B0%D0%BD%20%D1%82%D0%B5%D1%85%D0%BD%D0%B8%D1%87%D0%B5%D1%81%D0%BA%D0%B8%D0%B9,%D1%82%D0%B5%D0%BD%D0%B3%D0%B5%20%D0%B7%D0%B0%201%20%D0%BC%D0%B5%D1%82%D1%80%D0%B8%D1%87%D0%B5%D1%81%D0%BA%D1%83%D1%8E%20%D1%82%D0%BE%D0%BD%D0%BD%D1%83.
56. *Special Economic Zone*. Available from: https://investastana.kz/en/spetsialnaya-ekonomicheskaya-zona/#:~:text=A%20special%20economic%20zone%20is,implementation%20of%20priority%20activities%20operates.
57. *General information about SEZ*. Available from: https://nipt.kz/o-kompanii/55-obschaja-informacija-o-sjez.html.
58. Брославская, Н. *Налоги в Казахстане*. 2024; Available from: https://www.bcc.kz/bcc-journal/taxes-in-kazakhstan/.
59. *Налогообложение специальных экономических зон в Казахстане* 2013; Available from: https://online.zakon.kz/Document/?doc_id=31424148&pos=11;22#pos=11;22.
60. *О ставках таможенных пошлин на ввозимые товары*. 2006; Available from: https://adilet.zan.kz/rus/docs/P960001389_.
61. *Kazakhstan - Country Commercial Guide*. 2022; Available from: https://www.trade.gov/country-commercial-guides/kazakhstan-import-tariffs.
62. *Kazakhstan: Corporate - Other taxes*. 2024; Available from: https://taxsummaries.pwc.com/kazakhstan/corporate/other-taxes.

63. *О внесении изменений в приказ Министра национальной экономики Республики Казахстан от 17 февраля 2016 года № 81 "Об утверждении Перечня товаров, в отношении которых применяются вывозные таможенные пошлины, размера ставок и срока их действия и Правил расчета размера ставок вывозных таможенных пошлин на сырую нефть и товары, выработанные из нефти"*. 2020; Available from: https://adilet.zan.kz/rus/docs/V2000021932.
64. *Памятка налогоплательщику по налогу на имущество юридических лиц и индивидуальных предпринимателей*. 2012; Available from: https://online.zakon.kz/Document/?doc_id=30394320&pos=20;15#pos=20;15.
65. *Средняя рыночная цена сырой нефти (в долл. США), для определения ставки вывозной таможенной пошлины на сырую нефть и нефтепродукты*. 2024.
66. S. Moran, Process Plant Layout, 2nd ed. Oxford: Butterworth-Heinemann, 2016.
67. [1] Министерство сельского хозяйства Республики Казахстан, *Санитарные правила "Санитарно-эпидемиологические требования к водным объектам, используемым в хозяйственно-питьевых целях и для водоснабжения населения"*, № ҚР ДСМ-156, зарегистрировано 27 декабря 2016 г. [Online]. Available: https://adilet.zan.kz/rus/docs/V1600014360
68. U.S. Environmental Protection Agency, Technical Overview of TOXICS RELEASE INVENTORY (TRI) Reporting for the Butadiene Industry, EPA Document No. TO_B. [Online]. Available: https://www3.epa.gov/ttnchie1/mkb/documents/TO_B.pdf
69. Raadman Burner, “What is a Pilot Burner?” Raadman Burner Blog, [Online]. Available: https://raadmanburner.com/blog/pilot-burner/.
70. Elsevier, “Flame Arrestor,” ScienceDirect Topics. [Online]. Available: https://www.sciencedirect.com/topics/engineering/flame-arrestor
71. K. D. Edwards and D. A. Hitt, Hydrogen Combustion Fundamentals Applied to Advanced Propulsion and Power Concepts, NASA Technical Paper 3669, 1997. [Online]. Available: https://ntrs.nasa.gov/api/citations/19970033338/downloads/19970033338.pdf
72. U.S. Department of Energy, Waste Heat Recovery: Technology and Opportunities in U.S. Industry, Washington, DC: U.S. DOE, 2015. [Online]. Available: https://www.energy.gov/sites/prod/files/2016/02/f30/QTR2015-6M-Waste-Heat-Recovery.pdf
73. Government of the Republic of Kazakhstan, *On approval of the Rules for the use of water bodies for the needs of water supply*, No. 212, Aug. 21, 2007. [Online]. Available: https://adilet.zan.kz/eng/docs/K070000212
74. TA Instruments, *Safety Data Sheet: Nickel Cobalt Alloy*, Rev. E, Document No. 901135, [Online]. Available: https://www.tainstruments.com/pdf/safety-data-sheets/901135-Rev-E_SDS-Nickel-Cobalt-Alloy.pdf
75. ChemicalBook, *Nickel(II) Oxide: Material Safety Data Sheet (MSDS)*. [Online]. Available: https://www.chemicalbook.com/msds/nickel-ii-oxide.htm

76. Evonik Industries, *Industrial and Petrochemicals: Product and Safety Information*, 2018. [Online]. Available: https://products.evonik.com/assets/64/61/Industrial_and_Petrochemicals_2018_EN_196461.pdf
77. CONCAWE, *Management of Spent Catalysts from the Refining Industry*, Report No. 95/57, 2004. [Online]. Available: https://www.concawe.eu/wp-content/uploads/rpt_95-57-2004-01710-01-e.pdf
78. CFPA Europe, *Guideline No. 18: 2013 F – Fire Protection for Oil Heating Installations*, Confederation of Fire Protection Associations Europe, 2013. [Online]. Available: https://cfpa-e.eu/app/uploads/2022/03/CFPA_E_Guideline_No_18_2013_F.pdf

Appendices

Appendix A. Process Introduction

A.1 Market Analysis

Email Correspondence
Date: September 16, 2024

Translated Message to the "LLP Butadiene" (translated to English):

Dear Бутадиен representatives,

I hope this message finds you well. My name is Zhandarbek Sapargaliyev, and I am currently a student at Nazarbayev University, working on a capstone project focused on the production and market analysis of butadiene. As part of our project, we are reaching out to industry experts like you to gather essential data that will significantly contribute to the accuracy and relevance of our study.

1. We kindly request your assistance in answering the following questions related to your butadiene production process:
2. What is the purity of the produced butadiene?
3. What companies do you sell butadiene to, or plan to sell it to?
4. What are the current feedstock (butane) prices in the production?
5. What method (oxidative, catalytic or thermal dehydrogenation) and catalyst are used in the production process?
6. What are your company's costs for reactors and technical equipment?
7. What is the composition of the final product with impurities?
8. What is the demand for butadiene in the CIS market, both with and without Russia?

9. What is the annual production rate?
10. At what price will butadiene be sold?

Please be assured that any information you provide will be held in strict confidence and will not be shared with any third parties. The data will be used solely for the purpose of our capstone project and will not be included in any publications or publicly disseminated documents.

We greatly appreciate your time and consideration in assisting us with this project. Your insights will be invaluable to our research, and we look forward to potentially discussing this further with you.

Thank you for your support.

Warm regards,
Zhandarbek Sapargaliyev
Nazarbayev University

Original Message to the "LLP Butadiene" (in Russian):

Уважаемые представители компании Бутадиен,

Надеюсь, что это сообщение найдет вас в добром здравии. Меня зовут Жандарбек Сапаргалиев, я являюсь студентом Назарбаев Университета и работаю над дипломным проектом, посвященным производству и анализу рынка бутадиена. В рамках нашего проекта мы обращаемся к отраслевым экспертам, таким как вы, чтобы собрать важные данные, которые значительно повлияют на точность и актуальность нашего исследования.

Мы бы хотели попросить вас ответить на несколько вопросов, касающихся вашего процесса производства бутадиена:

1. Какова чистота производимого бутадиена?
2. Каким компаниям вы продаете бутадиен или планируете его продавать?
3. Какова текущая цена на сырье (бутан) в производстве?
4. Какой метод (окислительное, каталитическое или термическое дегидрирование) и какой катализатор вы используете в процессе производства?
5. Каковы затраты вашей компании на реакторы и техническое оборудование?
6. Каков состав конечного продукта с примесями?
7. Каков спрос на бутадиен на рынке СНГ, как с учетом России, так и без нее?
8. Каков ваш ежегодный объем производства?
9. По какой цене будет продаваться бутадиен?

Мы гарантируем, что любая предоставленная вами информация будет храниться в строгой конфиденциальности и не будет передана третьим лицам. Данные будут использоваться исключительно в рамках нашего дипломного проекта и не будут включены в какие-либо

публикации или открыто распространяемые документы.

Мы очень ценим ваше время и внимание к нашему проекту. Ваши ценные ответы будут неоценимы для нашего исследования, и мы надеемся на возможность дальнейшего обсуждения этих вопросов с вами.

Благодарим вас за поддержку.

С уважением,
Жандарбек Сапаргалиев
Назарбаев Университет

Response from the “LLP Butadiene” (translated to English):

Good afternoon. I apologize for the slight delay in responding.

1. Which purity of butadiene are you interested in? Are you asking about the purity after the dehydrogenation process or after the extraction process? I assume you mean after extraction, as the dehydrogenation process results in a mixture containing the produced butadiene. After extraction, the butadiene will have the following quality specifications: 1,3-butadiene – min. 99.7% by mass; 1,2-butadiene – max 20 ppm; methylacetylene – max 10 ppm; ethylacetylene – max 10 ppm; vinylacetylene – 5 ppm; carbonyls (as acetaldehyde) – max 10 ppm; N-methylpyrrolidone – max 5 ppm; butadiene dimer – max. 100 ppm; non-volatile residue – max. 100 ppm; inhibitor – max. 25-125 ppm.
2. The final and target products of "Butadiene" LLP are: divinyl-styrene synthetic rubber (DSSR), styrene-butadiene-styrene thermoplastic elastomer (SBS), MTBE as an octane-boosting additive for motor gasoline, isobutane-isobutylene fraction (IIF), and an off-balance remainder of 1,3-butadiene (totaling up to 45.2 thousand tons per year). Therefore, almost all of the produced butadiene (divinyl), which is 120,000 tons per year, serves as raw material for producing rubbers within the designed Complex. The off-balance remainder of butadiene is planned to be sold to PJSC Tatneft or other CIS and Chinese markets.
3. The price of raw butane from TCO is confidential under the terms of the contract and is calculated based on a separate formula linked to the market price.
4. The dehydrogenation of isobutane and butane is carried out through a catalytic process using an alumina-chrome catalyst (trivalent chromium).
5. At this current stage of the project's implementation, such data is not yet available. These will be determined during the EP (Engineering and Procurement) stage.
6. The composition of the final product (butadiene) is reflected in answer #1.
7. This information falls under the jurisdiction of the Shareholder, who handles the financial model and their marginal income.

8. The capacity of the "Production of Butadiene and its Derivatives in the Republic of Kazakhstan" project is based on the raw material (butane mixture) and amounts to 380,000 tons per year.
9. The answer is similar to the comment in point 7.

Best regards, V.G. Gatsko

If you have any further questions related to my area of expertise (technology and production), I am ready to assist.

Response from the “LLP Butadiene” (in Russian):

Добрый день. Извините за некоторую задержку с ответом.

1. Какая чистота бутадиена Вас интересует? После процесса дегидрирования или после процесса экстракции? Смею предположить, что все-таки после экстракции, т. к. после процесса дегидрирования получается смесь в которой содержится образовавшийся бутадиен. После экстракции бутадиен будет соответствовать следующим качественным показателям: 1,3-бутадиен - мин. 99,7% масс; 1,2-бутадиен - макс 20 ppm; метилацителен - макс 10 ppm; этилацетилен - макс 10ppm; Винилацителен - 5 ppm; карбонилы (в виде ацетальдегида) - макс 10 ppm; Н-метилпирролидон - макс 5 ppm; димер бутадиена - макс. 100 ppm; нелетучий остаток - макс. 100 ppm; ингибитор - макс. 25-125 ppm.
2. Конечными и целевыми продуктами ТОО "Бутадиен" являются: дивинил стирольный синтетический каучук (ДССК), стирол-бутадиен стирольный термоэластопласт (СБС), МТБЭ октаноповышающая присадка к автомобильным бензинам, изобутан-изобутеленовая фракция (ИИФ) и забалансовый остаток 1,3-будадиена (всего до 45,2 тыс.в год), то есть почти весь получаемый бутадиен (дивинил) 120,0 тыс. тонн в год, является сырьем для получения каучуков внутри проектируемого Комплекса. Забалансовый остаток бутадиена планируется продавать на мощности ПАО Татнефть либо на иные рынки СНГ и Китая.
3. Цена на сырьевой бутан с ТШО является конфиденциальной информацией по условиям договора и рассчитывается по отдельной формуле с привязкой к рыночной цене.
4. Дегидрирование изобутана и бутана производятся каталитическим процессом с использованием алюмо-хромного катализатора (3-х валентный хром).
5. На текущем этапе реализации проекта такие данный пока отсутствуют. Они будут определены на стадии ЕР.
6. Состав конечного продукта (бутадиена) отражены в ответе №1.
7. Данная информация находится в ведении Акционера, который считает финансовую модель и свой маржинальный доход.

8. Мощность проекта "Производства бутадиена и его производных в РК" считается по сырью (смеси бутанов) и составляет 380,0 тыс. тонн в год.
9. Ответ аналогичен комментарию в пункте 7.

С уважением, Гацко В.Г.

Если вопросы будут по моему профилю (технология и производство), то готов помочь.

A.2 Projected production rate

As a result of market analysis, it was mentioned that required information on current production rate in CIS countries is unavailable, as the information is not free and it was decided to project production capacity from US country to CIS excluding Russia, as this market is inaccessible. For estimation of the future production rate, we will base the calculation on available data from the US. In 2022 US production rate is announced as 2,550 thousand tons with a CAGR of 4.79% resulting in approximately 3,222 tons in 2027 [1].
The projection process used three methods by analyzing production rate using: GDP, Population and GDP per capita. GDP per capita was calculated using the first two values. Results are shown on Tables A.2.1-4:

Table **A.2.1**. US GDP, population and GDP per capita values

US GDP (billions)	US population	US GDP per capita
28,630 [2]	345,426,571 [3]	82,883.028

Table **A.2.2**. Values of US production rate divided by each of the values

Using US GDP	Using population	Using US GDP per capita
$1.125*10^{-7}$	$9.328*10^{-3}$	38.875

Table **A.2.3**. CIS GDP, population and GDP per capita values excluding Russia

CIS GDP	CIS population	CIS GDP per capita
2,584,745,000,000 [4]	239,735,323 [4]	10,781.66

Table **A.2.4**. Values of production rate for CIS region excluding Russia

GDP	Population	GDP per capita
63,398.11	898,213.99	227,423.77

As the purpose of the project is to satisfy the 25% demand of the CIS region in 2027 we can take 25% of each obtained value in Table A.2.4 and calculate the average to project required production rate of the plant. The resulting value is approximately **90 thousand tons per year.**

Appendix B. Major Equipment Design

B.1 Heat Exchanger E-101 Design

The design procedure of E-101 heat exchanger will be discussed further. The calculations are based on Equations and charts from the Chemical Engineering Design book by Towler and Sinnot [5].

Temperature

In Table B.1.1 the temperatures of cold and hot fluids were presented as well as true temperature difference and related parameters. The calculations were performed based on the following equations:

$$\Delta Tlm = \frac{(T1-t2)-(T2-t1)}{ln\frac{(T1-t2)}{(T2-t1)}} \quad \text{(B.1.1)}$$

$$R = \frac{T1-T2}{t2-t1} \quad \text{(B.1.2)}$$

$$S = \frac{t2-t1}{T1-t1} \quad \text{(B.1.3)}$$

$$Ft = \frac{\sqrt{(R^2+1)}ln[(1-S)/(1-RS)]}{(R-1)ln\left[\frac{2-S[R+1-\sqrt{(R^2+1)}]}{2-S[R+1+\sqrt{(R^2+1)}]}\right]} \quad \text{(B.1.4)}$$

$$\Delta Tm = Ft \times \Delta Tlm \quad \text{(B.1.5)}$$

Table B.1.1. Temperature parameters

Fluid	Inlet temperature, °C		Outlet temperature, °C		ΔT_{lm}, °C	R	S	F_t	ΔT_m,°C
Cold fluid	t_1	85.426	t_2	268.87	-50.67	0.895	0.476	0.875	-78.398
Hot fluid	T_1	490.88	T_2	354.27					

Heat duty

The heat duty equation:

$$Q = mC_p\Delta T \quad \text{(B.1.6)}$$

where m - mass flow rate (kg/s), C_p - heat capacity at mean temperature (J/kg°C), ΔT - temperature difference (°C) of the hot fluid.

Table B.1.2. Heat duty

Q_{total} , kW	Q_{one} , kW	C_p, J/kg°C	m_{total}, kg/s	ΔT, °C
17693.69	4423.42	2986.821	43.364	136.61

Velocity

The velocities of both sides were calculated via the equation:

$$u = \frac{G}{\rho} \quad \text{(B.1.7)}$$

where u - velocity (m/s), G - mass velocity (kg/sm^2), ρ - density (kg/m^3). The parameters such as Re, Pr numbers were calculated using the data obtained from Aspen Plus mixture analysis at mean temperature of the fluids (Table B.1.3, B.1.4).

$$\text{Re} = \frac{D\,u\,\rho}{\mu} \quad \text{(B.1.8)}$$

Table B.1.3. Hot fluid parameters

Temperature,°C	Pressure, bar	Mu, N-sec/sqm	Cp, J/kg-K	K, W/m-K	Rho, kg/cum
354.27	4.98	1.74E-05	2823.636	0.0833158	3.6083
422.575	4.98	1.90E-05	2986.821	0.0975414	3.246862
490.88	4.98	2.06E-05	3134.675	0.11256	2.952267

Table B.1.4. Cold fluid parameters

Temperature,°C	Pressure, bar	Mu, N-sec/sqm	Cp, J/kg-K	K, W/m-K	Rho, kg/cum
85.42567426	1	1.00E-05	1875.406	0.0273983	1.62619
177.1478371	1	1.24E-05	2230.346	0.0401362	1.287207
268.87	1	1.47E-05	2534.547	0.0546589	1.06639

Table B.1.5. Velocity

u_t, m/s	u_s, m/s
12.4	29.5

Tube design

Table B.1.6. Specifications for tube design

TEMA			Aspen Plus	
OD, D, m	ID, d, m	Δt, m	L, m	N_t
0.032	0.0286	0.0017	3.15	418

Shell design

The bundle diameter was calculated using the equation:

$$D_b = d_0 \left(\frac{Nt}{K1}\right)^{1/n1} \quad \text{(B.1.9)}$$

For one tube pass: $K_1 = 0.319$, $n_1 = 2.142$. Shell inside diameter-bundle diameter was found from Fig. B.1.1 split-ring floating head.

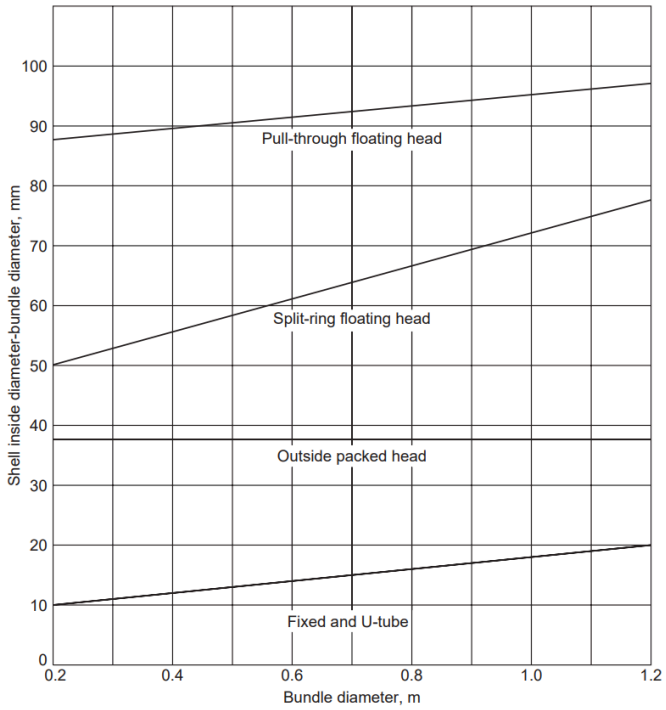

Figure B.1.1. Shell-bundle clearance

Table B.1.7. Shell design parameters

D_b, m	D_s	Clearance, m
1.42	1.5	0.084

Heat transfer coefficients

The tube side heat transfer coefficient (h_i) was calculated using the following correlations:

$$Nu = CRe^{0.8}Pr^{0.33}\left(\frac{\mu}{\mu_w}\right)^{0.14} \quad \text{(B.1.10)}$$

$$Nu = \frac{h\,d}{k} \quad \text{(B.1.11)}$$

where C=0.021 for gases, the ratio of μ to μ_w was assumed to equal 1, d - tube inside diameter (m). The shell-side coefficient (h_s) included the heat transfer factor j_h obtained from Fig. B.1.2. The baffle cut of 45% was chosen in order to minimize pressure drop on the shell side and a similar value was suggested by the Aspen simulation.

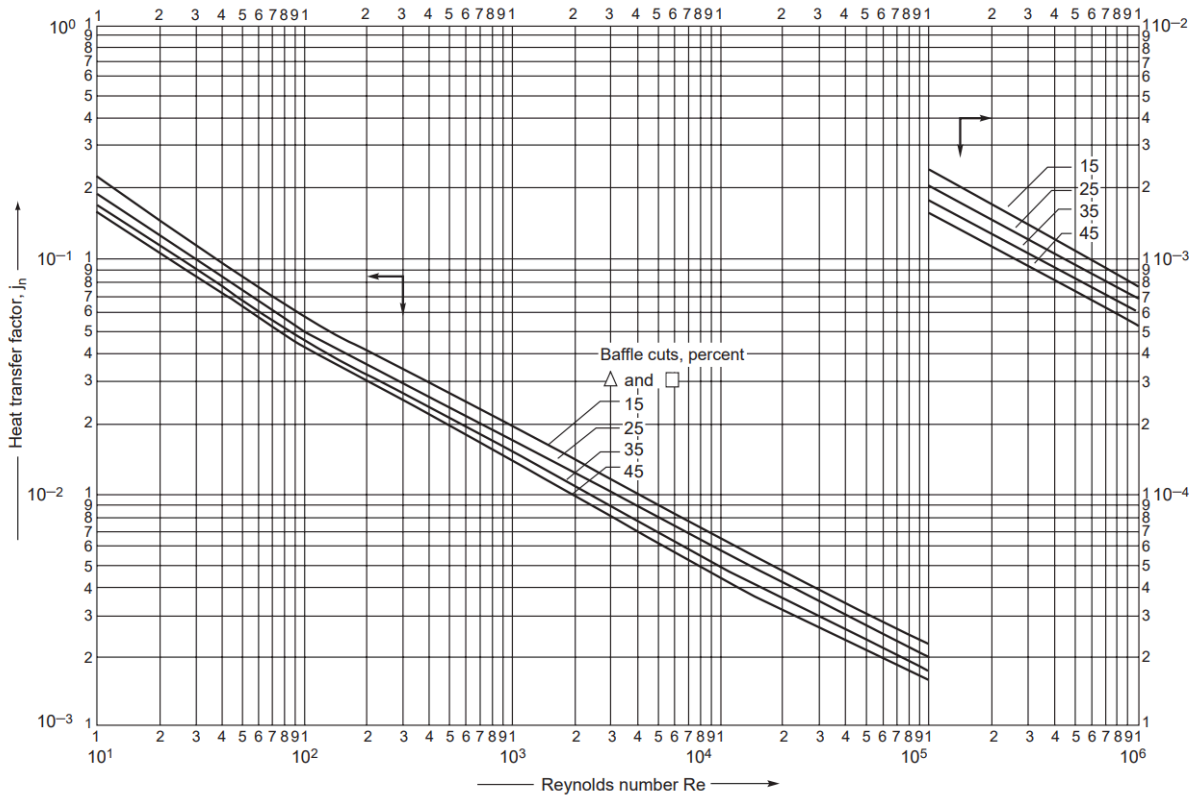

Figure B.1.2. Shell-side heat transfer factor

The shell-side heat transfer coefficient correlation:

$$Nu = j_h \, RePr^{1/3} \left(\frac{\mu}{\mu_w}\right)^{0.14} \tag{B.1.12}$$

Overall heat transfer coefficient

The coefficient, U, was calculated using the following equation:

$$\frac{1}{U} = \frac{1}{hs} + \frac{1}{f} + \frac{D\,ln(D/d)}{2k} + \frac{D}{d} * \frac{1}{f} + \frac{D}{d} * \frac{1}{hi} \tag{B.1.13}$$

The fouling factors for vapor organics are given as 5000 W/m^2°C.

Table B.1.8. Heat transfer parameters

U, W/m^2°C	U, W/m^2°C	h_s, W/m^2°C	f, W/m^2°C	h_i, W/m^2°C	k, W/m°C
Aspen	calculated				
158.4	149.5	274	5000	442.79	21.4

Pressure drop

Tube - side pressure drop was calculated via:

$$\Delta P_t = [8 j_f \left(\frac{L}{d}\right)\left(\frac{\mu}{\mu_w}\right)^{-m} + 2.5]\frac{\rho u^2}{2} \tag{B.1.14}$$

The friction factor was obtained from Fig. B.1.3.

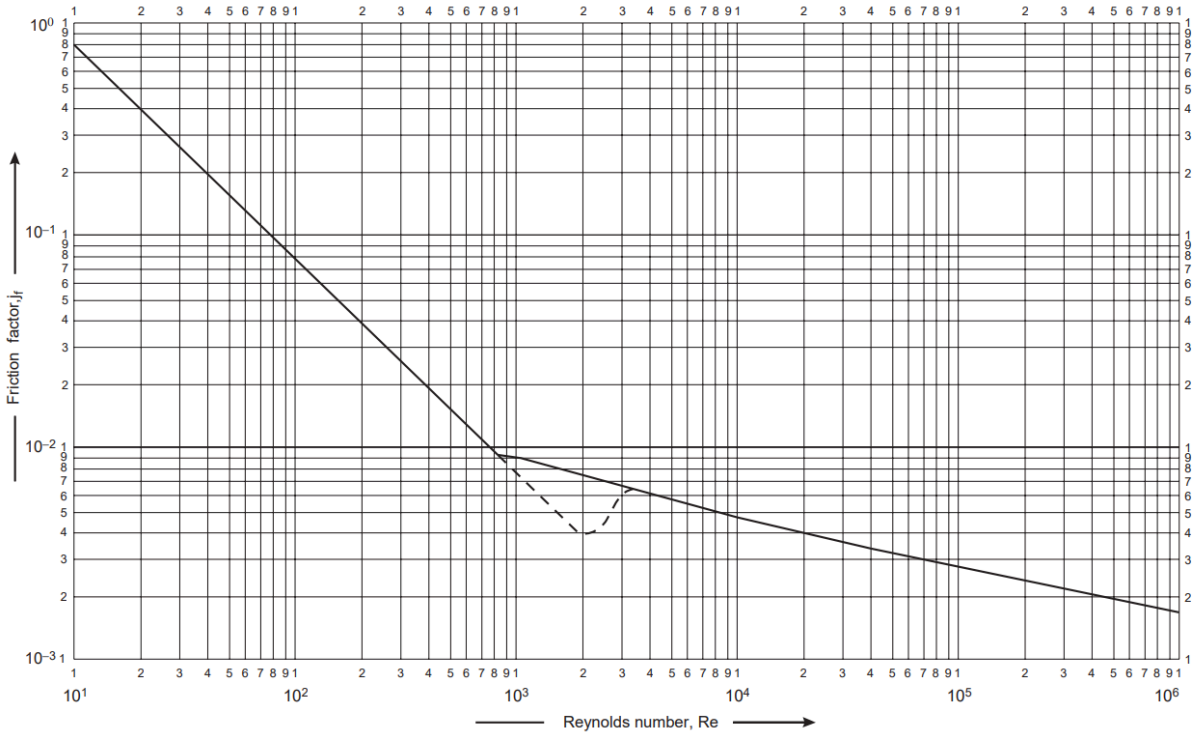

Figure B.1.3. Tube-side friction factor

While the shell-side pressure drop was calculated via:

$$\Delta P_s = 8 j_f \left(\frac{Ds}{de}\right)\left(\frac{L}{lb}\right)\left(\frac{\mu}{\mu_w}\right)^{-0.14}\left(\frac{\rho u^2}{2}\right) \qquad \text{(B.1.15)}$$

where D_s - shell diameter, d_e - equivalent diameter, L - tube length, l_B - baffle spacing. The friction factor is taken from Fig. B.1.4 - 45% baffle cut.

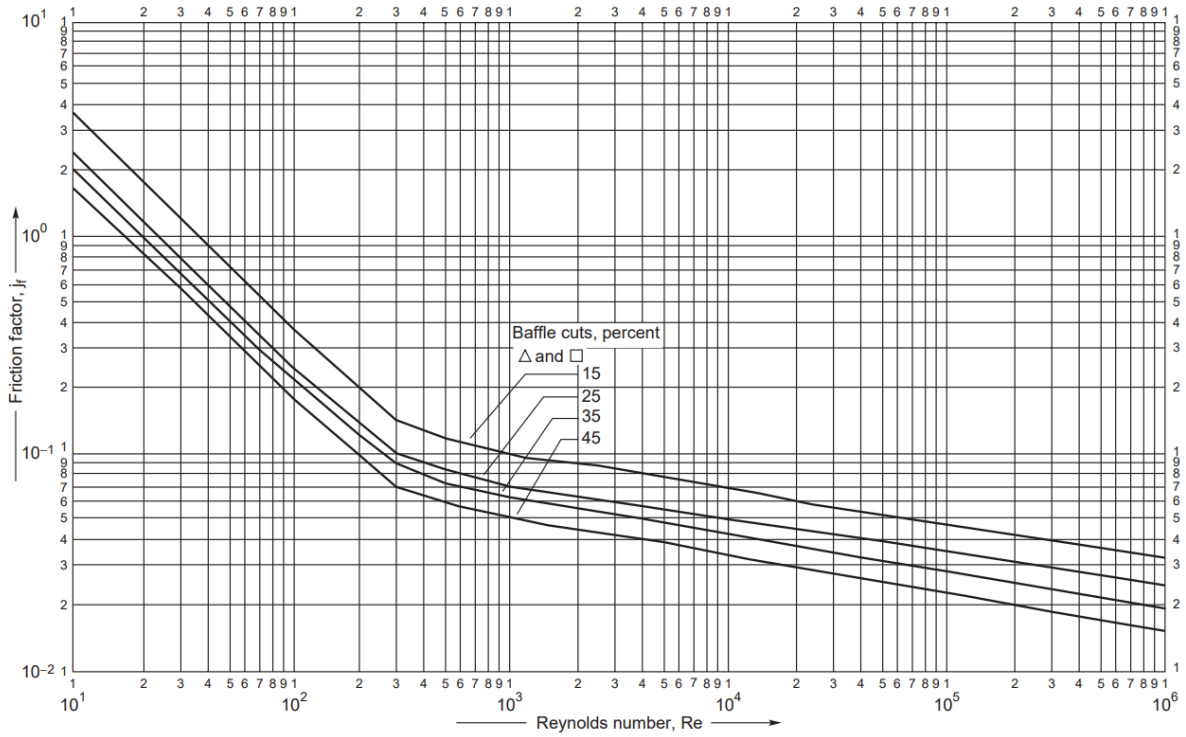

Figure B.1.4. Shell-side friction factor

Table B.1.9. Pressure drop

ΔP_t, bar		ΔP_s, bar	
calculated	Aspen	calculated	Aspen
0.0129	0.0487	0.2481	0.1109

Cost estimation

The equation for the cost calculation [6] is given as:

$$C_e=a+bS^n \tag{B.1.16}$$

Lang estimation:

$$C_L = C_B*CS*L \tag{B.1.17}$$

Material cost estimation:

$$C_M = \sum_{i=1}^{i=M} Ce, i, CS[(1 + f_p)f_m + (f_{er} + f_{el} + f_i + f_c + f_s + f_l)] \tag{B.1.18}$$

Table B.1.10. Cost estimation factors

Area, m^2	Lang factor	SS 321 factor	Location factor
147.84	3.5	1.3	0.732

Table B.1.11. Cost estimation

C_e, USD	Lang estimation, USD	Material cost estimation, USD	Cost escalation by CEPSI 2010, USD	Cost escalation by CEPSI 2024, USD	Overall cost, USD
49,684	226,063	185,819	248,419	204,195	816,781

B.2 Reactor R-101 Design

Sizing detailed calculations

Table B.2.1. Catalyst density calculation

Metal	Ni	Fe	Co	Bi	Al2O3
Density (kg/m^3) at 25°C	8900 [7]	7860 [8]	8900 [3]	9747 [10]	3890 [11]
Density (kg/m^3) at 625°C	8638 [12]	7670 [13]	8710* [14]	9580 [15]	3834* [16]
Weight percent (%)	10	5	5	30	50
$\rho_{cat} = \frac{1}{\rho_{Ni}} + \frac{1}{\rho_{Fe}} + \frac{1}{\rho_{Co}} + \frac{1}{\rho_{Bi}} + \frac{1}{\rho_{Al2O3}}$ = 5389 kg/m^3					

* - calculated using linear thermal expansion factor (volume expansion = 3* linear expansion [17])

Table B.2.2. Reactor volume density

Mass of catalyst	100,000 kg

Bed voidage, ε	0.4
Number of reactors, N:	4
$V_{cat} = \frac{m_{cat}}{\rho_{cat}} = \frac{100{,}000}{5389} = 18.56$ m^3 $V_{1\,reactor} = \frac{V_{cat} + 20\%}{N * (1-\varepsilon)} = \frac{15.56 * 1.2}{4*(1-0.4)} = 9.28$ m^3	

Table B.2.3. Reactor flow rates and dimensions

Volumetric flow rate (inlet), Q	2.98 m^3/s
Diameter, D	1.5 m
Length, L	5.22 m
Cross-sectional area, A	1.77 m^2
Velocity (superficial), Q/A	1.6 m/s
Velocity (superficial), Q/(A*ε)	4 m/s

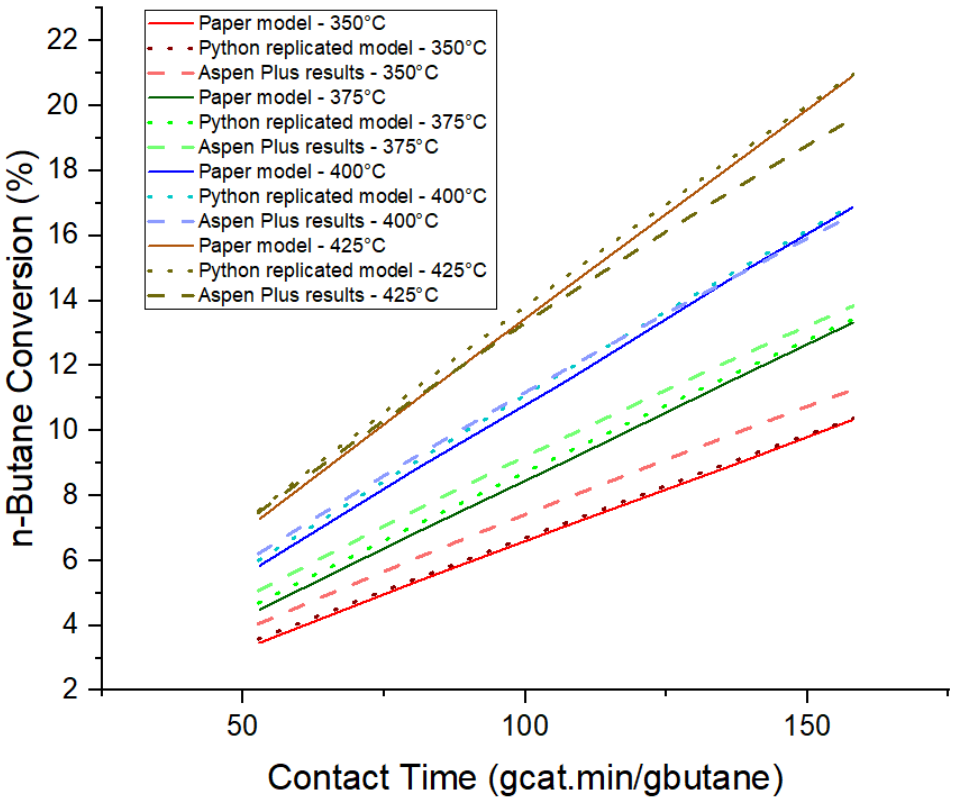

Figure B.2.8. Comparison of all data (Paper, Aspen, Python)

Material Selection

Table B.2.4. Design Pressure and Design Temperature Calculation.

Operating Temperature, °C/°F	625 / 1157
Operating Pressure, bar/psi	6 / 87.02
Design Temperature, (1157+50°F) °C/°F	650* / 1210*
Design Pressure (87.02 -> 90 psi) bar/psi	6.2 / 90

* - rounded to multiple of 10

Table B.2.5. Material Comparison [18].

Material	N06625	S31008
Allowable Stress, MPa	133	16.9
Weld strength reduction factor, W	1	1

Coefficient of material used. Y	0.7	0.7
Weld quality factor. E	1	1
Corrosion resistance	High	High
Wall thickness (assuming 0 corrosion), mm	3.50	27.53
Wall thickness (6 mm corrosion allowance), mm	9.53	33.78
Closest ASME standard thickness, mm	9.53	-

It can be seen that both materials have very different allowable stress at design temperature, showing that inconel is much stronger in given conditions. It can also be seen that to maintain the stainless steel with a tube 1.5 m internal diameter, the thickness of the wall should be at least 27.53 mm, which is too high and has no close ASME standard to it. Therefore, the N06625 is chosen as our reactor material.

Pressure Drop

Using Ergun's equation, the pressure drop in the fixed bed reactor can be estimated as

$$\frac{\Delta P_{drop}}{5.22} = \frac{180*2.29*10^{-5}*(1-0.4)^2*1.6}{0.003^2*0.4^3} + \frac{1.75*3.871*(1-0.4)*1.6^2}{0.003*0.4^3}$$

$$\Delta P_{drop} = 2.87\ bar$$

However, this drop is also partially compensated with a pressure increase due to an increase in moles of gases. Overall growth is estimated as

$$\Delta P_{inc} = (3792.5/3258.9 - 1) * 6$$

$$\Delta P_{inc} = 0.98\ bar$$

$$\Delta P_{total} = \Delta P_{drop} - \Delta P_{inc} = 2.87 - 0.98 = 1.89\ bar$$

Cost estimation

For a pressure vessel, the size parameter is shell mass. Therefore, the mass of the Inconel shell was found using the corresponding formula:

$$m = \rho * V = \rho * L * \frac{\pi(D_o^2 - D_i^2)}{4}$$

Table B.2.6. Size parameter (S) calculation:

Inside Diameter Di	1.501 m	$m = \rho * V = 844 * 5.22 * \frac{\pi(1.52-1.501)}{4}$

Outside diameter Do	1.52 m	$= 198.5\ kg$
Length, L	5.22 m	
Inconel density, ρ	844 kg/m^3	

Table B.2.7.Vertical pressure vessel cost estimation:

a	10200	$C_e = 10200 + 31 * 198.5^{0.85} = 14652$
b	31	Lang factor (+ Location, material, cost escalation):
S	198.5	$C = C_e * L * M = 14652 * 1.7 * 4 = 99634\ \$$
n	0.85	$C = 99634 * CL = 99634 * 0.732 = 72932\ \$$
Lang factor (L)	4	$C = \frac{CEPCI\ 2024}{CEPCI\ 2010} * 72932 = \frac{800}{532.9} * 72932 = 109487\ \$$
Inconel factor (M)	1.7	Equation (7.12) (+ Location, material, cost escalation):
CEPCI Jan 2010 (book)	532.9	$C = (1 + 0.8)* C_e + (0.3 + 0.2 + 0.3 + 0.3 + 0.2 + + 0.1) = 65348\ \$$
CEPCI 2024	800	$C = 65348 * CL = 65438 * 0.732 = 47835\ \$$
Location factor (CL)	0.732	$C = \frac{CEPCI\ 2024}{CEPCI\ 2010} * 47385 = \frac{800}{532.9} * 47385 = 71811\ \$$

B.3 Compressor C-102 design

Operating discharge pressure of MCOMP

The final pressure of 20.2 bar for the multistage compressor (MCOMP) was determined through a sensitivity analysis of the streams exiting the flash drum F-101. As the pressure increases, the amount of butadiene in the top product decreases (Fig. B.3.1), which is beneficial for the production rate. At the same time, the operating pressure of the de-propanizer T-101 is set at 20.2 bar to ensure effective separation. This value was chosen as it also eliminates the need for an additional compressor before the de-propanizer.

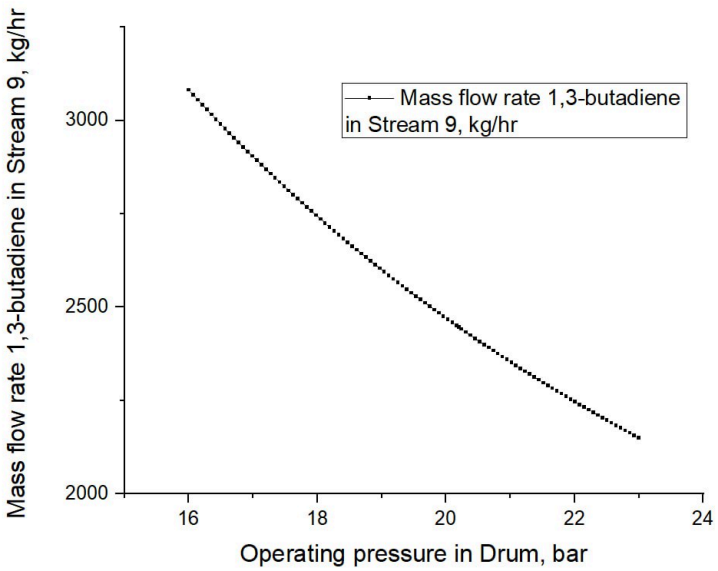

Figure B.3.1. Mass flow rate of 1,3-butadiene of TOP stream vs operating temperature in flash unit

Multistage compressor system

According to Table B.3.1, the most suitable compressor frame for a MCOMP system is 46M. This compressor frame can handle the required pressure increase from 4.5 bar to 20.2 bar (≈ 300 psig) while accommodating a gas flow rate of approximately ≈ 44,000 m3/h (26,000 CFM) for whole multistage compressor system from C-102 to C-103, ensuring reliable performance under the given operating conditions. Therefore, a nominal speed of 6300 rpm, polytropic efficiency of 0.8 and nominal H/N^2 (per stage) of $2.28*10^{-4}$ are chosen for further calculations.

Table B.3.1. Summary of Typical Multistage Centrifugal Compressor Data [19]

2 M-Line and MB-Line Frame Data							
Frame	Nominal Flow Range (cfm)	Nominal Max. No. of Casing Stages	Max. Casing Pressure (psig)	Nominal Speed (r/min)	Nominal Polytropic Efficiency	Nominal H/N^2 (per stage)	Maximum Q/N
29M	750–9,500	10	750	11,500	0.78	7.5×10^{-5}	0.83
38M	6,000–22,000	9	625	7,725	0.79	1.52×10^{-4}	2.85
46M	16,000–34,000	9	625	6,300	0.80	2.28×10^{-4}	5.40
60M	25,000–58,000	8	325	4,700	0.81	3.85×10^{-4}	12.34
70M	50,000–84,000	8	325	4,200	0.81	5.67×10^{-4}	20.
88M	70,000–135,000	8	325	3,160	0.81	39.1×10^{-4}	42.7
103M	110,000–160,000	8	45	2,800	0.82	11.6×10^{-4}	57.1
110M	140,000–190,000	8	45	2,600	0.82	13.4×10^{-4}	73.1
10MB	90–1,600	12	10,000	18,900	0.77	2.6×10^{-5}	0.085
15MB	200–2,350	12	10,000	15,300	0.77	3.6×10^{-5}	0.153
20MB	325–3,600	12	10,000	12,400	0.77	6.2×10^{-5}	0.29
25MB	500–5,500	12	10,000	10,000	0.78	9.5×10^{-5}	0.55
32MB	2,000–8,000	10	10,000	8,300	0.78	1.39×10^{-4}	0.96
38MB	6,000–22,000	9	1,500	7,725	0.79	1.52×10^{-4}	2.85
46MB	16,000–34,000	9	1,200	6,300	0.79	2.28×10^{-4}	5.40
60MB	25,000–58,000	8	800	4,700	0.80	3.85×10^{-4}	12.34
70MB	50,000–84,000	8	800	4,200	0.80	5.67×10^{-4}	20.

The mechanical losses from Table B.3.2 are considered in estimation of the brake horsepower based on the calculated actual power of the compressor. Since the compressor's C-102 power output is 5433.1 kW, the mechanical loss of 2.5% is applied in the estimations. For the compressors C-101, C-103, the mechanical losses are 2% and 2.5%, respectively (Table B.3.2).

Table B.3.2. Approximate Mechanical Losses as Percentage of a Gas Power Requirement [19]

Gas Power Requirement		
English (hp)	Metric (kW)	Mechanical Losses %
0 – 3,000	0 – 2,500	3
3,000 – 6,000	2,500 – 5,000	2.5
6,000 – 10,000	5,000 – 7,5000	2
10,000+	7,5000+	1.5

Compressor calculations

Based on the works of A. Kayode Coker [1] and Klaus H. Lüdtke [2], the following equations are used to calculate compressor parameters, including polytropic, adiabatic, and actual work, efficiency, and head values. Additionally, discharge temperature, stage head, number of stages, power (with and without losses), brake horsepower, and flow coefficient are determined. Impeller characteristics such as tip speed, rotational speed, Mach number, sound velocity, and blade inlet angle are also considered. The detailed calculations results are presented in ESI.

Main calculation points:

Compression ratio:

To determine the final pressure for compressor C-102, Equation B.3.1 was used to calculate the compression ratio, which is 2.12 for multistage compressor system MCOMP. Therefore, the final pressure for compressor C-102 is 9.53 bar, which serves as the inlet pressure for heat exchanger E-103 and the initial pressure for compressor C-103 is equal to the final pressure at the outlet of heat exchanger E-103, which is 9.5 bar.

Polytropic efficiency:

The polytropic efficiency (which is 80%) was selected based on Table B.3.1, as it corresponds to the most suitable compressor frame.

Aspen-derived values:

Values such as heat capacity ratio, compressibility factor, molecular weight, density of the mixture, specific volume, volumetric flow rate, enthalpy, and polytropic head (C-103) were taken from Aspen and used in Equations B.3.{2, 7, 8, 10, 11, 18, 20, 23, 25} for estimations.

Casing stages:

For the entire compressor system MCOMP, the number of casing stages is determined. This is calculated using the sum of the polytropic heads of the two compressors and the head per stage, as defined by Equation B.3.20. The head per stage is obtained using values from Table B.3.1 and Equation B.3.21. Additionally, the number of casing stages for each compressor is calculated separately by considering the polytropic head of each unit and the head per stage of the entire system, allowing for an analysis of the required casings for each compressor.

Compression ratio [19]:

$$R_c = \left(\frac{P_2}{P_1}\right)^{\frac{1}{N}} \tag{B.3.1}$$

$N = 2$ (for 2 compressors in multistage system)

Polytropic exponent [19]:

$$n = \frac{log_{10}(P_2/P_1)}{log_{10}(v_1/v_2)} \tag{B.3.2}$$

Adiabatic efficiency [19]:

$$E_{ad} = \frac{H_{ad}}{H_p}(E_p) \tag{B.3.3}$$

$$E_{ad} = \frac{adiabatic\ work}{polytropic\ work} = \left(\frac{(P_2/P_1)^{(k-1)/k}-1}{(P_2/P_1)^{(n-1)/n}-1}\right) \tag{B.3.4}$$

Polytropic efficiency [19]

$$E_p = \frac{n(k-1)}{k(n-1)} \tag{B.3.5}$$

$$k = \frac{-n}{E_p n - n - E_p}$$

Polytropic Head [19]:

$$H_p = \frac{H_{ad}}{E_{ad}}(E_p) \tag{B.3.6}$$

$$H_p = \frac{Z_{avg}RT_1}{M_w}\left(\frac{n}{n-1}\right)\left((P_2/P_1)^{\frac{n-1}{n}} - 1\right) \tag{B.3.7}$$

Adiabatic Head [19]:

$$H_{ad} = \frac{Z_{avg}RT_1}{M_w}\left(\frac{k}{k-1}\right)\left((P_2/P_1)^{\frac{k-1}{k}} - 1\right) \tag{B.3.8}$$

Discharge Temperature [19]:

$$T_2 = T_1\left((P_2/P_1)^{\frac{n-1}{n}}\right) \tag{B.3.9}$$

Polytropic Work [19]:

$$(-W)_{poly} = \left(\frac{n}{n-1}\right)\frac{Z_1RT_1}{M_w}\left((P_2/P_1)^{\frac{n-1}{n}} - 1\right) \tag{B.3.10}$$

Adiabatic Work [19]:

$$(-W)_{ad} = \left(\frac{k}{k-1}\right)\frac{Z_1RT_1}{M_w}\left((P_2/P_1)^{\frac{k-1}{k}} - 1\right) \tag{B.3.11}$$

Actual Work [19]:

$$(-W)_{actual} = \frac{(-W)_{poly}}{E_p} \tag{B.3.12}$$

Power [19]:

$$P = \frac{(-W)_{actual}\,m}{3600} \tag{B.3.13}$$

Brake Horsepower [19]:

$$Bh_p = P + Mechanical\ losses\ (from\ Table\ B.3.2) \tag{B.3.14}$$

Peripheral velocity (tip speed) [19]:

$$u = \frac{\pi D\omega}{60} \tag{B.3.15}$$

Rotative speed [19]:

$$\omega = \frac{1300}{D}\sqrt{\frac{H'}{\mu}} \tag{B.3.16}$$

Mach number [19]:

$$M' = \frac{u}{V_s} \tag{B.3.17}$$

Velocity of sound in a gas [19]:

$$V_s = \sqrt{\frac{C_p}{C_v} RTg} \tag{B.3.18}$$

Fan law [19]:

$$\omega_{adj} = \omega_{nom} \sqrt{\frac{H'}{H_p}} \tag{B.3.19}$$

No. stages [19]:

$$No.\,stages = \frac{H_p}{(Max.\,H\,per\,stage)} \tag{B.3.20}$$

Head per stage [19]:

$$H' = (H/N^2)(\omega)^2 \tag{B.3.21}$$

Slip ratio [20]:

$$\sigma = 1 - \frac{0.63\pi}{z} \tag{B.3.22}$$

Flow coefficient [20]:

$$\Phi = \frac{Q_{in}}{\frac{\pi}{4} d_2^{\,2} u_2} \tag{B.3.23}$$

Blade Inlet Angle [20]:

$$tan\,\beta_{1B} = \frac{c_{m1}}{u_1} \tag{B.3.24}$$

Euler head (actual work) [20]:

$$\Delta h = h_2 - h_1 \tag{B.3.25}$$

where,

R_c - compression ratio, bar

N - number of compressors, N = 2 (for MCOMP with 2 compressors)

P_1 - Suction pressure, bar

P_2 - Discharge pressure, bar

T_1 - Temperature at inlet, K

T_2 - Temperature at inlet, K

v_1 - Specific volume at inlet, m^3/kg

v_2 - Specific volume at outlet, m^3/kg

H_{ad} - Adiabatic head, kJ/kg

H_p - Polytropic head, kJ/kg

E_{ad} - Adiabatic efficiency

E_p - Polytropic efficiency

k - Adiabatic exponent

n - Polytropic exponent
Z_{avg} - Compressibility factor Average
Z_1 - Compressibility factor inlet
R - Gas constant, R = 8.31432 kJ/kg mol K
M_w - Molecular weight of a mixture
W_{poly} - Polytropic work, kJ/kg
W_{ad} - Adiabatic work, kJ/kg
P - Power, kW
m - Mass flow rate, kg/h
Bh_p - Brake horsepower, bhp
D - diameter of the impeller part, m
ω_{nom} - Rotative speed (nominal speed), rpm
ω_{adj} - Adjusted rotative speed (nominal speed), rpm
H' - Head per stage, kJ/kg
μ - Pressure coefficient, $\mu = 0.55$
M' - Mach number
V_s - Velocity of sound in a gas, m/s
C_p/C_v - Heat capacity ratio
g - acceleration constant, g = 9.81 m/s
H/N^2 - Nominal H/N^2 per stage (set according to the Table B.3.1)
z - Number of blades
σ - slip ratio
Φ - flow coefficient
Q_{in} - Volumetric flow rate at inlet, m^3/s
d_2 - Outlet diameter of impeller, m
u_2 - Peripheral velocity of impeller tip, m/s
β_{1B} - Blade inlet angle, deg.
c_{m1} - Abs. velocity mid-LE (meridional component)
u_1 - Peripheral velocity of impeller eye tip, m/s

Table B.3.3. Comparison of estimation of values for Compressor C-102

	Discharge Temperature, K	Polytropic head compressor, kJ/kg	Total power, kW	Brake Horsepower, hp
Hand calculated	669.33	97.670	5433.11	7285.91
Aspen Plus	670.96	97.141	5437.15	7291.34

Compressor characteristics and dimensions

Horizontally split casing:

A horizontal split casing is chosen, since it is usually applicable for discharge pressure up to 40-60 bar (moderate-to-high pressure), additionally, this type of casing is used for high-flow rates [21].

The shrouded 3D impeller:

A shrouded 3D impeller was chosen for the compressor because of its high efficiency, ability to handle high rotational speeds, and improved aerodynamic performance, making it ideal for high-pressure applications like 20 bar. Additionally, since the volume flow is high and the flow coefficient is 0.14 (which is near to 0.15), 3D shrouded impellers are typically used to ensure efficient performance and minimize losses [20].

The vaneless diffuser:

A vaneless diffuser was chosen because it provides a wider operating range, allowing different flow rates to be handled without significant efficiency loss. This makes it more adaptable to process variations. Additionally, its simpler design reduces manufacturing complexity and maintenance requirements, leading to lower costs and improved reliability [22].

Assumptions on Impeller dimensions:

According to the design guidelines of Process Centrifugal Compressors by Lüdtke [20], the following assumptions on ratio is established:

$$\frac{r_6}{r_2} = 0.25 - 0.45 \text{ and } \frac{r_6}{r_2} = 0.33 \ (according\ to\ Fig.\ B.3.2) \tag{B.3.26}$$

$$\frac{r_1}{r_4} = 0.85 \tag{B.3.27}$$

$$\frac{d_{20}}{d_2} = 1.044 \tag{B.3.28}$$

$$\frac{d_{20}}{d_2} = 1.044 \tag{B.3.29}$$

$$\frac{b_2}{d_{20}} = 0.13 \tag{B.3.30}$$

$$\frac{s}{d_{20}} = 0.001 \tag{B.3.31}$$

$$\frac{D_{out}}{D_{in}} = 1.65 \tag{B.3.32}$$

$$\frac{c_{m1}}{u_{20}} = 0.393 \tag{B.3.33}$$

$$\frac{D_v}{d_2} = 2.11 \tag{B.3.34}$$

$$\frac{d_1}{d_{20}} = 0.523 \tag{B.3.35}$$

$$\frac{b_1}{d_2} = 0.07 \tag{B.3.36}$$

According to the Figure B.3.2, the hub/tip ratio is 0.33 (with flow coefficient ≈ 0.14)

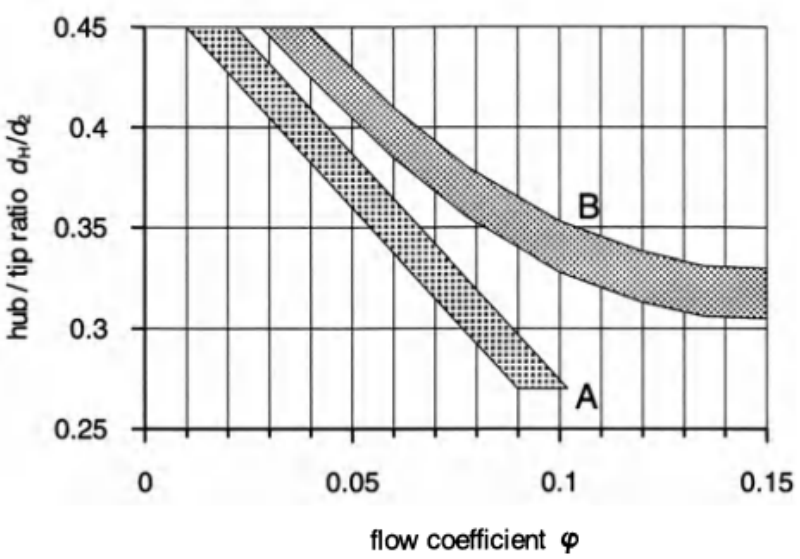

Figure B.3.2. Rough guidelines for hub/tip ratio. A low to medium flow coefficients for medium number of impellers per shaft, B medium to high flow coefficients for high number of impellers per shaft [20].

Based on the design guidelines from Aerodynamic Design of Centrifugal Compressor [23], the following ratio assumptions are defined (for comparison with the obtained results regarding the impeller inlet radius, trailing edge blade height, and leading-edge hub radius):

$$\frac{r_1}{r_2} = 0.6 - 0.65 \tag{B.3.37}$$

$$\frac{b_1}{r_2} = 0.05 - 0.15 \tag{B.3.38}$$

$$\frac{r_6}{r_1} = 0.3 - 0.7 \tag{B.3.39}$$

According to the design guidelines of Turbomachinery Design and Theory [24], the following assumptions on ratio is established (to obtain additional value for eye root radius of impeller):

$$\frac{r_5}{r_1} = 0.533 \tag{B.3.40}$$

Based on the design guidelines from The design of a family of process compressor stages

[25], the following formula is applied to calculate the impeller axial length:

$$l_{imp} = (0.08 + 3.16) * r_2 \quad \text{(B.3.41)}$$

where,
r_1 - Blade inlet radius
r_2 - Blade outlet radius
r_4 - Eye radius
r_5 - Eye root radius
r_6 - Leading-edge hub radius
b_1 - Impeller inlet width
b_2 - Impeller outlet width
d_2 - Blade diameter
d_{20} - Disk diameter
s - blade thickness
D_{in} - Diffuser inlet diameter
D_{out} - Diffuser outlet diameter
D_v - Volute outer diameter
c_{m1} - Absolute velocity mid-LE (meridional component)
u_{20} - Disk peripheral speed
l_{imp} - impeller axial length

As shown in Fig. B.3.3, blade exit angle β_{2B} is 50 degrees (with flow coefficient ≈ 0.14).

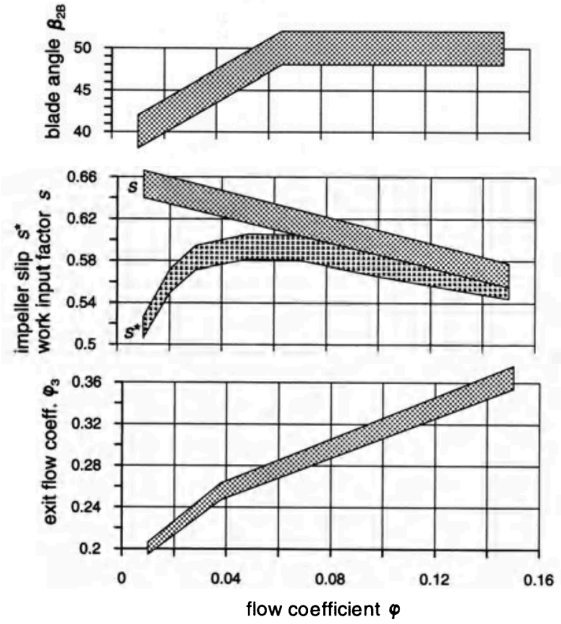

Figure B.3.3. Impeller exit flow coefficient, impeller slip factor, work input factor and blade exit angle as functions of the inlet flow coefficient (empirically determined values for the best efficiency point). s includes work of shroud leakage and disk friction [20].

Referring to Fig. B.3.4, the shaft can accommodate a maximum of 5 impellers, with a Mach number of approximately 0.9.

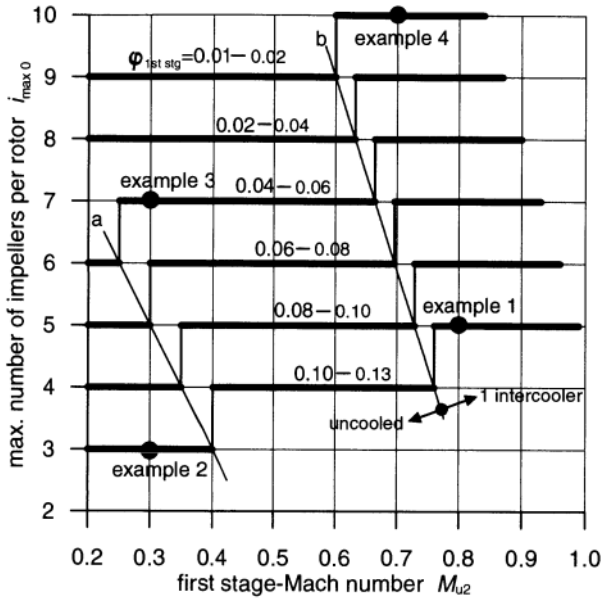

Figure B.3.4. Prevailing tendency for maximum feasible number of impellers per rotor [20]

Appendix 3.E. CapCost estimation for C-102

The cost estimation for the compressor was carried out using the guidelines outlined in Chemical Engineering Design by G. Towler [6]. The calculations took into account driver power (kW).

Purchased equipment cost formula is given as:

$$Ce = a + bS^{n} = 580,000 + 20,000 * (5433.11)^{0.6} = 4,063,847\ USD \qquad \text{(B.3.42)}$$

Table B.3.4. Purchased equipment cost for centrifugal compressor

Constants	a	b	n
Value	580,000	20,000	0.6

Table B.3.5. Factors for estimation centrifugal compressor

Factors		Value

Lang factor for compressors	L	2.5
High alloy steel factor	f_m	1.3
Location factor of China	L_f	0.61
Scaling factor	S	1.2
CEPCI (Chemical Engineering Plant Cost Index) for Jan 2010	Cost index in year A	532.9
CEPCI for 2024	Cost index in year B	800

Lang estimation:

$$C_L = C_e * f_m * L = 4,063,847\ USD * 1.3 * 2.5 = 13,207,501\ USD \quad \text{(B.3.43)}$$

Location estimation

$$Location = C_L * (S * L_f) = 13,207,501\ USD * 1.25 * 0.61 = 9,667,891\ USD \quad \text{(B.3.44)}$$

Cost Escalation

$$Cost\ in\ year\ A = Cost\ in\ year\ B * \frac{Cost\ index\ in\ year\ A}{Cost\ index\ in\ year\ B} = \quad \text{(B.3.45)}$$
$$= 9,667,891\ USD * \frac{800}{532.9} = 14,513,629\ USD$$

B.4 Heat Exchanger E-103 design calculations.

All the equations and steps of designing a heat exchanger are taken from the Chemical Engineering Design book by Towler and Sinnot [5].

Assumed Heat transfer coefficient: 200 W/m^2 K

Table B.4.1. Temperature calculations

Fluid	Inlet temperature, °C	Outlet temperature, °C	ΔT_{lm}, °C	R	S	F_t	ΔT_m,°C
Cold fluid	20	29.81	-29.46	23.09	0.026	0.99	-31.04
Hot fluid	397.81	166.04					

$$\Delta Tlm = \frac{(T1-t2)-(T2-t1)}{ln\frac{(T1-t2)}{(T2-t1)}} \quad \text{(B.4.1)}$$

$$R = \frac{T1-T2}{t2-t1} \quad \text{(B.4.2)}$$

$$S = \frac{t2-t1}{T1-t1} \quad \text{(B.4.3)}$$

$$Ft = \frac{\sqrt{(R^2+1)}ln[(1-S)/(1-RS)]}{(R-1)ln\left[\frac{2-S[R+1-\sqrt{(R^2+1)}]}{2-S[R+1+\sqrt{(R^2+1)}]}\right]} \quad \text{(B.4.4)}$$

$$\Delta Tm = Ft \times \Delta Tlm \quad \text{(B.4.5)}$$

Heat duty calculation:

$$Q = mC_p\Delta T \quad \text{(B.4.6)}$$

m - mass flow rate (kg/s)

C_p - heat capacity at mean temperature (J/(kg°C))

ΔT - temperature difference (°C) of the hot fluid

Q = 22,208,896.73 W

Velocity calculation:

Table B.4.2. Hot fluid parameters

Temperature, K	Pressure, bar	Mu, N-sec/sqm	Cp, J/kg-K	K, W/m-K	Rho, kg/cum
444.28	6.994	1.31E-05	2329.605	0.054	10.64134
557.62	6.994	1.59E-05	2663.053	0.077	8.296159
670.96	6.994	1.86E-05	2934.268	0.102	6.830426

Table B.4.3. Cold fluid parameters

Temperature, K	Pressure, bar	Mu, N-sec/sqm	Cp, J/kg-K	K, W/m-K	Rho, kg/cum
293.15	1	1.02E-03	4525.96	0.599	998.77
298.06	1	9.14E-04	4524.05	0.606	994.04
302.97	1	8.23E-04	4522.97	0.613	989.30

$$u = \frac{G}{\rho} \quad \text{(B.4.7)}$$

u - velocity (m/s)

G - mass velocity (kg/s m^2)
ρ - density (kg/m^3)

According to the heat exchanger standards, velocity on the tube side should be around 10-30 m/s (for gas) and on the shell side 0.3-1 m/s (for liquid):

u (tube) = 76.297/6.698 = 18.03 m/s
u (shell) = 487.16/974.02 = 1.015 m/s

Tube design:

Following TEMA standards tube side values were taken as:
Outside D = 0.05 m
Δt = 0.0021 m
Inside D = 0.0458 m
Tube length = 4.65 m
Tube passes = 2
Number of tubes (Nt) = 300

Shell design:

$$D_b = d_0 \left(\frac{Nt}{K1}\right)^{1/n1} \quad \text{(B.4.8)}$$

D_b - Bundle diameter (m)
d_0 - tube outside diameter (m)
Values for K1 and n1 are taken for 2 tube passes as:
K1=0.156
n1=2.291

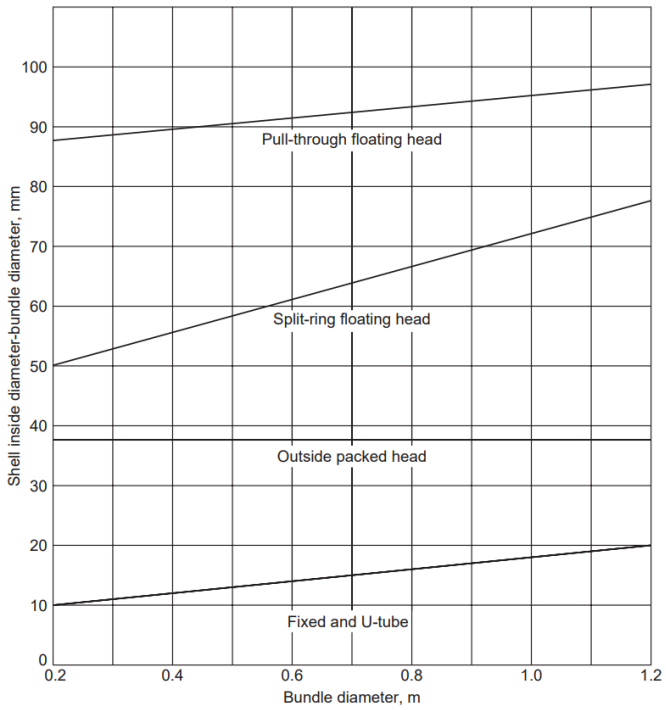

Figure B.4.1. Shell-bundle clearance

Bundle diameter, D_b = 1.820 m

As we use a Split-ring floating head, using Figure B.4.1 and interpolating to our value of bundle diameter we can identify the shell inside diameter-bundle diameter equal to 0.095 m.

Clearance = 0.095 m
Shell diameter, D_s = 3 m

Heat transfer coefficients:

Tube side heat transfer factor:

$$Nu = CRe^{0.8}Pr^{0.33}\left(\frac{\mu}{\mu_w}\right)^{0.14} \quad \text{(B.4.9)}$$

$$Nu = \frac{h\,d}{k} \quad \text{(B.4.10)}$$

C=0.021 for gases

the ratio of μ to μ_w was assumed to be equal to 1

d - tube inside diameter

Re = 4.29E+05 (calculated as $\frac{D\,u\,\rho}{\mu}$)

Pr = 5.54E-01 (calculated as $\frac{Cp\,\mu}{k_f}$)

k = 0.0767

Using equations (B.4.9) and (B.4.10) we can calculate tube side heat transfer coefficient h:

Tube side heat transfer factor, h_i = 928.65 W/(m^{2}K)

Shell side heat transfer factor:

$$Nu = j_h \, RePr^{1/3} \left(\frac{\mu}{\mu_w}\right)^{0.14} \quad \text{(B.4.11)}$$

Re = 3.94E+04

Pr = 6.82

From Fig. B.4.2 we can find j_h:

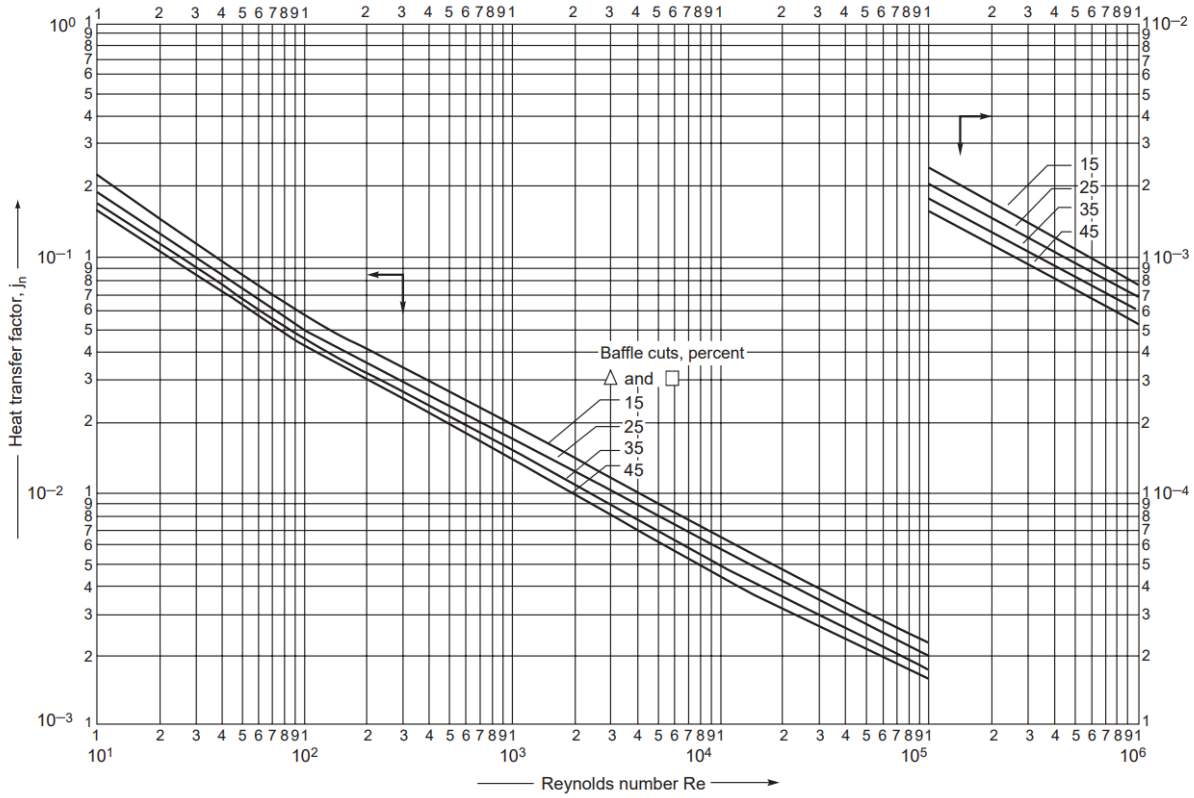

Figure B.4.2. Shell-side heat transfer factor

j_h = 0.0031 (30% baffle cut)

Shell side heat transfer factor, h_s = 2.42E+03

Overall heat transfer coefficient:

The coefficient, U, was calculated using the following equation:

$$\frac{1}{U} = \frac{1}{hs} + \frac{1}{hod} + \frac{D\,ln(D/d)}{2k} + \frac{D}{d} * \frac{1}{hid} + \frac{D}{d} * \frac{1}{hi} \quad \text{(B.4.12)}$$

Outside fouling coefficient, h_od = 5000 W/m°C (organic gas)

Inside fouling coefficient, h_id = 2000 W/m°C (water)

Thermal conductivity, k = 45 W/m°C (carbon steel)

$U_{calculated}$ = 424.4 W/(m²°C)
U_{Aspen} = 427.8 W/(m²°C)

Calculated and Aspen values are close to each other meaning heat exchanger efficiency is acceptable.

Tube - side pressure drop:

$$\Delta P_t = [8j_f (\frac{L}{d})(\frac{\mu}{\mu_w})^{-m}+2.5]\frac{\rho u^2}{2} \quad (B.4.13)$$

j_f = 0.0024 (from Fig. B.4.3)

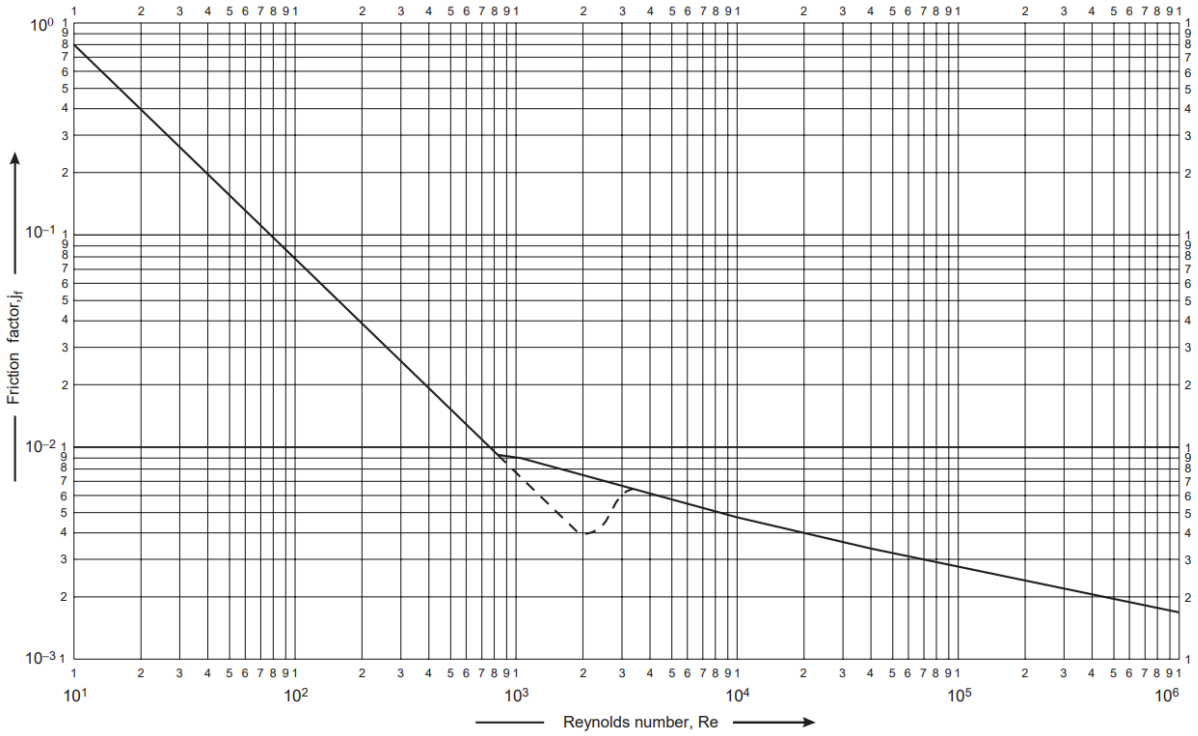

Figure B.4.3. Tube-side friction factor

ΔP_t = 0.06 bar

Shell-side pressure drop:

$$\Delta P_s = 8j_f (\frac{Ds}{de})(\frac{L}{lb})(\frac{\mu}{\mu_w})^{-0.14}(\frac{\rho u^2}{2}) \quad (B.4.14)$$

D_s - shell diameter
d_e - equivalent diameter
L - tube length
l_B - baffle spacing
Friction factor, j_f = 0.038 (from Fig. B.4.4)

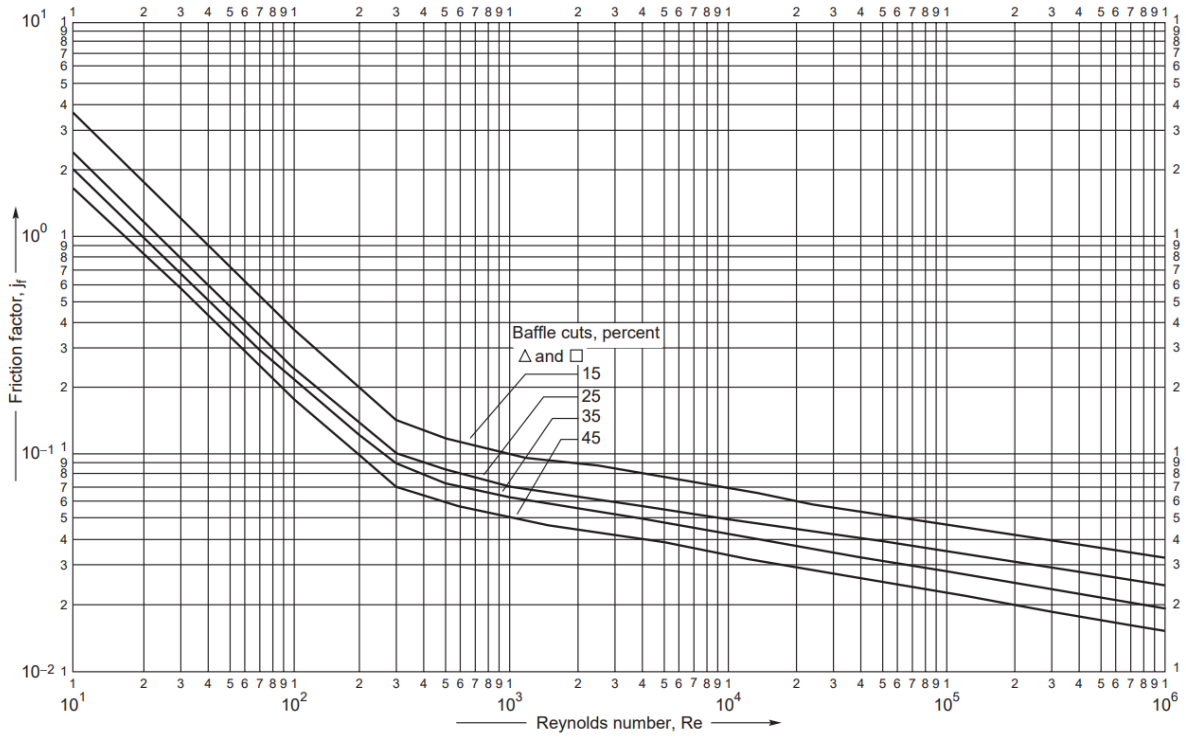

Figure B.4.4. Shell-side friction factor

ΔP_s = 0.53 bar

Both tube and shell side pressure drops are acceptable for heat exchanger design.

E-103 Cost estimation.

Base equipment cost of the Heat Exchanger E-103 can be calculated using the cost constants a and b for U-tube shell and tube heat exchanger are given as 28000 and 54 respectively [2]. Scaling factor is taken as 1.2 and the area is 256.68 m^2. The equation for the calculation is given as:

$$C_e=a+bS^n \quad \text{(B.4.15)}$$

C_e = 122257.7 USD

Lang factor for heat exchangers is given as 3.5, CS factor = 1.

Location factor of China (0.61) is multiplied by the scaling factor 1.2.

CEPCI (Chemical Engineering Plant Cost Index) book time (Jan 2010) = 532.9

CEPCI for 2024 is obtained as approximately 800.

Lang estimation:

$$C_L = C_e * CS * L \quad \text{(B.4.16)}$$

Material cost estimation:

$$C_M = \sum_{i=1}^{i=M} Ce, i, CS[(1 + f_p)f_m + (f_{er} + f_{el} + f_i + f_c + f_s + f_l)] \quad \text{(B.4.17)}$$

Installation factors are taken from the Towler's Chemical Engineering Design book [6]

Lang estimation:

C_L = 245140.504 USD

Location factor applied C_L = 179442.849 USD

Cost escalation L = 269383.148 USD

Material cost estimation:

C_M = 224128.461 USD

Location factor applied C_M = 164062.034 USD

Cost escalation L = 246293.164 USD

B.5 Depropanizer Distillation Column T-101 Design

The type of column chosen to be tray is based on several academic papers. Van Duc Long and Lee (2011) for improvement of depropanizer fractionation with simulation on Aspen HYSYS used a sieve tray type column with 34 stages, diameter 4.9m, condenser duty 26.03 MW and reboiler duty 21.54 MW [26]. Carling and Wood (1986) have done work with 29 ideal trays for the depropanizer column [27]. Thus, the type of column is chosen as a tray and not packed.

In order to find optimal conditions for the depropanizer column, 6 shortcut RadFrac columns with different numbers of stages were simulated using Aspen Plus V14. The reflux ratio of 14, distillate rate of 15 kmol/hr, pressure of column - 20 bar with pressure drop of 0.2 bar, condenser temperature of 2.8°C were held constant for these columns. The file with these simulations is "T-101 Optimization" in ESI. Table B.5.1 shows how recovery of propane changes with increase of total number of stages.

Table B.5.1. Dependence of propane recovery in distillate of total number of stages.

N total	Recovery of propane in distillate
15	0.9316
20	0.9778
25	0.9925
30	0.9960
35	0.9998
40	0.9999

While this approach is a little bit complicated, sensitivity analysis can be applied, however it may lead to slightly different values. The difference can be neglected, because they have the same trend. The reflux ratio of 14, distillate rate of 15 kmol/hr, pressure of column - 20 bar with pressure drop of 0.2 bar, condenser temperature of 2.8°C were held constant for these columns and feed stage was 4.

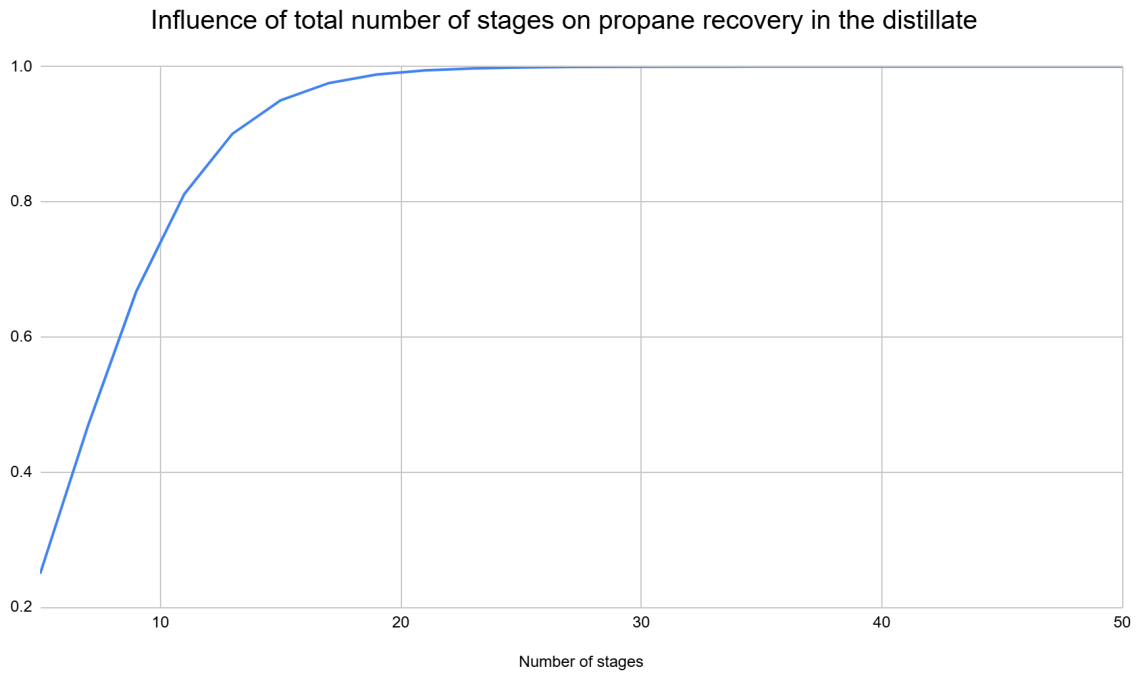

Figure B.5.1. Dependence of propane recovery in distillate with increase of total number of stages

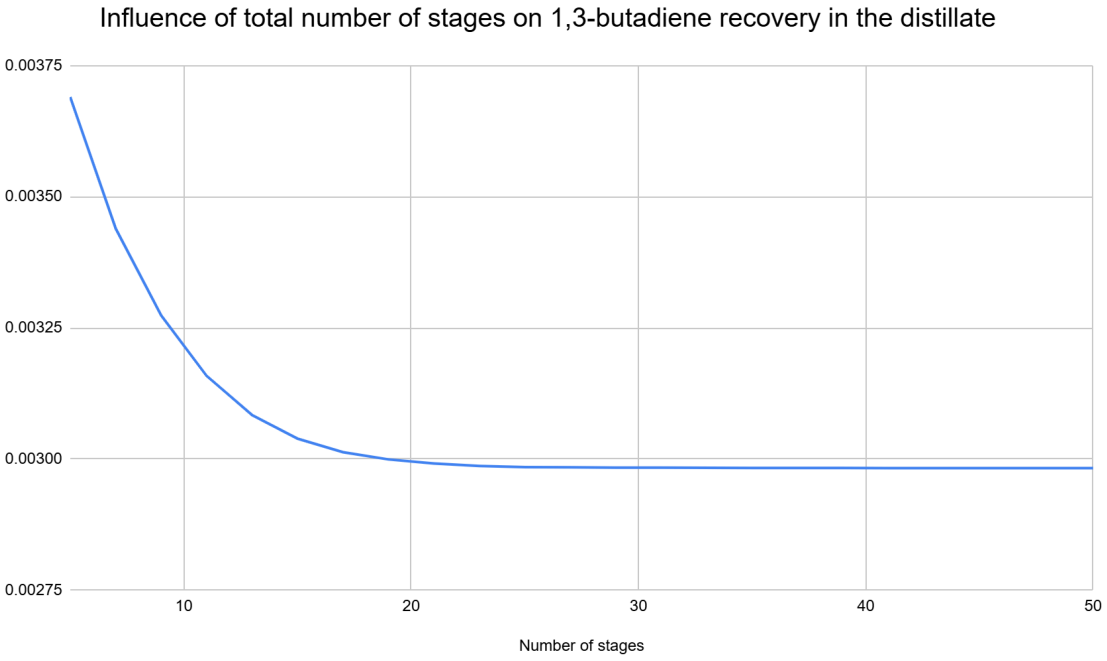

Figure B.5.2. Dependence of butadiene recovery in distillate with increase of total number of stages

It can be seen that, the more propane and less 1,3-butadiene is recovered in top product as the number of stages increases. However, it is not economically efficient to have a high number of stages. 25 total number of stages is taken as optimal to ensure efficient separation of propane and lighter components.

In order to find optimal reflux ratio, sensitivity analysis was done on a shortcut model of RadFrac with number of stages -25, distillate rate of 15 kmol/hr, pressure of column - 20 bar with pressure drop of 0.2 bar, condenser temperature of 2.8°C and feed stage-10-above stage.

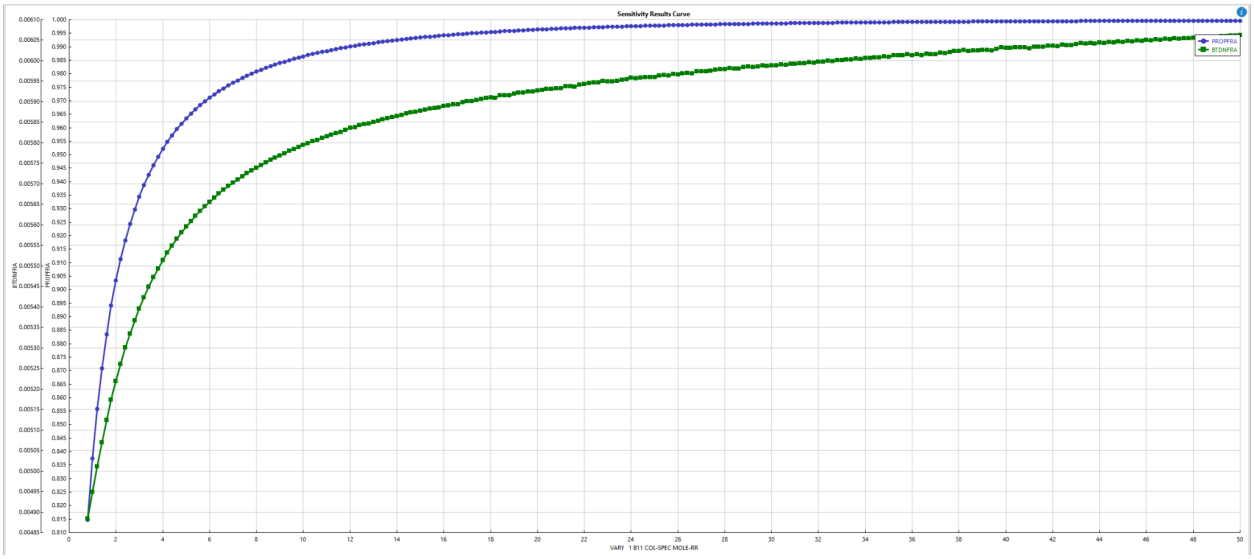

Figure B.5.3. Dependence of propane and butadiene recovery in distillate with increase of reflux ratio

Reflux ratio of 16 is taken as efficient, as with more increase in ratio the changes in recoveries almost stays the same, but will require more energy consumption for condenser. It should be noted that just to heat feed mixture 10 MW is already required, thus for the separation it would require more. Less reflux ratio can be used, but it will decrease the recovery of propane in the distillate, affecting the purity of the bottom stream. Analysis on finding optimal efficient distillate rate is needed in order not to lose a lot of butadiene in the top stream, as it is considered as by-products and will be taken away. Based on the result of sensitivity analysis shown in Figure B.5.4, distillate rate of 15 kmol/hr is chosen to be efficient.

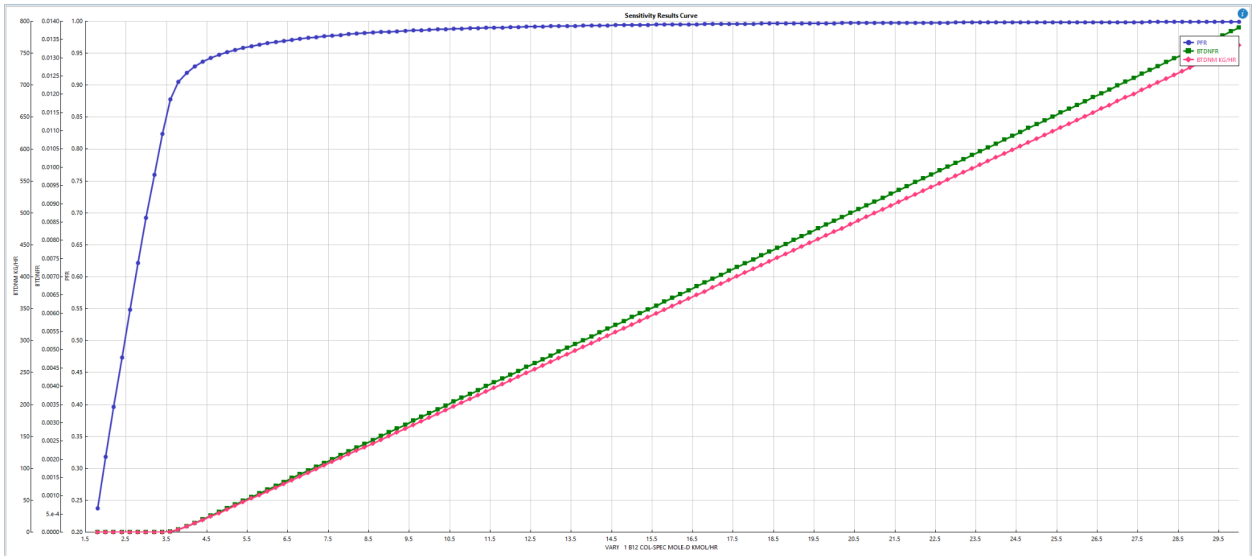

Figure B.5.4. Dependence of propane and butadiene recovery and butadiene mass flow rate in distillate with increase of distillate rate

The sensitivity of influence of the feed stage on separation is also done and can be seen in Figure B.5.5. It is required to get the most efficient recovery of propane, but also not getting high mass flow rate of butadiene in the top product. Since it is made on shortcut model of column with total 25 stages, the reflux ratio of 16, distillate rate of 15 kmol/hr, pressure of column - 20 bar with pressure drop of 0.2 bar, condenser temperature of 2.8°C, the results can be incorrect for the detailed model. For the detailed model feed stage is chosen to be 5 above stage.

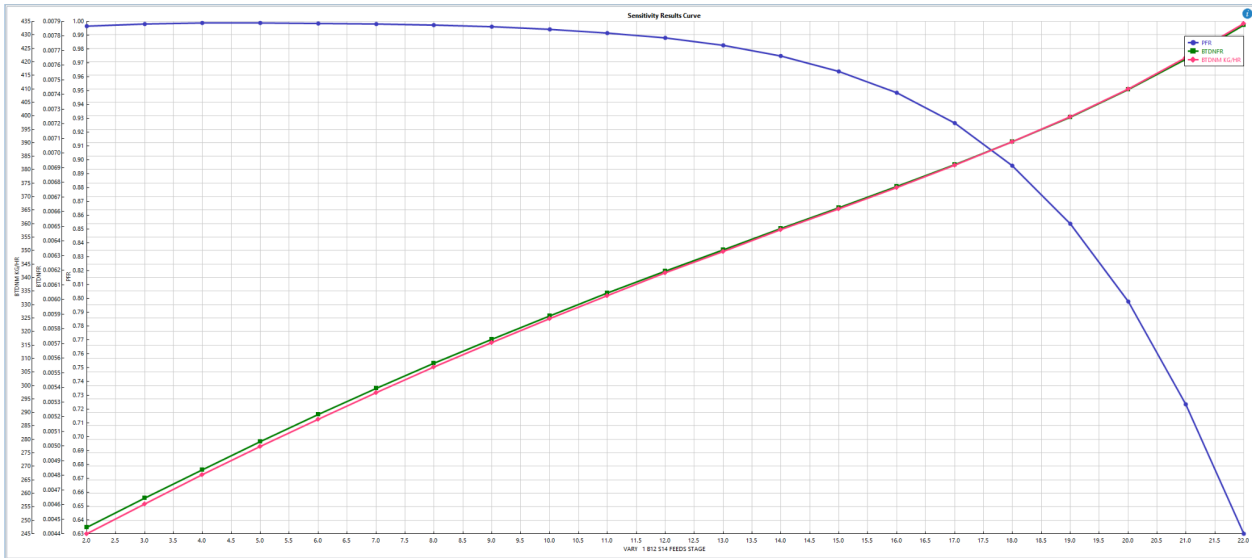

Figure B.5.5. Dependence of propane and butadiene recovery and butadiene mass flow rate in distillate with feed stage

Overall recovery of components in rate-based models differ with that of in shortcut. For instance recovery for propylene in top is 0.91, while for propane is 0.97. Similar tendency can be

seen with butadiene, the recovery of it on top is more than of butane or butene. The main reason is the presence of π-bonds in unsaturated compounds. The π-electrons in double bonds enable intermolecular interactions, such as π–π stacking or temporary associative forces with other molecules. These interactions can increase the apparent intermolecular attractions, which in turn lowers the volatility of the compound. As volatility decreases, the compound is less likely to vaporize and rise to the top of the column, resulting in greater accumulation in the lower sections and lower top product recovery. Rate-based models not only consider these subtle effects but also consider how separation undergoes in each tray, so it provides more accurate recovery estimates for components. [28]

In the column separation profile of propane's, butene's liquid flow and vapor flows across stages corresponds to different and correct separation of components. The partial-vapor condenser is considered as stage 1 and thus there is a different pattern. Same tendency with stages near the reboiler. It can be seen that almost no separation occurs in most of the trays, so they can be decreased. However, with decrease of total number of stages the mole flow rate of propane in distillate decreases influencing purity as seen in Figure B.5.6. This behavior arises because the concentration gradient between adjacent trays in the middle section becomes minimal, resulting in very low mass transfer driving force and, hence, negligible separation. Most of the effective separation takes place near the condenser and reboiler, while the intermediate stages operate close to equilibrium. This indicates that separation undergoes less, but is required to obtain required purity. As a result, reducing the number of stages for cost reduction is not feasible without adversely affecting the separation performance. As shown in Figure B.5.1, propane recovery increases rapidly at low stage numbers, but plateaus beyond ~25 stages, suggesting a low separation difference at higher number of stages, where recovery for propane is almost 1. It should be noted that more energy requirements can be compensated by energy obtained through burning waste streams. The detailed sensitivity analysis with multiple variables and how they influence recoveries of propane and butadiene in top and also how they influence reboiler's duty can be seen in Aspen file named "T-101 Design with sensitivity".

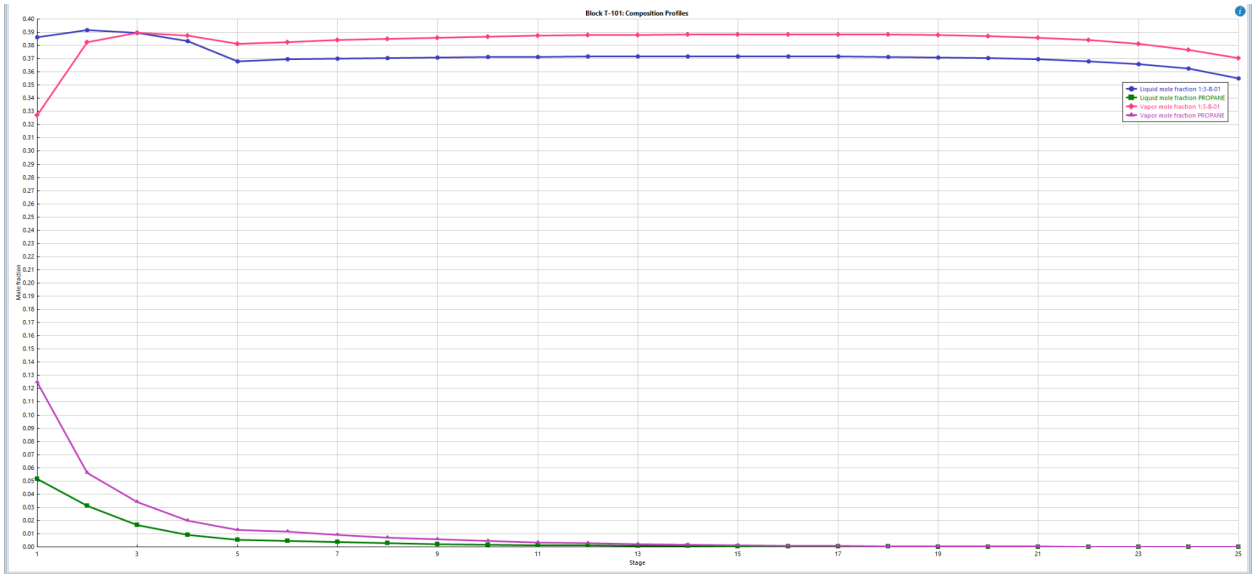

Figure B.5.6.Column separation profile across stages

Overall, the columns condenser and reboiler's duty, diameter is similar or even less than values used in papers on depropanizer simulations. Thus design is within realistic values. In the future with sufficient data for correct property estimation, the more accurate design can be done, but it is most likely that no big changes will occur as the amount of hydrogen in the feed is very low.

Appendix C. Environment and Waste Streams.

C.1 Health, safety, and regulatory considerations

Health and Safety

Before assessing health and safety concerns during production of butadiene it is important to identify major and minor components in the process, since only major components will be discussed in detail. Mainly, properties and possible hazards are studied for n-butane, 1-butene, 2- butene, 1,3-butadiene and hydrogen.

Explosions and fire risks

n-Butane, 1,3-butadiene and hydrogen gasses are extremely flammable substances, and their gas-air mixtures are explosive. Many reactions for hydrogen may cause fire or explosion. The auto ignition temperatures are 365°C for n-butane, 385°C for 1-butene, 324°C for 2-butene, 414°C for 1,3-butadiene and 560°C for hydrogen, trans form of 2-butene has the same characteristics as cis form [29-33]. All these substances should be kept away from all ignition sources like sparks, hot surfaces and open flames and should be protected from sunlight[34-36]. According to Occupational Safety and Health Administration the explosion limit for butane is from 1.6% to 8.4% [37]. For butadiene lower explosion limit - 2.0%, upper explosion limit - 12.0% [38]. For hydrogen flammability limits - 4% to 75%, explosion limits - 18.3% to 59%

[39]. Explosion limits for 1-butene and 2-butene are from 1.6% to 10% and from 1.7% to 9.7%, respectively [31, 34].

Toxicity

n-Butane is mostly non-toxic at low concentrations and can only cause low acute respiratory toxicity. If inhaled in high concentrations that are higher than lower explosion limit, it causes depression of the central nervous system and many different symptoms [40]. Risks of exposure to high concentrations of butadiene include acute toxicity, mutagenicity both in vivo and in vitro and high carcinogenicity, as it is a group 1 carcinogen [41,42]. Butadiene at very high concentrations is irritating to the eyes and respiratory tract and if inhaled may cause depression of the central nervous system. Rapid evaporation of its liquid may cause frostbite. Also, it is able to cause heritable genetic damage to human germ cells [29]. Inhalation of hydrogen can lead to headache, dizziness, lethargy or suffocation [32]. Both butenes do not have high toxicity; however, they may cause suffocation by lowering the oxygen content in the air [31,33]. Most catalysts used in the production of butadiene are metal oxide based and some of them like vanadium and magnesium oxides are toxic and may cause eye, skin and respiratory irritation, especially in dust form [42].

Preventive and safety measures

There should be no open flames, sparks or smoking in the area where the process will take place. There should be a closed system with ventilation, explosion-proof electrical equipment and lighting. Non-sparking hand tools should be used [30]. Personnel should work with cold insulating gloves and wear a face shield [29,30,32].

Regulations and legal considerations

According to Occupational Safety and Health Standards Permissible exposure limit for butadiene is 1 ppm for the 8-hour time weighted average (8-hr TWA) exposure and 5 ppm for 15 minutes of short-term exposure [44]. For butane, the recommended exposure limits up to 10-hour TWA - 800 ppm [37], however for hydrogen there is no specific exposure limit. According to OSHA regulations, customers should be provided with the latest Safety Data Sheet for the product, and it should be regularly updated [45]. Even though OSHA is the US federal agency, its regulation can be used as a basis and reference for the process regulation because data for regulations in Kazakhstan is hardly available. Since “LLP Butadiene” is already under construction and their process also includes the same major compounds, the compounds can be considered legal in the country.

Transportation of the product

Butadiene may be transported in liquid form in ships, barges, pipelines, bulk liquid containers and rail tank cars [45]. During transportation butadiene should be inhibited and one of the most common inhibitors is tertiary butyl catechol or TBC [45]. Since there is a possibility of formation of peroxides in butadiene, it is essential to keep the oxygen level below 1000 ppm during shipping [45]. In addition, it is required to label all containers with butadiene in

accordance with chemical hazard classification, thus “flammable gas” labels are needed. As all manufacturers are obligated to exclude the possibility of emission of butadiene in the atmosphere and sewage, it is needed to use exposure monitoring methods like charcoal tube method or gas chromatography [45].

C.2 Hazard identification tables

Table C.2.1. NFPA 704 for 1,3-butadiene [46]

Diamond	Hazard	Value	Description
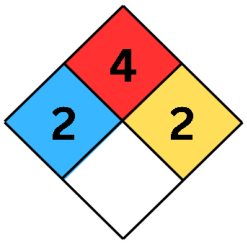	Health	2	Can cause temporary incapacitation or residual injury
	Flammability	4	Burns readily. Rapidly or completely vaporizes at atmospheric pressure and normal ambient temperature
	Instability	2	Readily undergoes violent chemical changes at elevated temperatures and pressures
	Special		

Table C.2.2. NFPA 704 for butane [47]

Diamond	Hazard	Value	Description
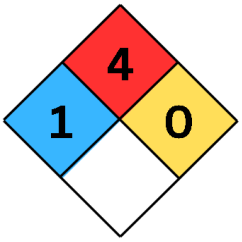	Health	1	Can cause significant irritation
	Flammability	4	Burns readily. Rapidly or completely vaporizes at atmospheric pressure and normal ambient temperature
	Instability	0	Normally stable, even under fire conditions
	Special		

Table C.2.3. NFPA 704 for hydrogen [48]

Diamond	Hazard	Value	Description
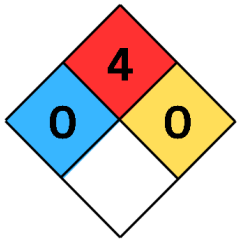	Health	0	No hazard beyond that of ordinary combustible material
	Flammability	4	Burns readily. Rapidly or completely vaporizes at atmospheric pressure and normal ambient temperature
	Instability	0	Normally stable, even under fire conditions
	Special		

Table C.2.4. NFPA 704 for 1-butene [49]

Diamond	Hazard	Value	Description
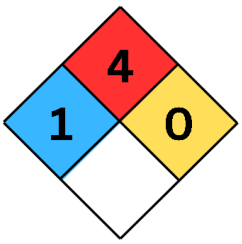	Health	1	Can cause significant irritation
	Flammability	4	Burns readily. Rapidly or completely vaporizes at atmospheric pressure and normal ambient temperature
	Instability	0	Normally stable, even under fire conditions
	Special		

Table C.2.5. NFPA 704 for 2-butene [50]

Diamond	Hazard	Value	Description
	Health	1	Can cause significant irritation
	Flammability	4	Burns readily. Rapidly or completely vaporizes at atmospheric pressure and normal

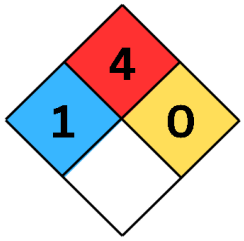			ambient temperature
	Instability	0	Normally stable, even under fire conditions
	Special		

Table C.2.6. NFPA 704 for 10Ni–5Fe–5Co–30Bi with 50% γ-Al_2O_3 [51, 52]

Diamond	**Hazard**	**Value**	**Description**
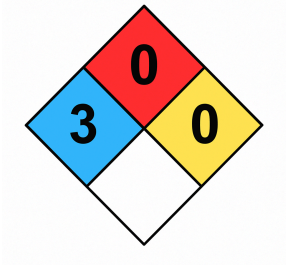	Health	3	Serious health hazard; toxic heavy-metal dust can cause lung damage or cancer if inhaled and may trigger skin/respiratory allergies
	Flammability	0	Non-flammable solid
	Instability	0	Stable and not reactive; no unusual explosion or reaction hazards
	Special		No special hazards

Reference list for Appendix

1. *USA Butadiene Market Analysis: Industry Market Size, Plant Capacity, Production, Operating Efficiency, Demand & Supply, End-User Industries, Sales Channel, Regional Demand, Company Share, Manufacturing Process, Policy and Regulatory Landscape, 2015-2032*. 2023; Available from: https://www.chemanalyst.com/industry-report/usa butadiene-market-736.
2. *Gross Domestic Product, Second Quarter 2024 (Advance Estimate)*. 2024; Available from: https://www.bea.gov/news/2024/gross-domestic-product-second-quarter-2024-
3. *United States Population*. 2024; Available from: https://www.worldometers.info/world population/uspopulation/#:~:text=the%20United%20States%202024%20population,(and%20depende ncies)%20by%20population.
4. *Commonwealth of Independent States*. Available from: https://countryeconomy.com/countries/groups/cis.
5. Towler, G.&Sinnott,R. (2008). Chemical Engineering Design. Elsevier Inc.
6. G. Towler and R. Sinnott, "Capital Cost Estimating," *Chemical Engineering Design*, pp. 307–354, 2013, doi: https://doi.org/10.1016/b978-0-08-096659-5.00007-9.
7. "Key properties of nickel," *Nickelinstitute.org*, 2020. https://nickelinstitute.org/en/nickel-applications/properties-of-nickel
8. "Iron - Density, Specific Heat and Thermal Conductivity vs. Temperature," *www.engineeringtoolbox.com*. https://www.engineeringtoolbox.com/iron-specific-heat-density-thermal-conductivity-vs-temperature-d_2226.html
9. Encyclopedia Britannica, "cobalt | Definition & Facts," *Encyclopædia Britannica*. Jan. 11, 2019. Available: https://www.britannica.com/science/cobalt-chemical-element
10. R. T. Sanderson, "bismuth | Properties, Uses, Symbol, & Facts," *Encyclopædia Britannica*. 2019. Available: https://www.britannica.com/science/bismuth
11. Accuratus, "Aluminum Oxide | Al2O3 Material Properties," *accuratus.com*, 2013. https://accuratus.com/alumox.html
12. R. N. Abdullaev, Y. M. Kozlovskii, R. A. Khairulin, and S. V. Stankus, "Density and Thermal Expansion of High Purity Nickel over the Temperature Range from 150 K to 2030 K," *International Journal of Thermophysics*, vol. 36, no. 4, pp. 603–619, Jan. 2015, doi: https://doi.org/10.1007/s10765-015-1839-x.
13. "Iron - Density, Specific Heat and Thermal Conductivity vs. Temperature," *www.engineeringtoolbox.com*. https://www.engineeringtoolbox.com/iron-specific-heat-density-thermal-conductivity-vs-temperature-d_2226.html
14. I. Sh. Valeev, V. I. Sergeev, and Kh. Ya. Mulyukov, "Thermal expansion of cobalt in various structural states," *Physics of the Solid State*, vol. 51, no. 3, pp. 593–596, Mar. 2009, doi: https://doi.org/10.1134/s1063783409030263.

15. Y. Greenberg *et al.*, “Evidence for a temperature-driven structural transformation in liquid bismuth,” *EPL (Europhysics Letters)*, vol. 86, no. 3, pp. 36004–36004, May 2009, doi: https://doi.org/10.1209/0295-5075/86/36004.
16. Accuratus, “Aluminum Oxide | Al2O3 Material Properties,” *accuratus.com*, 2013. https://accuratus.com/alumox.html
17. “12.3: Thermal Expansion,” *Physics LibreTexts*, Jan. 15, 2019. https://phys.libretexts.org/Courses/Prince_Georges_Community_College/PHY_2030%3A_General_Physics_II/12%3A_Temperature_and_Kinetic_Theory/12.3%3A_Thermal_Expansion?utm_source
18. *BPVC.II.D.C - BPVC Section II-Materials-Part D-Properties-(Mertric)*. ASME, 2019.
19. Coker, A. Kayode. (2015). Ludwig's Applied Process Design for Chemical and Petrochemical Plants, Volume 3 (4th Edition). Elsevier. Retrieved from
 https://app.knovel.com/hotlink/toc/id:kpLAPDCP12/ludwigs-applied-process/ludwigs-applied-process
20. K. H. Lüdtke, *Process centrifugal compressors* : basics, function, operation, design, application /. Berlin ; London: Springer, 2010.
21. "Theory at a Glance," *CST Firenze*. Available: https://www.cstfirenze.com/knowledge/theory-at-a-glance
22. J. M. Sorokes and M. J. Kuzdzal, "How diffusers in centrifugal compressors have evolved over the years," Turbomachinery International, Apr. 12, 2019. Available: https://www.turbomachinerymag.com/view/how-diffusers-in-centrifugal-compressors-have-evolved-over-the-years
23. A. Karlsson, *Aerodynamic Design of Centrifugal Compressor for Heavy Duty Truck Applications,* Technology and Engineering, 2018. ISSN: 0282-1990. https://lup.lub.lu.se/luur/download?func=downloadFile&recordOId=8950826&fileOId=8950857
24. R. S. R. Gorla and A. A. Khan, *Turbomachinery: Design and Theory*. 1st ed. Boca Raton, FL, USA: CRC Press, 2003. https://ftp.idu.ac.id/wp-content/uploads/ebook/tdg/ADVANCED%20ENGINE%20TECHNOLOGY%20AND%20PERFORMANCE/epdf.pub_turbomachinery-design-and-theory-dekker-mechanical.pdf
25. H. Hazby, M. Casey, C. Robinson, R. Spataro, and O. Lunacek, "The design of a family of process compressor stages," *in Proc. European Turbomachinery Conf.*, 2017, doi: 10.29008/ETC2017-134.
26. Van Duc Long, N., & Lee, M. (2011). Improvement of the deethanizing and depropanizing fractionation steps in NGL recovery process using dividing wall column. *JOURNAL OF CHEMICAL ENGINEERING OF JAPAN*, *45*(4), 285–294. https://doi.org/10.1252/jcej.11we187
27. Carling, G., & Wood, R. (1986). The dynamics and control of a depropanizer. *IFAC Proceedings Volumes*, *19*(15), 167–173. https://doi.org/10.1016/s1474-6670(17)59417-3

28. *π-stacking interactions, conducting organic materials - Department of Chemistry*. (2014, May 7). Department of Chemistry. https://chemistry.georgetown.edu/research_6/?utm_source
29. *1,3-BUTADIENE*. 2017; Available from: https://chemicalsafety.ilo.org/dyn/icsc/showcard.display?p_lang=en&p_card_id=0017&p_version=2.
30. *BUTANE*. 2003; Available from: https://chemicalsafety.ilo.org/dyn/icsc/showcard.display?p_lang=en&p_card_id=0232&p_version=2.
31. *cis-2-BUTENE*. 2019; Available from: https://chemicalsafety.ilo.org/dyn/icsc/showcard.display?p_lang=en&p_card_id=0397&p_version=2.
32. *HYDROGEN*. 2014; Available from: https://chemicalsafety.ilo.org/dyn/icsc/showcard.display?p_lang=en&p_card_id=0001&p_version=2.
33. *n-BUTENE*. 1999; Available from: https://chemicalsafety.ilo.org/dyn/icsc/showcard.display?p_lang=en&p_card_id=0396&p_version=2.
34. *BUTANE*. Available from: https://chemicalsafety.com/sds1/sdsviewer.php?id=33976120&name=BUTANE.
35. *HYDROGEN*. Available from: https://chemicalsafety.com/sds1/sdsviewer.php?id=33976331&name=HYDROGEN.
36. *BUTENE-1*. Available from: https://chemicalsafety.com/sds1/sdsviewer.php?id=33976484&name=BUTENE-1.
37. *BUTANE*. 2020; Available from: https://www.osha.gov/chemicaldata/49. 172.
38. *BUTADIENE (1,3-BUTADIENE)*. 2024; Available from: https://www.osha.gov/chemicaldata/50.
39. P. R. Lewis, C.G., *Forensic Polymer Engineering*. 2010.
40. Lee, J.-S. *n-Butane and Isobutane*. 2012; Available from: https://www.tceq.texas.gov/downloads/toxicology/dsd/final/butanes.pdf.
41. Birnbaum, L.S.J.E.h.p., *A brief survey of butadiene health effects: a role for metabolic differences*. 1993. **101**(suppl 6): p. 161-167.
42. Chen, W.-Q., X.-Y.J.G. Zhang, and Environment, *1, 3-Butadiene: a ubiquitous environmental mutagen and its associations with diseases*. 2022. **44**(1): p. 3. 177.
43. *MAGNESIUM OXIDE*. Available from: https://chemicalsafety.com/sds1/sdsviewer.php?id=33707644&name=Magnesium%20ox ide.
44. *1,3-Butadiene.*; Available from:

https://www.osha.gov/lawsregs/regulations/standardnumber/1910/1910.1051.
45. *BUTADIENE: PRODUCT STEWARDSHIP GUIDANCE MANUAL*. 2024. 47.
Butadiene Production from n-Butane. 2021; Available from: https://cdn.intratec.us/docs/reports/previews/butadiene-e11a-b.pdf.
46. *Database of Hazardous Materials | 1,3-Butadiene*. 2010; Available from: https://cameochemicals.noaa.gov/chemical/4891.
47. *Database of Hazardous Materials | Butane*. 2010; Available from: https://cameochemicals.noaa.gov/chemical/5668.
48. *Database of Hazardous Materials | Hydrogen*. 2010; Available from: https://cameochemicals.noaa.gov/chemical/8729.
49. *Database of Hazardous Materials | 1-Butene.* . 2010; Available from: https://cameochemicals.noaa.gov/chemical/18041.
50. *Database of Hazardous Materials | 2-Butene*. 2010; Available from: https://cameochemicals.noaa.gov/chemical/18045.
51. ChemicalBook, Nickel(II) Oxide Material Safety Data Sheet, [Online]. Available: https://www.chemicalbook.com/msds/nickel-ii-oxide.htm
52. TA Instruments, *Safety Data Sheet: Nickel Cobalt Alloy*, Rev. E, Document No. 901135, [Online]. Available: https://www.tainstruments.com/pdf/safety-data-sheets/901135-Rev-E_SDS-Nickel-Cobalt-Alloy.pdf